Dissertations   Electronic Theses and Dissertations

12-31-2023

Assessing the feasibility and mechanism of destructive removal of per- and polyfluoroalkyl substances (PFAS) from water

Kaushik Vinaykumar Londhe
New Jersey Institute of Technology, kvl4@njit.edu

Follow this and additional works at: https://digitalcommons.njit.edu/dissertations

Part of the Chemical Engineering Commons, and the Environmental Engineering Commons

ABSTRACT

ASSESSING THE FEASIBILITY AND MECHANISM OF DESTRUCTIVE REMOVAL OF PER- AND POLYFLUOROALKYL SUBSTANCES (PFAS) FROM WATER

by
Kaushik Vinaykumar Londhe

One of the most pertinent challenges faced by the drinking water community is the widespread contamination of per- and polyfluoroalkyl substances (PFAS). These anthropogenic chemicals have been ubiquitously used in everyday products such as carpets, stain repellents, dyes, shampoos, non-stick cookware as well as in aqueous firefighting foams. PFAS are linked with adverse health effects in humans such as thyroid disease, obesity, immunological and reproductive disorders and linked to cancer in adults and low birth weight and developmental defects in infants.

Conventional water treatment technologies have proven to be largely ineffective in PFAS remediation, due to their extreme stability and resistance to degradation. The overall goal of this dissertation is to assess the feasibility and performance of novel destructive technologies in treating PFAS. The specific objectives of this study are to: (i) investigate the impact of water quality and operating parameters on the treatment of a suite of PFAS using two destructive techniques, a) electron beam (e-beam) and b) electrochemical oxidation process (eAOP); (ii) elucidate the primary degradation mechanism of PFAS in these systems; (iii) differentiate the performance (energy requirements) of these systems in treating PFAS isomers; and (iv) develop a novel air-bubbling system to extract PFAS from contaminated soils to combine with destructive technologies via a treatment-train approach. The effect of chain length and functional group is observed while treating PFAS with e-beam technology with the short chain perfluorobutanoic acid and

perfluorobutanesulfonic acid showing highest resistance to degradation. This chapter additionally highlights previously unknown degradation pathways of PFAS using a combination of fluorine mass balance and suspect screening. In eAOP system, the composition of supporting electrolyte and anodic voltage did not impact PFAS degradation. PFAS degradation strongly correlates with compound hydrophobicity and this study is the first to differentiate between degradation and loss in concentration due to the phenomena of electrochemical aerosolization of PFAS. Branched PFAS isomers preferentially degrade by e-beam treatment but show comparative/poorer removal in an eAOP system, compared to their linear forms. Soil washing is studied as a removal approach for PFAS-contaminated soils, that can be used as a standalone technique or along with destructive techniques in a treatment train system. A novel air-bubbling assisted soil washing system is used to investigate the removal of adsorbed PFAS from contaminated soils. The extraction efficiency from the soil is found to be inversely proportional to PFAS hydrophobicity, with poorest results observed for long chain perfluorodecanoic acid. Results from this dissertation (i) identify ideal conditions and energy requirements for the destructive removal of PFAS, (ii) highlight the challenges and knowledge gaps for the remediation of contaminated soils, and (iii) provide insight into the variable mechanisms of PFAS destruction and removal, impacted by the PFAS structure and operating parameters in both aqueous and soil matrices.

ASSESSING THE FEASIBILITY AND MECHANISM OF DESTRUCTIVE REMOVAL OF PER- AND POLYFLUOROALKYL SUBSTANCES (PFAS) FROM WATER

by
Kaushik Vinaykumar Londhe

A Dissertation
Submitted to the Faculty of
New Jersey Institute of Technology
in Partial Fulfillment of the Requirements for the Degree of
Doctor of Philosophy in Environmental Engineering

John A. Reif, Jr. Department of Civil and Environmental Engineering

December 2023

ASSESSING THE FEASIBILITY AND MECHANISM OF DESTRUCTIVE REMOVAL OF PER- AND POLYFLUOROALKYL SUBSTANCES (PFAS) FROM WATER

Kaushik Vinaykumar Londhe

Dr. Arjun Venkatesan, Dissertation Advisor   Date
Associate Professor of Civil and Environmental Engineering, NJIT

Dr. Taha Marhaba, Committee Member   Date
Professor and Chair of Civil and Environmental Engineering, NJIT

Dr. Oladoyin Kolawole, Committee Member   Date
Assistant Professor of Civil and Environmental Engineering, NJIT

Dr. Xinwei Mao, Committee Member   Date
Associate Professor of Civil Engineering, Stony Brook University, Stony Brook, NY

Dr. Carrie McDonough, Committee Member   Date
Assistant Professor of Chemistry, Carnegie Mellon University, Pittsburgh, PA

BIOGRAPHICAL SKETCH

Author: Kaushik Vinaykumar Londhe

Degree: Doctor of Philosophy

Date: December 2023

Undergraduate and Graduate Education:

- Doctor of Philosophy in Environmental Engineering,
  New Jersey Institute of Technology, Newark, NJ, 2023

- Master of Science in Chemical Engineering,
  Arizona State University, Tempe, AZ, 2018

- Bachelor of Science in Chemical Engineering,
  D.J. Sanghvi College of Engineering, Mumbai, India, 2016

Major: Environmental Engineering

Publications:

Lee, C. S., **Londhe, K**., Cooper, C., Grdanovska, S., & Venkatesan, A. (2023). Emerging investigator series: Low doses of electron beam irradiation effectively degrade 1, 4-dioxane in water within a few seconds. *Environmental Science: Water Research & Technology,* doi:10.1039/D3EW00111C

Cooper, C., Grdanovska, S., **Londhe, K**., Venkatesan, A.K., Lange, C. (2023), *Destruction of PFAS in Water via Electron Beam. Per- and Polyfluoroalkyl Substances Treatment: Theories, Technology, and Practice*, Royal Society of Chemistry (Book chapter, accepted)

Londhe, K., Lee, C. S., McDonough, C. A., & Venkatesan, A. K. (2022). The Need for Testing Isomer Profiles of Perfluoroalkyl Substances to Evaluate Treatment Processes. *Environmental Science & Technology, 56*(22), 15207-15219. doi:10.1021/acs.est.2c05518

Li, D., **Londhe, K**., Chi, K., Lee, C. S., Venkatesan, A. K., & Hsiao, B. S. (2021). Functionalized bio-adsorbents for removal of perfluoroalkyl substances: A perspective. *AWS, 3*(6). doi:10.1002/aws2.1258

Londhe, K., Lee, C.-S., Zhang, Y., Grdanovska, S., Kroc, T., Cooper, C. A., & Venkatesan, A. K. (2021). Energy Evaluation of Electron Beam Treatment of Perfluoroalkyl Substances in Water: A Critical Review. *Environmental Science & Technology Engineering, 1*(5), 827-841. doi:10.1021/acsestengg.0c00222

Presentations:

Lee, C. S., **Londhe, K**., Grdanovska, S., Cooper., C. A., & Venkatesan, A. K. Effective degradation of 1,4-dioxane in waters by low doses of electron beam irradiation, *Association of Environmental Engineering and Science Professors 2023 Conference*, Poster presentation, 2023.

Londhe, K., Lee, C. S., Schneider, O., & Venkatesan, A. K. . Degradation of long and short chain PFAS using a bench scale Magneli phase Ti_4O_7 anode based electrochemical oxidation system, *American Chemical Society Fall Symposium*, Oral presentation, 2022.

Londhe, K., Lee, C. S., Zhang, Y., Grdanovska, S., Cooper, C. A., & Venkatesan, A. K. . Application of electron beam for the degradation of perfluoroalkyl substances (PFAS) in drinking water., *Civil Engineering Graduate Student Research Symposium*,Stony Brook University, Stony Brook, NY, Poster presentation, 2022.

Londhe, K., Lee, C. S., Grdanovska, S., Cooper, C. A., Kalb, P., Paquette, D., Mills, M., & Venkatesan A. K. . Treatment of PFAS and 1,4-dioxane using e-beam technology*, American Chemical Society Spring Symposium*, Oral presentation, Virtual, 2021.

Londhe, K., Lee, C. S., Grdanovska, S., Cooper, C. A., Kalb, P., Paquette, D., Mills, M., & Venkatesan A. K. . Application of electron beam for the degradation of 1,4 dioxane and perfluoroalkyl substances in drinking water., *Strategic Environmental Research and Development Program & Environmental Security Technology Certification Program Symposium*, Poster presentation, Virtual, 2020.

I would like to dedicate this PhD dissertation to my family who have supported me throughout my life, starting right from elementary school, all the way to this day. I would like to recognize and thank my parents, Dr. Vinaykumar Londhe and Mrs. Nanda Londhe, who have been a pillar of strength especially during the ups and downs of the MS and PhD program. I would also like to acknowledge and thank my sister, Dr. Priya Londhe, who has not only been a source of inspiration, but also a mentor and a confidant throughout this journey. Finally, I would like to recognize and acknowledge my uncle, Mr. Vijaykumar Londhe, who strongly encouraged and supported me to follow my dream of higher education in the United States.

ACKNOWLEDGMENTS

I would like to thank my advisor, Dr. Arjun Venkatesan at the Department of Civil and Environmental Engineering at NJIT for his support and guidance throughout my PhD process.

I would also like to acknowledge my committee members, Dr. Taha Marhaba, Dr. Oladoyin Kolawole, Dr. Xinwei Mao and Dr. Carrie McDonough and my collaborators, Dr. Charlie Cooper and Dr. Slavica Grdanovska, who provided guidance, input, and suggestions to improve the quality of the research.

I would like to thank Dr. Cheng-Shiuan Lee and Dr. Michael Bentel, who have been my mentors throughout the PhD process. I would also like to acknowledge and thank Dr. Xiayan Ye and all current and former members of New York State's Center for Clean Water Technology for their input and suggestions.

I would like to acknowledge my funding agencies: U.S Department of Energy (award# 86233), U.S Department of Health (award# 86325) and US Army Corps. Engineers (award# 93408) for all their help and support.

I would like to take the opportunity to recognize some of the special peers and friends that I have met during my academic journey. My heartfelt gratitude goes out to Dr. Samantha Roberts and Dr. Molly Graffam, have gone above and beyond as friends and mentors, since the first day of my PhD. I would like to recognize a few of my friends; Erin Giuliano, Hilary Brooks, Michelle Horsham, Meghan Oates, Ram Telikicherla, Courtney Tello, Samruddhi Jewlikar, Annapoorani Hariharan, Kristen Burk, Juee Joshi, Kavyaja Hambardikar, Lavya Kedare, Shweta Panchal, Vaibhavi Sanghvi, Robin Denny, Apoorva

Telukuntla, Mangalam Lalpuria, Jake Wiersig and Kendall Byers who helped me celebrate good times and provided support during bad times.

Finally, I would like to thank all members, staff and coaches of Orangetheory Fitness, Long Island, that helped me maintain and improve my physical and mental well-being.

TABLE OF CONTENTS

LIST OF TABLES

LIST OF ABBREVIATIONS AND ACRONYMS

PFAS	Per and polyfluoroalkyl substances
GAC	Granular Activated Carbon
PAC	Powdered Activated Carbon
IX	Ion exchange
NF	Nanofiltration
ARP	Advanced Reduction Processes
PFSA	Perfluorosulfonic Acid
PFCA	Perfluorocarboxylic Acid
PFOA	Perfluorooctanoic Acid
PFHpA	Perfluoroheptanoic Acid
PFHxA	Perfluorohexanoic Acid
PFOS	Perfluorooctanesulfonic Acid
PFBA	Perfluorobutanoic Acid
PFBS	Perfluorobutanesulfonic Acid
PFNA	Perfluorononanoic Acid
6:2 FTS	6:2 fluorotelomer Sulfonate
FOSA	Perfluorooctane Sulfonamide
DIW	Deionized Water
GW	Groundwater
WW	Wastewater
TOC	Total Organic Carbon

A2D2	Accelerator Application Development and Demonstration
SBU	Stony Brook University
AOP	Advanced Oxidation Process
eAOP	Electrochemical Advanced Oxidation Process
HALT	Hydrothermal Alkaline Treatment
BDD	Boron Doped Diamond
EC	Electrical Conductivity
PP	Polypropylene
ORP	Oxygen Reduction Potential
HDPE	High-density Polyethylene
pCBA	para chlorobenzoic acid
OC	Organic Carbon
CTAC	Cetyltrimethylammonium Chloride

CHAPTER 1

INTRODUCTION

1.1   Objective

The objective of this dissertation is to focus on the treatment technologies employed for the remediation of per and poly-fluoroalkyl substances (PFAS) in aqueous and soil matrices.

The first technique studied as a part of this dissertation was electron beam (e-beam) technology. The main objective of utilizing this technique was to identify optimal treatment parameters while investigating the effects of PFAS structure and effects of sample matrix on the degradation process.

The second technique chosen was electrochemical oxidation (eAOP) by utilizing a specialized boron-doped diamond electrode. The main objectives of this technology were to investigate the impact of supporting electrolyte, anode potential and PFAS structure on the degradation of PFAS.

Finally, the main objective of the soil-washing process was to design a novel air-bubbling assisted system to extract PFAS of different chain lengths and functional groups. The secondary objective was to study the effect of organic matter, washing solution and additives on the extraction process, while studying PFAS compartmentalization.

1.2   Background Information

In 1962, Ludwig Von Drake, in an episode of 'Walt Disney's Wonderful World of Color' explained why people were actually the biggest challenge facing people these days. He further added that because they cause the most problems, without them, there would be none. Although nature has tested the very existence of our lives several times over the course of mankind's history, the sheer damage that we, as the 'smartest' and most 'advanced' species are causing to both us and the world around us, is both, extreme and saddening.

This is especially true when we look at the pollution caused by human activities and its effects on several flora and fauna, as well as the natural balance. The onset of the scientific revolution led to a deeper understanding of the world around us, leading to new scientific breakthroughs and discoveries. Although this greatly improved our quality of life and life expectancy, the 'use now, worry later' philosophy , as we are slowly learning has led to some devastating and irreversible consequences.

Access to clean, drinking water is not a luxury, but a fundamental right of every human being. Today, about 74% of the world's population has access to clean water, with this number constantly rising. Through scientific advancements, we have been able to design and develop technologies to remove naturally occurring substances such as copper, lead, selenium as well as arsenic and mercury. However, a group of anthrophonic chemicals, invented less than a century ago, may prove to be one of our biggest water treatment challenges yet.

1.2.1 Introduction to PFAS

Per and polyfluoroalkyl substances (PFAS) are a group of man-made chemicals that were first invented in the 1930s. However, these chemicals did not become commercially popular and/or manufactured until the 1940-50s. These chemicals have a carbon-carbon skeleton with the degree of defluorination varying with the chemical structure. Simply put, PFAS can be thought of as having the structure of a common straight chain hydrocarbon with a terminal functional group(s) attached at the end and with the C-H bonds replaced partially or fully with C-F bonds. This substitution with fluorine, the most electronegative element, meant that it greatly changed the physicochemical properties of the parent compound. PFAS were found to be highly resistant to chemical and thermal degradation and their water-repelling and oil-repelling properties led to their implementation in a variety of industrial and military non-stick applications. Teflon, a PFAS commercially manufactured by 3M company for DuPont, was used in the Manhattan project during WW2 to manufacture warheads, liquid-fuel tanks and linings of nuclear bombs.[1] The fallout of the war led to a focus on widespread manufacture and implementation of PFAS into commercial products and applications. Two years after 3M company started producing PFAS for DuPont, 3M invented the ScotchGard fabric coating, another iconic brand that they went on to coat everything from pans to pants. Teflon and ScotchGard, for their oil and water-resistant properties, went on to coat non-stick cookware, upholstery, carpeting, clothing etc. However, PFAS had still not achieved its full potential for military applications yet.

In 1967, there was a deadly fire aboard the U.S. Navy aircraft carrier, the USS Forrestal. This was caused by the accidental launch of a rocket into loaded fuel tanks and

armed planes. This accident destroyed the ship and killed more than 130 people. This led to more research into aqueous fire-fighting foams (AFFFs) with PFAS being the primary ingredient in the formulations. This foam mixture rapidly extinguished fires and was easy to spread, making it highly effective against fires caused by petroleum and flammable-liquid fires. This led to PFAS-containing AFFFs installed on military and civilian ships as well as both airplanes and airports.[1]

1.2.2   Fate and Transport of PFAS

Since the 1960s and 1970s, PFAS have been used ubiquitously in a variety of household, industrial and military applications. PFAS have been used in a variety of consumer products such as dyes, detergents, plastic and food wrappers, non-stick cookware, carpets and upholstery, water-resistant clothing. This has led to the detection of PFAS in several environmental compartments such as surface, ground, drinking, ocean and waste waters, air, rainwater and soils.[2-8] PFAS have been detected in the bodies of humans, oceanic and terrestrial animals and birds, plants as far as in the blood of polar bears in the arctic, showing the widespread distribution of PFAS. For humans, there is both direct and indirect routes for PFAS exposures through the air we breathe, the water and food we consume and through other products that we use such as cosmetics, dyes and detergents. As we learnt about the widespread distribution and compartmentalization of PFAS, more and more research pointed towards the health effects of these compounds, that raised several concerns.

PFAS are extremely persistent, bioaccumulative and toxic.[9] They are linked to a variety of immunological and reproductive disorders in humans.[10, 11] PFAS are linked to kidney and testicular cancers in men as well as increased cholesterol levels and increased

risk of high blood pressure or pre-eclampsia in pregnant women.[12] PFAS can also cause birth defects, including reduction in birth weight and vaccine response in children.[12] In adults, PFAS are linked to obesity as well as damage to the liver, kidney, thyroid and placenta causing disruption of regulatory hormones and metabolic functions.[2, 6, 12, 13]

1.2.3   Current Status of PFAS Treatment Technologies

The treatment technologies currently applied or investigated for PFAS remediation can be grouped into two categories, depending on the removal mechanism. Sequestration techniques involve physical/chemical separation techniques such as granular activated carbon (GACs), ion-exchange resins, (IX), nano/ultrafiltration, reverse osmosis (RO) and foam fractionation. These technologies mainly aim to remove PFAS from the source matrix, leading to a reduction in PFAS concentrations in the final treated product. Techniques such as GACs, IX, and RO have been used in both pilot and full scale applications for PFAS removal with the treatment efficiencies ranging from 40-100%.[2, 6, 14-17] The wide range of efficiency can be attributed to the variation of interactions between the adsorbent media and PFAS molecules influenced by the structure of the PFAS molecules (chain length, functional group, degree of defluorination etc.) that influences the removal mechanisms during the process. These sequestration processes are easy to scale up, are efficient, can be modified, based on the initial PFAS concentration and distribution to achieve excellent removal efficiencies. However, the biggest problem lies when the media reaches the end of its life cycle. Utilizing these removal technologies leads to a concentrated waste stream that may be several orders of magnitude higher in concentration than the recommended levels. This means that the final steps are appropriate treatment and/or disposal of such concentrated waste streams that requires careful planning, but also

increases capital and operational costs. This is usually done either by incineration or landfill disposal, both of which have the potential to release PFAS back into the environment.

Destructive technologies, on the contrary, aim to breakdown the C-F or the C-C bonds present in PFAS molecules, with the ultimate goal of transforming the parent PFAS into less toxic, more manageable byproducts. This is done by the production of highly unstable, short-lived but reactive radicals that target C-C or C-F bonds present in the molecules of PFAS. It is important to note that due to the presence of multiple C-F bonds, PFAS are largely resistant to destructive technologies following oxidative pathways. Hence, some of the destructive technologies such as DC plasms, advanced reduction processes, electron beam (e-beam) focus on breaking down PFAS molecules using a reductive pathway. Other techniques such as electrochemical oxidation, supercritical water oxidation, hydrothermal alkaline water treatment involve high temperatures, pressures or additional steps prior to PFAS oxidation. The ultimate goal of these techniques is to fully convert the poly/perfluoroalkyl substances into inorganic fluorine and CO_2. However, it should be noted that so far, no technology has achieved this goal. Incomplete degradation of the parent PFAS can lead to the formation of known and unknown byproducts that can potentially be more toxic and harder to treat. Utilizing destructive technologies, especially for PFAS remediation involves high energy demands, driving up the overall treatment costs. Thus, more research is needed in the field of destructive treatment of PFAS to be able to find a solution to ultimately dispose and solve the PFAS problem.

For my PhD work, I focused on two advanced oxidation/reduction technologies for PFAS remediation in predominantly aqueous matrices. The first technology I studied was electron beam (e-beam) technology. This study was performed in collaboration with the

Fermi National Accelerator Laboratory (Fermilab), Batavia, Illinois, utilizing their novel accelerator. Prior to actually utilizing the treatment for PFAS remediation, I discovered a knowledge gap that existed, specifically on utilizing this technique for PFAS remediation. Hence, Chapter 2 of this dissertation is a critical review paper that focuses on the energy evaluation of e-beam technology for primarily PFAS treatment.

Chapter 3 is building on the lessons learnt from Chapter 1, advances in the field during that time period to apply e-beam technology for destruction of PFAS of different chain length and functional groups, under different water quality and operating parameters in aqueous matrices.

For my next chapter, I was lucky to have been able to use my interest in electrochemistry to design and build a two-electrode electrochemical oxidation system. Chapter 3 focuses on utilizing this system, with an inactive BDD anode to study the impact of PFAS structure, supporting electrolyte and operating parameters for PFAS destruction and identify potential degradation mechanisms.

Chapter 5, interestingly builds on lessons learnt from Chapters 3 and 4 on the variation in treatment performance observed for PFAS isomers. This is a critical review demonstrating how the behavior of PFAS isomers varies, depending on the choice of treatment technologies, for both sequestration and destruction approaches.

The general consensus along with the data obtained from investigating the two destructive technologies for PFAS remediation was that the overall treatment efficiency could be enhanced by using a 'concentrate and destroy; approach, meaning a pre-concentration step could be utilized prior to ultimate destruction. Thus, for my final Chapter (6), I combined a novel technique combining air-bubbling with soil washing to

extract and concentrate PFAS from contaminated soil matrices. Figure 1 is a map detailing my journey throughout the PhD process.
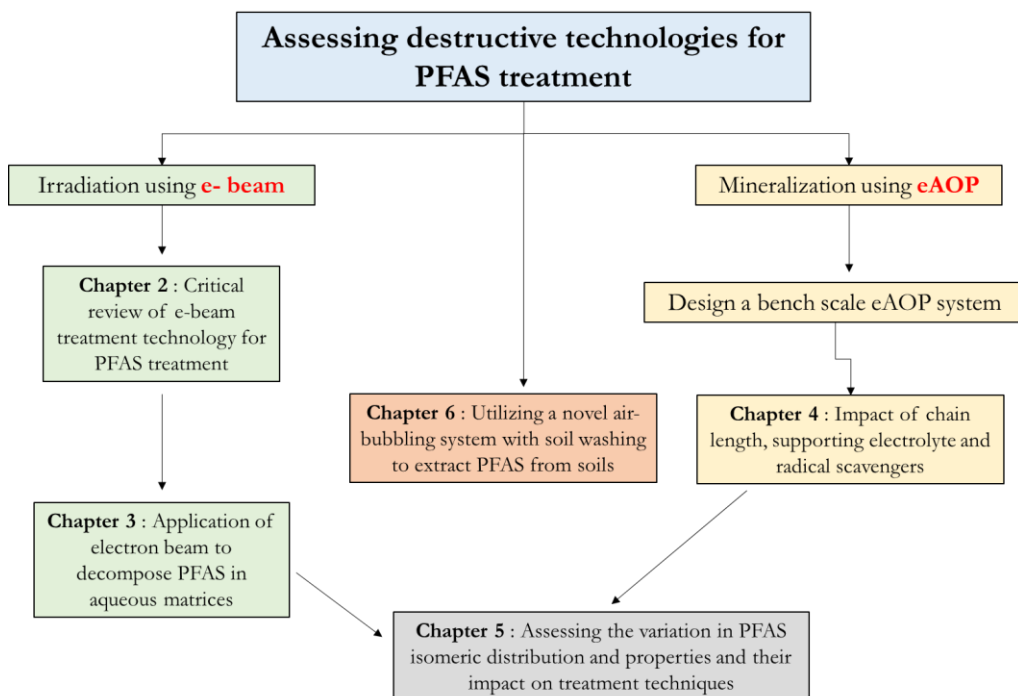
Figure 1.1 Overall PhD map and chapters for the PhD process.

CHAPTER 2

ENERGY EVALUATION OF ELECTRON BEAM TREATMENT OF PERFLUOROALKYL SUBSTANCES IN WATER: A CRITICAL REVIEW

2.1   Introduction

E-beam accelerators are multipurpose tools that can deliver beams with a large energy span and are used in applications that range from fundamental science to industrial processing including water treatment, environmental waste remediation, medical sterilization and materials processing. It has been historically reported[18-22] that radiation treatment is suitable to replace advanced oxidation technologies for both water purification and flue gases in environmental remediation processes.

E-beam treatment is unique in that it produces highly oxidizing and reducing species at the same time. There is no other advanced oxidation process that has the capability of generating as high an overall free radical yield per unit energy input as high energy e-beam treatment[23]. It removes organic impurities with radiation-initiated chemical reaction, removes colors by destroying double bonds and removes odors by opening the rings of aromatic compounds[24]. Similarly, this treatment is very effective in disinfection of microorganisms due to the ability to destroy DNA, causing chemical dissociation of organic matter as well as rupturing cell walls.[25]

Multiple efforts have shown the effectiveness of e-beam technology for full scale wastewater treatment. In the 1990s, the Miami Dade County municipal waste water treatment system demonstrated the capability of e-beams to effectively kill bacteria in sludge[25]. E-beam treatment has been explored by Samsung Heavy Industries (SHI) in

Korea since the 1970s. They established a pilot plant for industrial wastewater from dyes and petrochemical processes in Taegu Dyeing Industrial Complex.[26] Another example is the Deer Island Electron Research Facility in Boston, established in 1976 to disinfect municipal wastewater effluents and decompose organic pollutants using a 0.8 MeV ICT type accelerator[18]. Similarly, the Takasaki Radiation Research Establishment utilized a Cockcroft-Walton accelerator generating 2 MeV electrons to treat 10 mm thick water streams.[27]

Irradiation of aqueous solutions with e-beam results in the decomposition of water molecules and the creation of various reactive species (radiolysis products of water) with the greatest number of protons (H^+_{aq}), hydrated electrons (e^-_{aq}), and hydroxyl radicals (OH·) produced as compared to other products[28]. Amongst these, hydrated electrons have shown to be critical in the degradation of PFAS due to their high reactivity and high reduction potential of -2.9 eV[29, 30]. e^-_{aq} are primarily responsible for the cleavage of C-F bonds, resulting in degradation and defluorination of PFAS compounds, with rate constants[31-33] ranging from 1.7 x 10^7 to 7 x 10^7 $M^{-1}s^{-1}$. The production and abundance of e^-_{aq} can change with e-beam operating parameters such as dose, dose rate[28] as well as the water quality parameters such as pH, dissolved oxygen (DO), and other additives[34, 35], affecting the decomposition of PFAS.

To date, very few studies have investigated e-beam treatment for PFAS in aqueous solutions. One important challenge in the application and commercialization of e-beam technology for water treatment is the high energy demand for its operation. Hence, the present study provides a critical review of the recent literature from the perspective of energy consumption of e-beam technology to treat PFAS, while highlighting and

summarizing operational parameters that influences e-beam performance. In addition, this review further discusses opportunities to maximize the efficiency of e-beam technology to treat PFAS.

2.2 Research Questions

1. How to normalize data and compare different e-beam techniques for PFAS treatment?

2. What are the effects of operating parameters (dose, dose rate) on e-beam treatment of contaminants?

3. What are the effects of water quality parameters (pH, DO, radical scavengers) on e-beam treatment of PFAS and what are the conditions that have yielded the optimum performance?

4. How does e-beam compare with other destructive techniques utilized for PFAS treatment, from an energy perspective?

2.3 Influence of Key Operating Parameters of E-Beam to Treat PFAS

2.3.1 Dose Rate

In radiation processing, a commonly used measure is the radiation-chemical yield or the G value, defined as the number of molecules of a reactant produced or number of molecules of the contaminant degraded per 100 eV of absorbed energy.[28] Studies that looked at the degradation of PFAS using e-beam used dose rates ranging from 1.58 kGy s^{-1} to 20 [1 36-38]. Although the dose rate is an inherent parameter of the e-beam technology used, it can influence the overall degradation process by affecting the G-value. The radiolysis yield is mostly affected by high dose rates which increase the probability of interradical reactions in both the medium and the particle tracks. For instance, when oxygenated aqueous phenol degradation was investigated[39] by lowering the dose rate from 100 to 13 Gy h^{-1}, the overall

G-value for phenol increased from 2.6 to 250 molecules per 100 eV. A similar observation was made by Pikaev and Shubin[40] where high G-values (250-500) were reported for phenol with very low dose rates (0.1 Gy s^{-1}). In the case of phenol, the chain reactions causing the degradation process are mainly initiated by radicals such as OH· , HO$_2$·, and O$_2$·$^-$. While these reactive species are formed at higher concentrations at high dose rates, they are quickly consumed by reactions with other radical species that compete with the target contaminant.[28]

In the case of PFAS, the e_{aq}^- react with PFAS, leading to formation of unstable PFAS radicals[31, 37, 38], according to Reactions 1.1 and 1.2 shown for PFOA[31] and PFOS (Perfluorooctanesulfonic acid) below[34]. This has been agreed upon as the initiating step of PFAS degradation mechanism.

$e_{aq}^- + C_7F_{15}COO^- \rightarrow C_7F_{15}COO \cdot ^{2-}$ (Reaction 1.1 (k = 1.7 x 10^7 M^{-1}s^{-1} - 7 x 10^7 M^{-1}s^{-1}))

$e_{aq}^- + C_8F_{17}SO_3^- \rightarrow C_8F_{17}SO_3 \cdot ^{2-}$ (Reaction 1.2 (k = 0.56 x 10^7 M^{-1}s^{-1} - 7 x 10^7 M^{-1}s^{-1}))
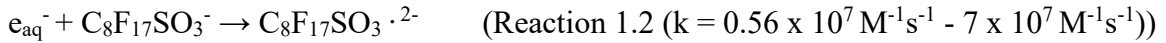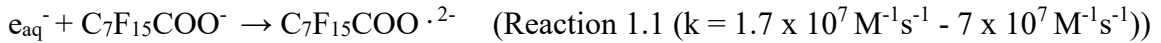
Similar to the observations made for phenol, the dose rate may influence the steady state concentration of hydrated electrons in the system available for reaction with PFAS. e_{aq}^- can be consumed by radical-radical combinations with other species such as OH·, H$^+$ and H· radicals amongst others[41] as well as with degradation products such as PFAS radicals, e_{aq}^- can also react with itself, although at a slower rate, as shown below.

$e_{aq}^- + OH· \rightarrow OH^-$ (Reaction 1.3 (k = 3 x 10^{10} M^{-1}s^{-1}))

$e_{aq}^- + H^+ \rightarrow H·$ (Reaction 1.4 (k = 2.2 x 10^{10} M^{-1}s^{-1}))

$e_{aq}^- + H· \rightarrow H_2 + OH^-$ (Reaction 1.5 (k = 2.5 x 10^{10} M^{-1}s^{-1}))

$e_{aq}^- + e_{aq}^- \rightarrow H_2 + OH^- + OH·$ (Reaction 1.6 (k = 5 x 10^9 M^{-1}s^{-1}))

In the presence of other e_{aq}^- scavenging pathways competing with PFAS degradation, an optimal dose rate, which generates both e_{aq}^- and other scavenging radicals (Reaction 3-6), should be carefully selected to improve both PFAS degradation and energy efficiency. Thus, similar to studies involving other contaminants[39, 40], a lower dose rate might be preferable for PFAS degradation as it will enhance the abundance of hydrated electrons needed to initiate the cleavage of C-F bonds by reducing the reactions 1.3-1.6 with competing molecules.

2.3.2   Penetration Depth

In addition to the total dose delivered, how the dose is distributed in the target is important. The Percent Depth Dose (PDD) curve (Figure 2.1) describes the variation in the delivered e-beam dose with sample depth. The useful range of electrons depends on the initial e-beam energy and the density of the irradiated material. Figure 2.1 shows PDD curves at 6, 9 and 12 MeV in water. The PDD curve increases to a certain depth, and the depth that receives the maximum dose (approximately 100 %) is referred to as Z_{max}. Z_{max} increases with an increase in accelerator energy (MeV) capacity.[42] Beyond this depth, the PDD curve drops rapidly. The intercept of the slope of this portion of the PDD with the x-axis is referred to as the "practical range," R_p[22]. This drop in the PDD curve is due to scattering and continuous energy loss by incident electrons.[42] Beyond the practical range are the electrons produced from bremsstrahlung photons that were produced by the initial electron beam, referred to as the "bremsstrahlung tail". The contribution of these electrons is less than 5% of the maximum dose.[49] Most of the available literature on PFAS uses a small sample volume[36, 38, 43] (15 to 100 mL) for treatment. As can be seen in Figure 2.1, if the depth of solution is controlled appropriately, the change in dose delivered throughout the

sample can be minimized. For any e-beam treatment process, the MeV and thus, the Z_{max} is a fixed quantity. Hence, the sample thickness for a batch or a continuous process should be chosen in such a way that the depth of the solution undergoing treatment utilizes the useful range of electrons.
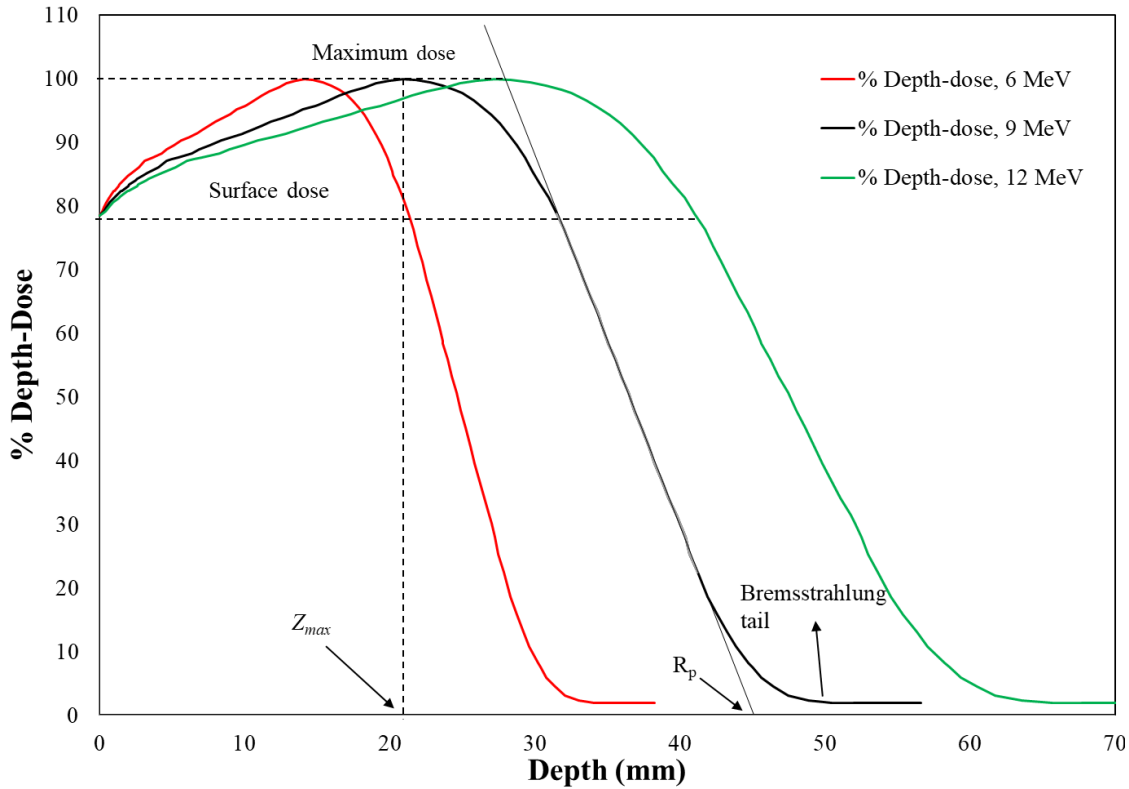
Figure 2.1 Depth-dose profile of electron beam in water.

2.3.3. G-Value and Electrical Energy Per Order as Performance Parameters

Previous studies have utilized e-beam as a potential treatment method to degrade a variety of contaminants in drinking water, groundwater, and wastewater.[38, 44, 45] However, the vast variation in the sampling and operating parameters makes it difficult to compare results reported in different e-beam studies. Normalization of the reported data is needed to compare and assess trends in the treatment of contaminants using e-beam. G-value is an inherent function of dose rate and e-beam accelerator energy, and hence is not an ideal

parameter to compare the performance of different e-beam accelerators utilized to degrade PFAS in different studies. Electrical energy per order (EE/O) is a quantity defined as the energy required for one log removal (90% removal) of a contaminant in a unit volume of water. This parameter is typically used to evaluate the energy efficiency of advanced oxidation processes (AOP) to degrade a target contaminant[46]. EE/O is calculated for AOP systems using the following equation[3, 46]:

$$
\text{EE/O (kWh m}^{-3}\text{ order }^{-1}) = \frac{P*t*1000}{V*60*\log(\frac{[C]in}{[C]out})} \tag{1.1}
$$

Where, P is the power (kW), t is the time (min), V is the sample volume (L), C_{in} is the influent concentration and C_{out} is the effluent concentration of the target contaminant. This equation can be modified for e-beam treatment of 'y' mL water sample receiving a dose of 'x' kGy by using unit conversion as follows:

$$
\text{EE/O (kWh m}^{-3}\text{ order }^{-1}) = \frac{x\ kGy*\left(\frac{kJ}{kGy*kg}*\frac{kg}{1000\ ml}*y\ ml\right)*\frac{kWh}{3600\ kJ}}{y\ ml*\frac{1\ L}{1000\ ml}*\frac{1\ cu.m}{1000\ L}*\log(\frac{[C]in}{[C]out})} \tag{1.2}
$$

$$
\text{EE/O (kWh m}^{-3}\text{ order }^{-1}) \text{ for e-beam} = \frac{Dose\ (kGy)}{3.6*\log(\frac{[C]in}{[C]out})} \tag{1.3}
$$

Where *Dose* denotes the dose delivered to the water sample in unit of kGy (kJ-kg^{-1} of water). Since, EE/O is based on measurable variables and can be confirmed by measuring contaminant log reduction and dose applied, this serves as a 'normalized'

parameter for comparing data reported in different e-beam studies. This allows for researchers and engineers to compare the performance of e-beam technology with other destructive technologies for PFAS treatment such as electrochemical oxidation, plasma technology, sonolysis amongst others.[3]

Figure 2.2 compares G-value and EE/O for different e-beam doses as a function of initial PFAS concentration calculated from previous studies. It can be seen that although G-values show a linear trend for each initial concentration set, the trends are different and influenced largely by the initial PFAS concentration. In comparison, EE/O can better normalize the effect of initial concentration and other operating parameters as seen in Figure 2.2b. Hence, in the present study, we utilize dose derived EE/O values to critically review the performance and the impacts of various operating parameters on the treatment of PFAS utilizing e-beam.
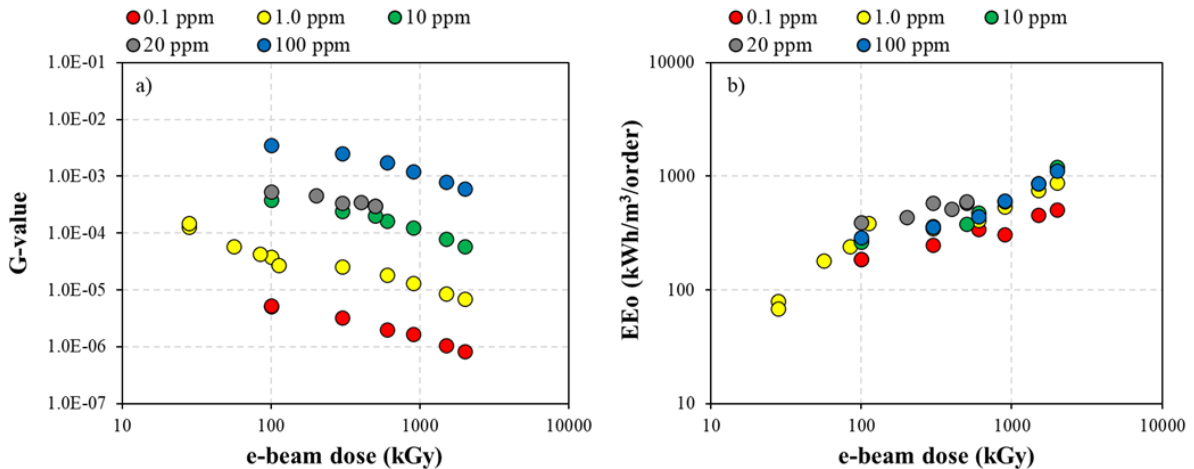
Figure 2.2 Calculated (a) G-values and (b) EE/O for a range of initial PFOS concentrations in DI water at varying e-beam doses. Data presented here were without air-purging and additives (minimal sample modification). Data source.[31, 34, 35, 37, 38]

A comparison of EE/O for the treatment of different contaminants by e-beam is shown in Figure 2.3. In the case of halogenated methanes, as the number of halogens on

the carbon atom increases, the EE/O value also proportionally increases. This is due to the greater stability of C-Cl bond as compared to C-Br bond. The bond energies of C-F, C-Cl, and C-Br are 485, 339, and 276 kJ mol^{-1}, respectively.[47] This explains why chloroform requires more energy to degrade and has a higher EE/O as compared to bromoform (CHCl$_3$ vs CHBr$_3$). Based on the bond energies, if the Cl atoms are replaced by F atoms, the EE/O values would increase as the C-F bond is harder to breakdown than the C-Cl and the C-Br bonds. PFOA and PFOS have 15 and 17 C-F bonds, respectively, imparting exceptionally high stability to these compounds. As a result, calculated EE/O values for PFAS (range: 187-1121 kWh m^{-3} order^{-1}) are several orders of magnitude higher than in comparison to many other contaminants, requiring more energy to breakdown the multiple C-F bonds present in PFAS.
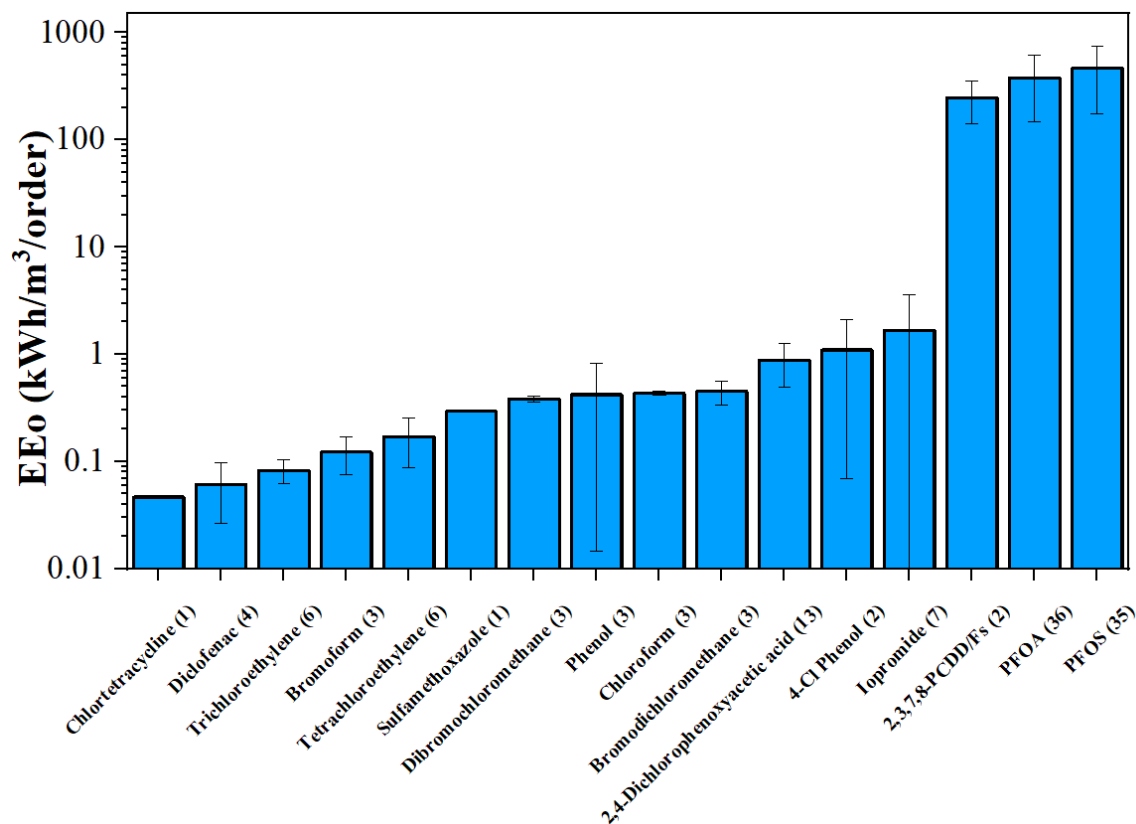
Figure 2.3 Calculated EE/O values for e-beam treatment of different contaminants at neutral pH [28, 35, 37, 38, 41, 44, 48-51]. Number within parenthesis represents the number of data points used to calculate EE/O and error bars represent standard deviation values.

2.4   Degradation of PFAS in DI Water Using E-Beam

There are very limited number of studies (n = 6) in literature that focus on the degradation and defluorination of PFAS using e-beam[31, 34, 35, 37, 38, 52], which is comparatively lower than the number of articles published on other destructive techniques such as electrochemical oxidation (n = 22), advanced reduction processes (n = 12), photolytic/photochemical oxidation (n = 20) and plasma technology (n = 12) based on Web of Science search results as of August 2020. Most of the e-beam (n = 5) studies used deionized (DI) water spiked with PFAS for treatment whereas some have used synthetic wastewater.[52] These studies

have focused on the degradation of solely either PFOA[52] or PFOS.[35, 38] A few of them have additionally compared the difference in decomposition of PFOA vs PFOS.[31, 36, 37] Owing to the high stability of PFAS, previous studies have used a wide range of e-beam doses (10 kGy to 2000 kGy) to test the degradation of PFAS.[31, 34, 35, 37, 38, 52] The initial PFAS concentrations tested ranged from 0.1 parts per million (ppm) to 100 ppm, which are several orders of magnitude higher than environmentally relevant levels. Different sample containers such as heavy glass-walled reactor[38], Pyrex glass petri dishes[52] and polyethylene bags[31, 37] were used for sample irradiation with the sample volumes ranging from 10 mL to 100 mL. In most cases, samples were irradiated in a batch treatment and a conveyor belt was used in some cases to move the sample rack for irradiation.[36]

Previous studies have reported an increase in the percent degradation of PFAS with an increase in applied e-beam dose.[34-36, 38, 52] Figure 2.4a summarizes the PFAS degradation and calculated EE/O as function of e-beam dose using the data reported in a previous study for PFOS treatment in DI water.[38] The increase in percent degradation of PFOS with e-beam dose can be associated with the generation of relatively a greater number of reactive species (e_{aq}^-) formed from water radiolysis at higher doses and successive reaction with PFOS [28, 31, 38, 39]. It can also be noted that the amount of PFOS degraded, beyond a particular dose, is eventually levelled off. However, the calculated EE/O keeps increasing, as expected, with the dose applied from 0 to 2000 kGy (Figure 2.4a). This observation suggests that at a given treatment condition (initial PFAS concentration, dose rate, and water matrix), there exists a 'threshold dose' beyond which there is no improvement in the PFAS degradation efficiency. Any further increase in the delivered dose beyond this threshold dose is not targeted on the PFAS of interest, and hence the efficiency of the

treatment process is reduced, as indicated by the increasing EE/O values beyond this point (~600 kGy in Figure 2.4a). Although there is an increase in the cumulative generation of e_{aq}^- at higher doses, the reason that threshold dose exists remains to be explored. It might be associated with more frequent radical-radical recombination (Reactions 3-6) at a higher cumulative dose, thus scavenging the available e_{aq}^-.[35] Another likely explanation is that byproducts derived from the target PFAS compound can accumulate in the solution over time and might preferentially react with e_{aq}^-, reducing the abundance of e_{aq}^- in the solution to react with the target PFAS.

Previous e-beam studies have also reported that the amount of PFOS degradation was inversely related to its initial concentration.[35, 37] When the initial concentration varied from 0.1 to 100 mg L^{-1} at a constant dose, the number of molecules of PFOS degraded also increased linearly (Figure 2.4b). This trend was observed for both 300 kGy and 2000 kGy. At a higher initial concentration, the relative abundance of PFAS molecules increases compared to other reactive species (OH·, H$^+$ and H· radicals) from water radiolysis. As a result, the competition from reactions 3-6 is minimized at higher initial PFAS concentrations.

It can also be noted in Figure 2.4b, that EE/O values are much lower for 300 kGy dose compared to 2000 kGy. This observation reiterates the concept of threshold dose: where 300 kGy may represent a dose below the threshold dose, while 2000 kGy may represent a dose much higher than the threshold dose for this system. Another important observation at 300 kGy dose, is that the calculated EE/O values are similar (average EE/O value = 329 ± 53 kWh m^{-3} order $^{-1}$) for treating 0.1 to 100 ppm of PFOS, *i.e.*, the same amount of energy was required to remove 90% of PFOS per unit volume of water.
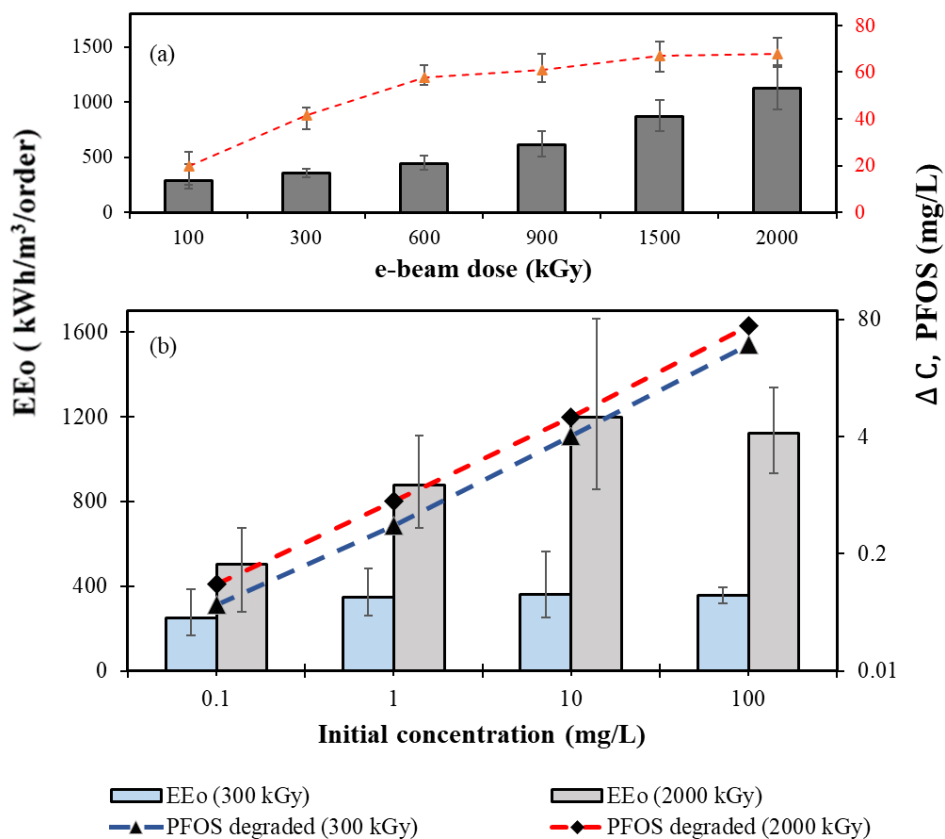
Figure 2.4 a) Variation of calculated EE/O and ΔC, PFOS at initial concentration of 100 mg L^{-1} with e-beam dose[35, 38] at the same dose rate (1.58 kGy s^{-1}) b) Variation of calculated EE/O and Δ C, PFOS with initial concentration at 300 kGy and 2000 kGy and at the same dose rate (1.58 kGy s^{-1}). ΔC, PFOS = PFOS $_{initial}$ – PFOS $_{remaining}$. Error bars represent standard deviation.

In other words, approximately 42, 4.2, and 0.41 mg L^{-1} of PFOS, representing 90% removal, can be degraded for a solution containing 100, 10, and 1 mg L^{-1} of initial PFOS concentration, respectively, at the same e-beam dose of 300 kGy. Hence, the energy efficiency of the treatment process can be improved by treating contaminated waters with high concentrations of PFAS. Combining e-beam technology with a pre-concentration step for treating natural waters (typically exhibiting ng L^{-1} of initial PFAS) can help to improve the overall efficiency of the treatment process. These perspectives, however, are based on limited number of papers that have observed the degradation of PFAS, both with e-beam

dose and concentration dependence. More research into this area will better elucidate the concept of threshold dose and variation in PFAS degradation with initial concentration.

2.5   Influence Of Water Quality and Chemical Additives on the Treatment of PFAS Using E-Beam

As observed in Figure 2.3, the EE/O values are higher for PFAS than for other contaminants. In order to improve the efficiency of e-beam treatment process, researchers have focused on altering the water chemistry with additives. These chemical additives mainly focus on promoting the abundance of e_{aq}^-, thus improving the degradation and defluorination efficiency.[31, 34, 35, 38, 52]

Two of the most commonly tested water quality parameters in e-beam studies are pH and DO of the solution. A study done by Ma et al.[37] analyzed the degradation of PFOS for varying sample pH at a constant dose of 500 kGy.[37] With an increase in solution pH, the calculated EE/O values show a linear decrease and are the lowest at highly alkaline pH conditions (Figure 2.5a). A similar observation was also made by Trojanowicz et al.[34], where the degradation efficiency of PFOS was shown to increase by 30 % when the solution pH was changed from pH 7 to pH 12. One of the proposed explanations by Trojanowicz et al[34] was the reaction of OH· with OH⁻ at high pH, according to Reaction 1.7, forming oxide radical ion. This ion can further react with dissolved oxygen in the solution, according to Reaction 1.8, forming an ozonide reaction ion.[34]
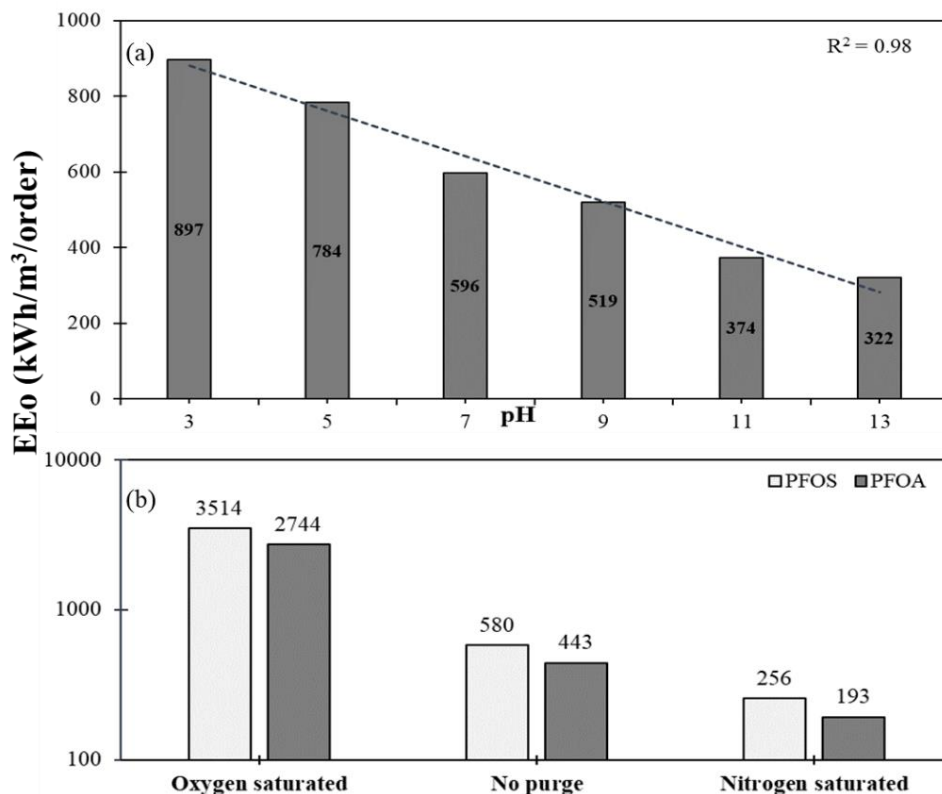
Figure 2.5 a) Variation of calculated EE/O as a function of initial solution pH for PFOS at 500 kGy and constant dose rate (Data source: Ma et al.[37]); b) Variations of calculated EE/O with DO conditions for PFOS (initial concentration of 20 ppm) at 500 kGy dose. Note: No purge implies no gas purging to remove DO (ambient levels of DO: 8-10 mg O_2 L^{-1}), O_2 saturated assumes oversaturated DO and N_2 saturated assumes very low DO. (Source: Ma et al. [37]).

$$OH \cdot + OH^- \rightarrow O \cdot^- + H_2O \qquad \text{(Reaction 1.7 (k = 1.2 x } 10^{10}\,M^{-1}s^{-1}))$$

$$O \cdot^- + O_2 \rightarrow O_3 \cdot^- \qquad \text{(Reaction 1.8 (k = 3 x } 10^9\,M^{-1}s^{-1}))$$

Thus, at high pH conditions, abundance of e_{aq}^- is increased due to the scavenging of competing species such as $OH \cdot$ and O_2, that could otherwise react with e_{aq}^-, and this results in an increase in the degradation efficiency. At low pH, the abundant H^+ ions scavenge e_{aq}^- according to Reaction 4, forming hydrogen radicals.[34, 37] As the pH increases, the abundance of H^+ ions in the system is reduced, resulting in an increased availability of e_{aq}^- to react with and decompose PFAS. Another mechanism proposed that increases the

overall abundance of e_{aq}^- is the reaction of hydrogen radicals, formed as a result of water radiolysis, with OH$^-$ ions[37], as per Reaction 1.9.

$$H\cdot + OH^- \rightarrow e_{aq}^- + H_2O \hspace{2cm} \text{(Reaction 1.9 (k = 2.1 x } 10^7 \text{ M}^{-1}\text{s}^{-1}\text{))}$$

High pH favors this reaction toward more hydrated electron production. However, the rate constant for this reaction is nearly three orders of magnitude lower than the reactions involving the consumption of e_{aq}^-, indicating that this may not be as significant as Reactions 1.3 -1.6 and 1.7, 1.8.

The levels of DO present in the samples can also affect the overall degradation process as seen in Figure 2.5b. The EE/O values decrease with a reduction in DO levels in the samples. This can be attributed to the scavenging of e_{aq}^- by oxygen molecules at high DO values, according to Reaction 1.10:

$$e_{aq}^- + O_2 \rightarrow O_2^- \hspace{2cm} \text{(Reaction 1.10 (k = 1.9 x } 10^{10} \text{ M}^{-1}\text{s}^{-1}\text{))}$$

Multiple studies have thus reported an increase in the overall degradation and defluorination efficiency in very low DO samples or in nitrogen or argon saturated samples[31, 36, 37]. The observed improvement in the degradation process is simply attributed to the increase in abundance of available e_{aq}^-. In another study[53], degradation efficiency of PFOS was found to be less than 15 % when the aqueous sample was saturated with N_2O[34], because the presence of N_2O improves the abundance of OH$\cdot$ by scavenging e_{aq}^-, according to Reaction 1.11. This results further confirm that e_{aq}^- are primarily responsible for initiating PFAS degradation.

$$e_{aq}^- + N_2O + H_2O \rightarrow N_2 + OH\cdot + OH^- \hspace{1cm} \text{(Reaction 1.11 (k = 9.1 x } 10^9 \text{ M}^{-1}\text{s}^{-1}\text{))}$$

Figure 2.6a summarizes the effect of a combination of additives[37] on PFAS degradation efficiency and calculated EE/O values. It can be inferred that a combination of

low DO conditions and high pH yield the best degradation efficiency, based on previous studies.[36, 38] Interestingly, even with the addition of t-butanol, an $OH^{\cdot}$ radical scavenger, the EE/O values for both PFAS and the degradation efficiencies remain fairly constant as compared to without t-butanol addition. A justification for possibly adding t-butanol could be given with the help of rate constants of PFAS reactions with e_{aq}^- by a study published by Trojanowicz et al. [34] Compared to other techniques, the pseudo-first order rate constant (k = 0.183 s^{-1}) for PFOS degradation with e_{aq}^-, in the presence of t-butanol, is an order of magnitude higher than other conditions reported previously.[34] Although the authors acknowledge that a detailed discussion was not possible due to the complexity of the reactions, the rate constant for the reaction of e_{aq}^- with PFAS increased from 0.56 x 10 ^{7} $M^{-1}s^{-1}$ to 3.3 x 10 ^{7} $M^{-1}s^{-1}$ in presence of t-butanol.[28] Thus, even though the EE/O values do not significantly increase, the 489 % increase in the rate might justify the use of hydroxyl radical scavengers to achieve faster degradation. Effects of other additives such as formate ions, sodium thiosulfate, 2-propanol, fulvic acid, alkalinity (as $CaCO_3$) on the degradation process have also been assessed.[31, 34-36, 38, 52] All these additions were tested in an attempt to scavenge competing radicals to improve the reaction of PFAS with e_{aq}^-. This resulted in more e_{aq}^- available to react with and degrade PFAS. As a result, the use of these additives improved the overall degradation efficiency and also increased the rate constant of PFAS degradation with e_{aq}^-.
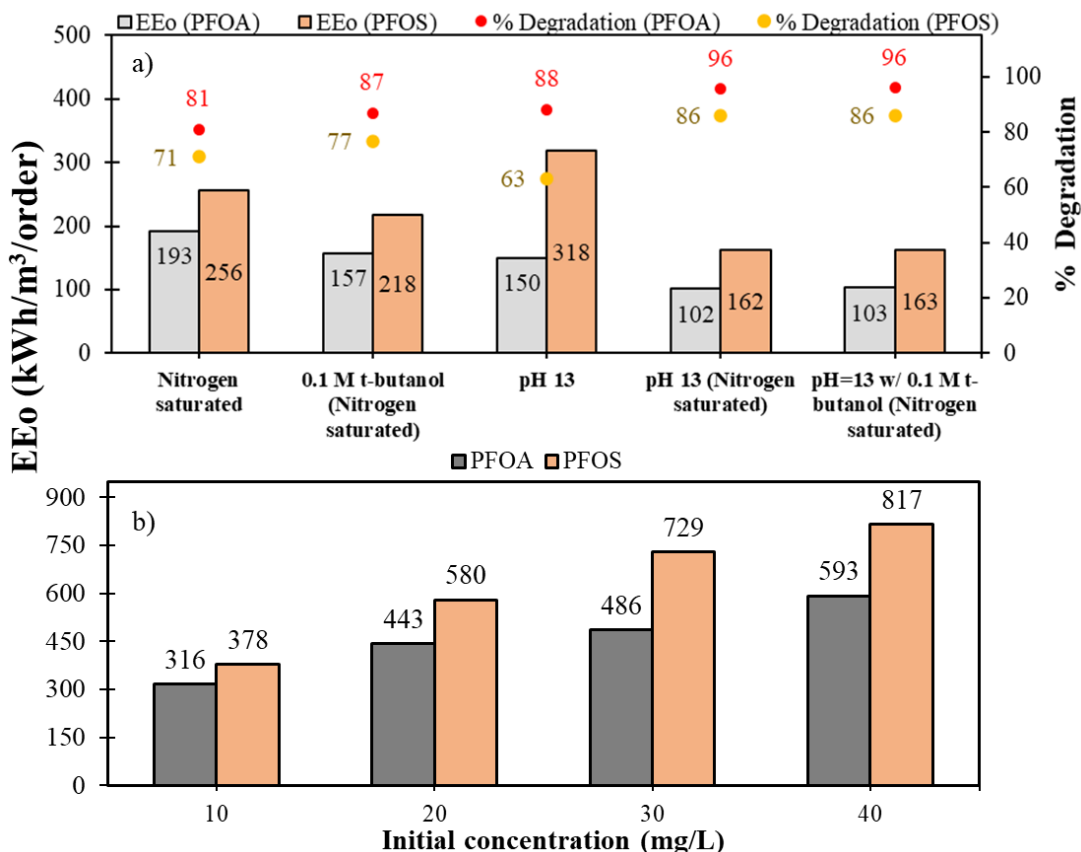
Figure 2.6 a) Variation of calculated EE/O and percent degradation of PFOA and PFOS with addition of a combination of additives at a constant dose rate and dose of 500 kGy. b) Comparison of calculated EE/O values for PFOA and PFOS at 500 kGy with varying initial concentrations[37] at a constant dose rate.
Data extracted from Ma et al[37].

Interestingly, a few studies have reported an improvement in overall degradation of PFAS with e-beam by addition of nitrate, even though they are known scavenger of e_{aq}^- [31, 37, 52] according to Reaction 1.12. [31]

$$NO_3^- + e_{aq}^- \rightarrow NO_3^{2-} \cdot \qquad \textbf{(Reaction 1.12 (k = 9.7 \times 10^9 \ M^{-1}s^{-1}))}$$

$$NO_3^{2-} \cdot + H_2O \rightarrow NO_2 \cdot + 2OH^- \qquad \textbf{(Reaction 1.13 (k = 5.5 \times 10^4 \ M^{-1}s^{-1}))}$$
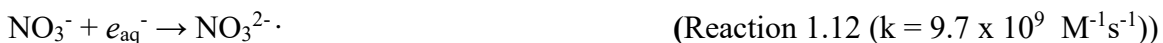
In spite of the scavenging action of nitrate, a study reported a 122% increase in degradation efficiency of PFOA when 10 mg L^{-1} of nitrate was used.[52] This was suspected to be due to the production of nitrate radicals (NO$_3^{2-}$ · : redox potential of -1.1 eV) and

nitrogen dioxide radicals ($NO_2 \cdot$: redox potential of 1.04 eV[31]) formed during irradiation and that these radicals reacted with PFOA to improve degradation efficiency.[52] However, this observation is not supported by the fact that the synthetic water used to prepare the samples in the study contained other chemicals such as 50 mg-$CaCO_3$ L^{-1} alkalinity, 50 µg-C L^{-1} DOC from fulvic acid, and 10 mg L^{-1} of additional background nitrate.[52] Also, this is unlikely as the formation of nitrogen dioxide radicals is a very slow reaction as compared to Reaction 13 and Reactions 3-6. When the effects of nitrate were observed on the photolytic decomposition of PFOS in the presence of sulfite[54], 30 mg L^{-1} nitrate did not affect the decomposition, and at even higher concentration of 0.6 g L^{-1}, the overall decomposition was suppressed. This was attributed to the scavenging of hydrated electrons by Reaction 1.12. Trojanowicz et al[31]. reported an increase in decomposition yield at 10 mg L^{-1} of nitrate for gamma and e-beam irradiation.[31] Some of the explanations proposed for this phenomenon are the slowing down of certain radical-radical combination reactions (Reactions 1.3-1.6), increasing the overall abundance of hydrated electrons, and the possible generation of a radical with strong reductive properties.[31] However, a clear explanation to the observed increase in the presence of nitrate ions is still not present and this topic needs further investigation.

2.6   Effect of PFAS Structure and Functional Groups

Although hydrated electrons are responsible for the reactions involving PFAS degradation, the overall degradation efficiency can change not only with the chain length but also with the functional group.[30] In previous studies that compared degradation of C_8 PFAS (PFOA and PFOS), it was generally observed that under similar conditions, PFOS had a lower

degradation efficiency than PFOA.[37] This has been attributed to the presence of sulfonate terminal group, which is more difficult to oxidize than the carboxylic acid group.[37] Bentel et al[30]. theorized that for perfluorosulfonic acids (PFSAs), in general, the degradation is highly dependent on the chain length[30]. It is theorized that the structure of PFSAs, in contrast to perfluorocarboxylic acid (PFCAs), limits the process of release of fluoride ions, limiting the degradation of the PFSAs. The terminal C-F bond energies in PFCAs (α position, adjacent to functional group) are slightly lower than the bond energies in PFSAs, leading to relatively higher reactivity of corresponding PFCAs than PFSAs.[30] Figure 2.6b shows the difference in EE/O values for PFOA and PFOS at a constant dose of 500 kGy and with increasing initial concentration.[37] The EE/O values show an upward trend as expected with an increase in initial concentration; however, PFOS showed more resistance to degradation compared to PFOA. PFOS showed 20 – 50 % higher EE/O values compared to PFOA for the same initial concentration ranging from 10 ppm to 40 ppm.

Interestingly, one study reported lower PFOA degradation than PFOS under similar conditions.[34] At a high pH (12 – 12.5) and at similar doses (26 kGy for PFOA and 28 kGy for PFOS), PFOA and PFOS showed 8% and 39% degradation, respectively. At neutral (pH 7) and near-neutral pH conditions (pH 6.7), PFOA showed almost no degradation at 26 kGy whereas PFOS showed 55 % degradation in the presence of t-butanol addition and argon purging.[31, 34] PFOS exists in the natural environment in linear (L-PFOS) as well as branched (br-PFOS) forms. The variation in the distribution of the branched isomers such as 1-PFOS, 6-PFOS, 3,5-PFOS, 4,5-PFOS and linear isomers (br-PFOS vs L-PFOS) is large.[34, 55] A study from Sweden[55, 56] reported the percent linear isomers of PFOS in surface waters to be 80.5 % and 92.2%, whereas the branched isomers accounted for 19.5% and

7.8% in two different samples. In river waters in Norway[55, 57], linear isomers accounted for 24.6-59.5 % of the total PFOS whereas branched isomers accounted for 43.5-75.4%. In previous studies that investigated degradation of PFOS by photolytic methods[34, 58], L-PFOS showed lower reaction rate constants (0.098 h^{-1}) than br-PFOS (0.115-0.127 h^{-1}). Although it is hypothesized that the difference in rate constants for reductive environments (such as e-beam) can vary with water chemistry, branched isomers are theorized to degrade much quicker.[30, 34] This coupled variance in distribution of L-PFOS vs br-PFOS isomers can lead to contrasting results when comparing the degradation of PFOA and PFOS, especially if the isomeric contribution to the overall degradation is unaccounted for.

2.7   Kinetic Scheme of PFAS Degradation

As observed in Figure 2.4a, PFAS degradation efficiency initially increase with an increase in delivered dose, but then levels-off after a certain threshold dose. From the energy efficiency perspective, e-beam operators will need to maintain their delivered dose less than or equal to this threshold dose (for a fixed initial PFAS concentration and water matrix) to maximize PFAS degradation efficiency. Here we propose a PFAS radiolysis degradation scheme to better understand the dependence of PFAS degradation on e-beam dose. Upon e-beam irradiation, the major reactive radical species generated from water radiolysis are $OH\cdot$, e_{aq}^- and $H\cdot$ following the reaction below in units of μmol J^{-1} [59] :

$$H_2O \rightarrow [0.28]OH\cdot + [0.27]\ e_{aq}^- + [0.06]H\cdot + [0.07]H_2O_2 + [0.27]H_3O^+ + [0.05]H_2$$
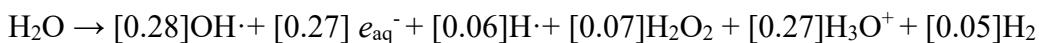
(Reaction 1.14)

Since e_{aq}^- are known to initiate the degradation of PFAS, the PFAS reaction is in competition with other oxidants for reducing the e_{aq}^- radical. The possible oxidants in the

PFAS water system include system oxidant, such as dissolved oxygen (DO), and e-beam generated oxidants, such as e_{aq}^- scavenging reactive species (RS) like e_{aq}^- (recombination), H$^+$, H·, OH·, and PFAS degradation products introduced to the water system during irradiation. Possible scavenging reactions of e_{aq}^- with generated RS in water system follow Reactions 3-6 and reactions with degradation products generated from parent compound. From these reactions, it can be inferred that the degraded PFAS products, DO, and RS are three major sinks of e_{aq}^-, and hence consumption rate of e_{aq}^- can be expressed as shown below:

$$\frac{d[e_{aq}^-]}{d_t} = -[e_{aq}^-] \times (k_{O_2}[O_2] + k_{RS} \times [R_{RS} \times \Delta t] + k_p[PFAS]_0) \qquad (1.4)$$

Where k_p, k_{O_2} and k_{RS} are second order rate constants for e_{aq}^- reacting with PFAS, DO, and RS, respectively (M^{-1}s^{-1}); $[O_2]$ and $[PFAS]_0$ are initial concentration in mM of DO and PFAS, respectively; R$_{RS}$ is the production rate (mM s^{-1}) of e_{aq}^- scavenging reactive species (RS), and $[R_{RS} \times \Delta t]$ is the concentration of generated RS at irradiation time t. Δt is total EB irradiation time (s). The formation of e_{aq}^- during e-beam irradiation can be expressed as:

$$\frac{d[e_{aq}^-]}{d_t} = R_{Dose} \times f_{e_{aq}^-} \qquad (1.5)$$

where, R_{dose} is e-beam irradiation dose rate (kGy s^{-1}); $[f_{e_{aq}-}] = 0.27$ µmol J^{-1} is the G

fraction of e_{aq}^- produced upon e-beam irradiation in the absence of an external catalyst. The

overall reaction rate of e_{aq}^- in the system can then be expressed as follows:

$$\frac{d[e_{aq}^-]}{d_t} = R_{Dose} \times f_{\overline{e_{aq}}} - [e_{aq}^-] \times (k_{O_2}[O_2] + k_{RS} \times [R_{RS} \times \Delta t] + k_p[PFAS]_0) \quad (1.6)$$

At steady state approximation, $\frac{d[e_{aq}^-]}{d_t} = 0$,

$$[e_{aq}^-]_{ss} = \frac{R_{Dose} \times [f_{e_{aq}-}]}{k_{O_2}[O_2] + k_{RS} \times [R_{RS} \times \Delta t] + k_p[PFAS]_0} \quad (1.7)$$

Where, $[e_{aq}^-]_{ss}$ represents the steady state concentration of e_{aq}^- in the solution.

PFAS degradation rate can be expressed as follows:

$$R_{PFAS} = \frac{dC}{dt} = -k_p[e_{aq}^-]_{ss}[PFAS]_0 \quad (1.8)$$

Where, R_{PFAS} is PFAS degradation rate, dC/dt is the PFAS concentration change (mM) over time (t), and $[PFAS]_0$ is the initial PFAS concentration in solution. Substituting for $[e_{aq}^-]_{ss}$ from Equation 1.7, the rate of PFAS degradation becomes:

$$\frac{dC}{dt} = -\frac{k_p[PFAS]_0 R_{Dose} \times [f_{e_{aq}^-}]}{k_{O_2}[O_2] + k_{RS} \times [R_{RS} \times \Delta t] + k_p[PFAS]_0} \tag{1.9}$$

At an initial PFAS concentration $[PFAS]_0$, total PFAS degradation (ΔC) is dependent on dose rate (R_{Dose}) and irradiation time (Δt) as follows:

$$\Delta C = -\frac{k_p[PFAS]_0 \times R_{Dose} \times f_{e_{aq}^-} \times \Delta t}{k_{O_2}[O_2] + k_{RS} \times [R_{RS} \times \Delta t] + k_p[PFAS]_0} \tag{1.10}$$

Equation (1.10) represents the kinetic model that explains the dependence of PFAS degradation on e-beam operating parameters and water quality. This model was fitted with PFOS degradation data from Kim et al.[38], with the input parameters as: $k_{O_2} = 1.9 \times 10^{10}$ M^{-1}s^{-1}, $[O_2] = 0.25$ mM at ambient conditions at 25 °C, $f_{e_{aq}^-} = 0.27$ μmol J^{-1},[33] and $R_{Dose} = 1.58$ kGy s^{-1} .The value of $k_{PFOS} = 5.1 \times 10^7$ M^{-1}s^{-1} employed was obtained from Szajdzjnska-Pietek et al.[33]. The e_{aq}^- scavenging RS could be a combination of system generated oxidants and/or competing species in solution including the byproducts of PFAS

degradation (*e.g.*, short-chain PFAS derived from long-chain PFAS degradation)[35, 37], and the rate constant (k_{RS}) and production rate of RS (R_{RS}) would vary depending on the reaction system and the water matrix. With the above model input parameters and other variables from Kim et. al.[38], the combined value of the term $k_{RS} \times R_{RS}$ for the DI water matrix was calculated to be $2.65 \times 10^4\,\text{s}^{-2}$ ($R^2 = 0.993$; Figure 2.7a).

To validate this kinetic model, we simulated the PFOA and PFOS degradation with increasing irradiation dose and compared the model output with data sets reported for DI water in previous studies (Figure 2.7 b-d). Simulation input parameters were kept the same from the above model fitting, and we made the assumption that the PFAS - e_{aq}^- rate constant (k_p) is similar for both PFOS and PFOA ($5.1 \times 10^7\ \text{M}^{-1}\text{s}^{-1}$). If R_{Dose} was not reported in the study, we combined the term R_{Dose} and Δt to represent the reported e-beam dose (kGy). The previously fitted value of $k_{RS} \times R_{RS} = 2.65 \times 10^4\,\text{s}^{-2}$ was employed under the assumption that the RS would be similar for the DI water matrix. Our simulation output matched the reported data well from the other three studies (RMSE = 0.0001-0.0039), suggesting that the RS were similar for all these systems in DI water matrix. The kinetic model was able to simulate the saturation trend for PFAS degradation with increasing e-beam dose as observed in Figure 2.7.
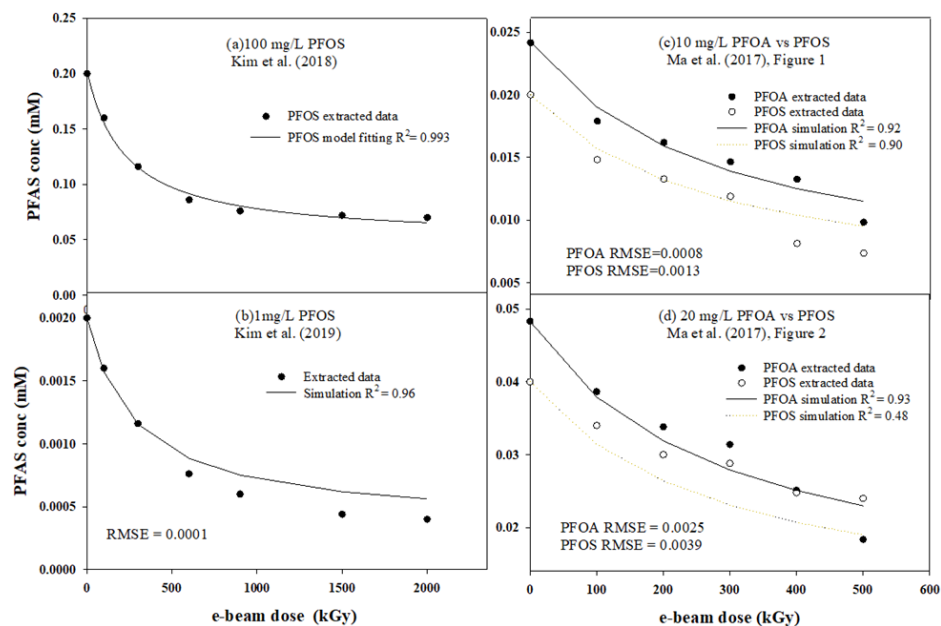
Figure 2.7 Model fitting with reported experimental data from Kim et al.[38] (a) and simulation comparison to reported experimental data[35, 37] (b-d) on PFOA and PFOS concentration (mM) as a function of irradiation dose (kGy) using Equation 10 at fixed DO concentration (0.25 mM) and dose rate (1.58 kGy s^{-1}).

The kinetic model developed here also helps to explain the effects of DO and pH on the degradation of PFAS. Based on Equation 10, we can see that PFAS degradation is inversely related to DO concentration, and hence high DO concentration in the solution will reduce the PFAS degradation efficiency as explained in Figure 2.5b. At ambient conditions, where DO concentration is 0.25 mM, and k_{O2} (1.9×10^{10} M^{-1}s^{-1}) is three orders of magnitude higher than k_P (5.1×10^7 M^{-1}s^{-1}), we have $k_{O_2}[O_2] \gg k_p[PFAS]_0$. Equation 10 can then be expressed as shown in Equation 11 below, and a linear relation between the amount of PFAS degraded (ΔC) and initial PFAS concentration employed ($[PFAS]_0$) would be expected, as observed in Figure 2.4b.

34

$$\Delta C = -\frac{k_p[PFAS]_0 R_{Dose} \times f_{e_{aq}^-} \times \Delta t}{k_{O_2}[O_2] + k_{RS} \times [R_{RS} \times \Delta t]} \tag{1.11}$$

As the solution pH increases, it is very likely that aqueous hydrogen radicals will be converted to the hydrated electron as shown in Reaction 1.15 below, increasing the $[e_{aq}^-]_{ss}$ in the solution[60]. This can help to explain the improved degradation efficiency of PFAS at alkaline conditions as shown in Figure 2.5a.

$$OH^- + H\cdot \rightarrow e_{aq}^- + H_2O \qquad (\text{Reaction 1.15 } (k = 2.2 \times 10^7 \text{ M}^{-1}\text{s}^{-1}))$$

We expect that the developed kinetic model (Equation 1.11) can help researchers to identify the threshold dose and the impacts of water quality parameters for optimizing the treatment of PFAS using e-beam.

Table 2.1 General Trends for Degradation Efficiency of PFAS Using E-Beam

Influencing parameter	Ideal parameter trend for improving degradation efficiency
E-beam dose	↑
Dissolved oxygen	↓
pH	↑
Hydroxyl radical scavengers[*]	↑

* formate ions, t-butanol, 2-propanol

2.8   Feasibility and Limitations of E-Beam Technology for Water Treatment

Other destructive techniques employed for the treatment of PFAS include photochemical, advanced reduction processes (ARPs), electrochemical oxidation, sonolysis, and high-energy plasma technology. These technologies have been reviewed in detail summarizing

their effectiveness for treating PFAS.[2, 3, 61] Figure 2.8 summarizes the range of EE/O values reported for these destructive techniques and are compared with the calculated EE/O values for e-beam treatment.[3, 61] E-beam, when combined with the ideal water quality parameters (*e.g.*, DO, pH) and additive concentrations gives a range of EE/O values that are comparable and, in many cases, much lower than other destructive techniques such as activated persulfate, ultrasound as well as electrochemical oxidation. This suggests that e-beam is a feasible technology from the point of energy consumption to decompose PFAS. The EE/O values for e-beam can be enhanced by changing the initial PFAS concentration. Based on our discussion of Figure 2.4, it might be more favorable to use high initial concentrations of PFAS at an optimized threshold dose with suitable additives, in order to get energy efficient conditions for PFAS decomposition.
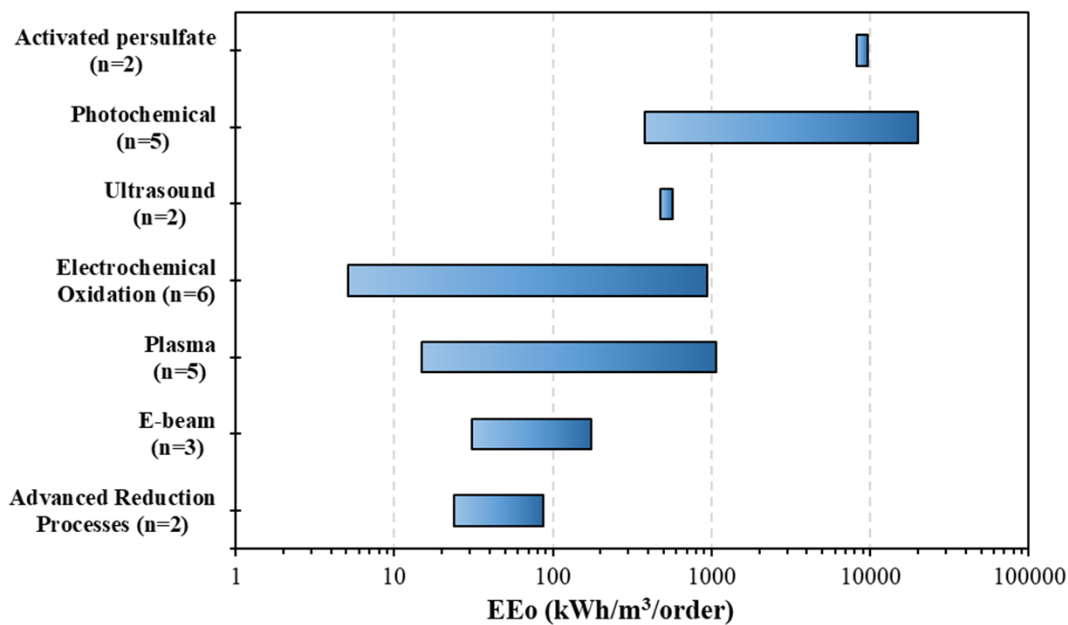
Figure 2.8 Calculated EE/O values of destructive techniques to treat PFOA with and without additives.[3, 31, 37, 38, 43, 62] Number within parenthesis represents the number of data points used to calculate EE/O.

Several studies have proposed a treatment train for destructive techniques to enhance the overall efficiency of the process and to reduce the cost of treatment. Some of the combinations proposed are nanofiltration/electrochemical anodic oxidation for PFHxA (Perfluorohexanoic acid), GAC adsorption/activated persulfate and ion exchange resin/electrochemical anodic oxidation for PFOA and PFOS.[63] An interesting combination proposed for e-beam was activated persulfate. One study showed an increase in the overall degradation efficiency in the presence of $Na_2S_2O_8$.[35] This improvement could be due to the production of more reducing species ($SO_4 \cdot^-$) that reacts with PFAS or the direct cleavage of C-F bonds by hydrated electrons in the presence of sulfate ions.[35, 63]

However, since e-beam is more efficient at treating higher initial PFAS concentrations, a pre-concentration step using adsorbents (*e.g.*, GAC and ion exchange resins) or other techniques could improve the overall efficiency of the process. The spent adsorbents from pre-concentration step can then either directly be irradiated with e-beam or could be extracted using solvents and the resulting concentrated waste stream could be treated with e-beam to achieve high energy efficiency as compared to direct treatment of water by e-beam. One study employed gas bubbling to enrich PFOA and PFOS at the air-water interface and then employed Direct current (DC) plasma treatment to decompose PFAS within gas bubbles.[64] A similar approach can also be utilized in combination with e-beam.

Although based on the EE/O values, e-beam shows potential for large-scale water treatment applications, there are a few limitations in our calculation of EE/O and to this technology. Firstly, the EE/O values calculated here were not based on complete defluorination or mineralization of PFAS. Very few studies have reported both the

decomposition and the defluorination efficiencies while using e-beam and the defluorination values are usually lower than decomposition values. For an initial concentration of 20 mg L^{-1} and at pH 13 and 500 kGy, decomposition[37] and defluorination efficiencies for PFOA were 88.1 and 37.5% and for PFOS were 63.4 and 51.8%, respectively. In a different study at an initial concentration of 1 mg L^{-1} and at pH 12, with argon saturated samples, decomposition[34] of PFOS at 28 kGy was 30% and defluorination efficiency of PFOS at 112 kGy was 15%. A few studies observed the formation of short-chain PFAS during the degradation of PFOA and PFOS, confirming incomplete defluorination during e-beam treatment.[31, 35, 38] Hence, EE/O values reported in this study are best-case scenarios and one could expect higher values if complete mineralization of PFAS is accounted for.

Another factor that limits e-beam technology is the energy efficiency of the overall process. While dose-based comparison offers advantages over G values for the ability of e-beam to break down various compounds in solution, to compare the EE/O values from Equation 2.3 with EE/O values of other water treatment techniques, the wall plug power efficiency must be considered. If the dose is divided by the wall plug power efficiency, the total power used by the accelerator to deliver the dose can be determined. Using an EE/O value calculated from the wall plug power would provide for the best comparison of EE/O values between e-beam and other technologies. In literature, often the accelerator efficiency is not listed, but the effect of the electrons on the target is independent of the particular accelerator being used given the same operating parameters such as dose, dose rate, and energy. The EE/O values calculated in this paper were based on the delivered dose to water and not the overall power consumption of the e-beam accelerator. The energy

efficiency of the DC accelerator itself usually ranges from 60 to 80% and for radio frequency (RF) linear accelerator systems, the efficiency ranges from 20 to 30%[65]. If this efficiency is considered in the EE/O calculations, the EE/O values will increase, leading to an energy-intensive treatment process. Better and more energy efficient accelerator designs will improve this efficiency and lower the overall energy required for the operation of e-beams.

E-beam technology has not been widespread to water treatment due to the general lack of understanding of the technology, often coupled with comparatively high capital and operating costs. Issues with most studies and pilot plants designed for e-beam treatment of water are that all use inefficient e-beam accelerators and therefore the operating cost was impractical for large scale applications. The 2010 Accelerator for America's Future report revealed a wealth of knowledge amongst the national labs on accelerator technology that could be adapted from discovery science to commercial applications.[66] The 2015 Department of Energy sponsored Workshop on Energy and Environmental Applications of Accelerators documents the necessity for high-power, high-efficiency e-beam accelerators that are economic for high flow rate water treatment.[67] Stemming from these workshops and reports, the Department of Energy created an accelerator stewardship program that has been funding the development of e-beam accelerators for high mass flow rate applications. Key to designing the next generation e-beam accelerators is high energy efficiency that correlates to reduced operating expenses.

Typically, the biggest losses of energy are seen in the power supply and the accelerating structure when accelerating the beam of electrons from the power source to the target. Consequently, the largest developmental efforts have been focused on increasing

the efficiency of RF power supplies and decreasing losses in the accelerating structure. Some other efforts devoted to minimizing the power loss in connections between major accelerator systems will not be discussed. One example is power loss between the beam of electrons exiting the accelerator vacuum and uniform deposition to the target.

Recent efforts to improve RF power supplies targets power efficiency of 80% and the ability to supply 1 MW of average power at a capital cost on the order of $1.5 per watt of average power[68]. For instance, this compares to currently available efficiencies of klystrons in the range[69] of 40-45%. The desire for a cheaper accelerator has pushed much of the developmental work towards magnetrons which have been demonstrated at capital costs on the order of the desired $1.5 per watt. Other RF power supplies, offering some desirable advantages such as increased uptime and decreased maintenance costs, like inductive output tubes (IOTs), and solid-state RF power sources, have not seen as much developmental work owing to higher installed costs in the range $5-15 per watt. A 2.45 GHz 1.2 kW CW magnetron[70] and a 1.3 GHz 100-kW peak, 10-kW average power magnetron[71] both recently demonstrated efficiencies above the target of 80%. However, these are just proof of principle validations and need to be developed for high powers in the range of 1 MW before capital costs can be estimated.

One of the major advances in reducing power losses in the accelerating structure is the use of superconducting materials. Using superconducting materials like niobium, the accelerating structure can be nearly lossless.[72, 73] In addition to increased energy efficiency, the superconducting accelerating structures can handle much higher power allowing for the treatment of higher mass flow rates. Conversely, there is a parasitic cost associated with the use of cryogens to cool the cavities to liquid helium temperatures. Current industrial

accelerators use normal conducting materials and suffer higher inefficiencies because they avoid the use of cryogens in order to minimize capital costs. The potential adoption of superconducting materials in industrial accelerators has been greatly aided by demonstrating the replacement of flowing cryogenic helium with cryocoolers and conduction cooling of the superconducting cavities.[74, 75] The use of cryocoolers compared to flowing liquid helium reduces the capital cost, operating cost and footprint of equipment required for an accelerator.

In the past 5-10 years, there have been great advancements in taking particle accelerator technology out of the national labs and developing it from high energy physics to an industrial platform. Low power prototypes are currently being built and high power (200-250 kW) are thought to be on the order of 5 years from the first prototype. The higher efficiency and higher power of these accelerators should open up more application of the technology for areas such as environmental remediation and possibly the destruction of PFAS.

TRANSITION 1

Chapter 1 demonstrated how the water quality and the operating parameters could impact the abundance of e_{aq}^-. the primary species responsible for PFAS degradation. It also emphasized the advantages of using EE/O as a normalizing parameter to compare previous studies utilizing e-beam technology. This parameter was also used to juxtapose e-beam technology with other destructive technologies currently employed for PFAS remediation.

The study introduced the concept of 'threshold dose' beyond which, for e-beam technology applications, the applied dose does not target the contaminant. This study also showed that under optimized treatment conditions, e-beam technology can compete with other destructive technology currently employed for PFAS destruction, while also stating the limitations and knowledge gaps.

The next chapter uses the lessons learnt from Chapter 1 to actually investigate destruction of PFAS using e-beam technology. This was done in collaboration with Fermi National Laboratory, Batavia using their novel A2D2 accelerator.

CHAPTER 3

APPLICATION OF ELECTRON BEAM TECHNOLOGY TO DECOMPOSE PER- AND POLYFLUOROALKYL SUBSTANCES IN WATER

3.1   Introduction

E-beam treatment is considered as an advanced oxidation/reduction process due to the simultaneous generation of both oxidizing and reducing species. A limited number of studies have utilized e-beam to study the degradation of PFAS in aqueous matrices.[16, 31, 76-83] The matrices studied have been deionized (DI) water, synthetic wastewater and groundwater[81, 84], and the studies have primarily focused on the degradation of PFOA and/or PFOS as model compounds[16, 31, 78, 80, 82], although a recent study investigated the degradation of PFHpA as a single solute.[83] The delivered e-beam dose in these studies varied from 10 to 2000 kGy (dose rate of 1.58 to 20 kGy s^{-1}) and the initial concentrations tested ranged from 0.1 to 400 mg/L or parts-per-million, with experiments primarily focused on higher concentrations that may not be environmentally relevant (µg/L or mg/L).[31, 77-80, 82] One recent study[81, 84] investigated the degradation of PFOA and PFOS in groundwater and soil matrices with initial concentrations at parts per trillion (ppt) levels at e-beam doses of 500 and 2000 kGy. Although this study looked at the degradation of other long- and short chain PFAS such as perfluorobutanoic acid (PFBA), perfluoropentanoic acid (PFPeA), perfluorobutane sulfonate (PFBS), perfluorononanoic acid (PFNA) as well as fluorotelomers such as 6:2 fluorotelomer sulfonate (6:2 FTS) in the soil matrix, the study discussed primarily the degradation of PFOA and PFOS in deionized water (DIW) and groundwater matrix.[81] e_{aq}^- (reduction potential = -2.9 eV)[40, 77] have been shown to initiate the degradation and defluorination of PFAS by cleavage of the C-F bonds, with rate

constants for PFOA and PFOS ranging from 1.7 x 10^7 to 7 x 10^7 $M^{-1}s^{-1}$.[31, 77, 80] Degradation efficiency of PFAS using e-beam was shown to be impacted by accelerator operating parameters such as dose and dose rate as well as water quality parameters such as pH, dissolved oxygen (DO), and the presence of other radical scavengers[16], as they impact the ratio of dominant radical species in the system. Reaction of PFAS with e_{aq}^- leads to the formation of unstable PFAS radicals, according to equations 1 and 2. This is theorized to be the first step in degradation of PFAS by e_{aq}^- while using e-beam treatment.[31, 77, 78]

The feasibility of e-beam to treat PFAS other than PFOA and PFOS in water still remains to be investigated. As natural waters can contain a suite of PFAS[85-87], it is also important to investigate the degradation (defined as transformation of the parent compound into subsequent byproducts) of a mixture of PFAS at environmentally relevant levels in source waters. To address this important knowledge gap, in this study, e-beam technology was utilized to treat a suite of PFAS in water samples (DI water and groundwater) at environmentally relevant levels to assess the effects of various operating and water quality parameters on treatment efficiency. Novelty of the present study include the investigation of: (i) degradation mechanisms for PFOA and PFOS utilizing a combination of targeted, suspect screening and total fluorine analysis; (ii) degradation of a suite of PFAS in real-world contaminated groundwater samples to observe the effect of sample matrix on PFAS degradation trends; and (iii) simultaneous transformation of PFAS precursors in real world samples. It was hypothesized that (i) e-beam technology could simultaneously transform PFAS precursors, due to the concurrent generation of oxidative radicals, and (ii) degradation of PFAS in real world samples would be suppressed due to the scavenging of e_{aq}^- by components of groundwater such as natural organic matter, nitrate/nitrites,

orthophosphates etc. The corresponding objectives of this study were to (i) test the impacts of pH, DO, and coexisting inorganic ions on the performance of e-beam to degrade PFAS, (ii) evaluate and compare the degradation and energy requirements of different PFAS as single solute and as mixtures, (iii) elucidate the degradation mechanism of PFAS by employing a combination of targeted and nontargeted/suspect screening of treated samples, and (iv) evaluate the effectiveness of e-beam technology to degrade environmentally relevant levels of PFAS in contaminated groundwater samples.

3.2 Research Questions

1. What are the optimized treatment conditions for PFAS treatment?

2. How does e-beam perform in treating PFOA, PFOS and what is the effect of increasing initial concentration?

3. What is the effect of chain length and functional group on PFAS degradation for 10 compounds chosen at a fixed dose ?

4. What are the degradation trends observed while treating an equimolar PFAS mixture with increasing e-beam dose?

5. How do the degradation trends for PFAS change while treating real world GW samples?

3.3 Research Hypotheses

1. Dissolved oxygen and $OH^{\cdot}$, H^{+} radicals will scavenge e_{aq}^{-} from the solution, reducing their availability to react with PFAS molecules. Low DO and alkaline conditions will be more suitable for PFAS treatment using e-beam technology.

2. Increasing the dose will enhance reactions between contaminants and reactive species, resulting in improved degradation.

3. PFOA will degrade more efficiently than PFOS as the carboxylic group in PFOA will be easier to oxidize than the sulfonic group in PFOS[78].

4. Short chain PFBA, PFBS will show highest resistance to degradation due to high BDE of C-F bonds due to their compact geometry[30].

5. For the same functional group, the degradation efficiencies will be a function of PFAS chain length, with the long chain PFAS showing better degradation efficiencies due to higher reactivity with e_{aq}^- and higher susceptibility to degradation.

3.4 Materials and Methods

3.4.1 Sample Preparation

All chemicals and solvents used in this research were of either certified ACS reagent grade or LC/MS with high purity and were purchased from Sigma-Aldrich (USA) and Fisher Scientific (USA). Samples were prepared in Stony Brook University in borosilicate glass vials or polypropylene jars, depending on the target dosage. Four different sample volumes were treated depending on the dimensions of the jars to ensure a constant beam penetration depth of 3 cm: 15 mL, 90 mL, 130 mL, and 160 mL. The empty weight of the containers was noted before sample preparation. The pH was adjusted by adding NaOH (for pH 10, 13 samples) or by using HNO_3 for pH 4 samples. Four PFAS-spiked samples were prepared for each sample set conditions. Three samples in the set were shipped to Fermi Accelerator National Laboratory (Fermilab) for e-beam treatment and one sample was retained to measure initial concentration of the contaminant prior to treatment. In each batch, control samples with known concentration of the contaminants and a sample containing only DIW (field and trip blanks) were simultaneously prepared and shipped to Fermilab to account for any loss and/or background contamination during shipping and sample processing. Samples were weighed before and after treatment to verify sample volume loss (if any).

3.4.2 E-Beam Treatment

Samples were treated in batches using the 9 MeV electron beam accelerator (Accelerator Application Development and Demonstration, (A2D2) located at Fermilab (SI). This is provided by a repurposed teletherapy linear accelerator that enables proof-of-concept studies. Upon receiving the samples at Fermilab, samples were purged with high purity N_2 gas to attain a final DO concentration of 2 mg/L, capped and treated immediately. The dose rate was fixed at 1.2 kGy/sec and the e-beam irradiation time determined the applied dose. Dosimetry is provided by a NIST certified dosimetry system that is available to measure/verify the amount of total dose given to each sample The sample depth in each of the containers was carefully chosen (set to 3 cm) to minimize the variation in dose delivered by the e-beam. To maximize usefulness of A2D2 beam time, capped samples were treated in set of six for each irradiation. For dose uniformity, the samples were placed in a revolving hexagonal shaped sample holder. After sample treatment, the samples were sealed and were shipped on ice back to Stony Brook University for PFAS analysis.

3.4.3 Sample Analysis

E-beam treated samples were diluted (1:1) with methanol to prevent any sorption prior to PFAS analysis. An aliquot of the diluted sample was taken out for further dilution (to fall within the calibration) and the pH was adjusted to near neutral using 10 % acetic acid. 10 µL of 100 µg/L isotopically-labeled standards (M2PFOA, MPFOS) were added prior to analysis to provide recovery-corrected PFAS concentrations. Samples were analyzed using an Agilent 6495B triple quadrupole liquid chromatography tandem mass spectrometer (LC-MS/MS) equipped with electron spray ionization (ESI). Details about the MRM transitions, analyte recovery, LC-MS/MS conditions, and relative percentage differences (RPDs) are

provided in Appendix A. Single solute samples post e-beam treatment for PFOA and PFOS at an initial concentration of 500 µg/L each were analyzed for total fluorine, inorganic fluorine and by high-resolution mass spectrometry (HRMS) suspect screening on an Agilent Infinity 1290 liquid chromatograph coupled to an Agilent 6545 quadrupole-time-of-flight mass spectrometer (LC-QTOF-MS) with negative electrospray ionization (ESI⁻). More details about the QTOF method and sample analysis can be found in SI. The rest of the sample was sent to PACE analytical laboratories (Massachusetts, USA) which applied TRUE TOF®, that can quantify both total and inorganic fluoride (IF) using two parallel IC modules, with the difference yielding the organic fluorine content of the samples.[88] Thus, the MDLs for organic fluorine (Total – Inorganic fluorine) are 0.005 ppm in trace system liquids/DIW and 0.1 ppm in mid-level system liquids/GW, WW.

3.5   Results and Discussion

3.5.1   Degradation of PFOA and PFOS

To test the impact of pH and DO, we tested PFOA and PFOS degradation at three pH (4,10 and 13) and two DO levels (2 and 4 mg/L). More details about DO and pH optimization can be found in SI. Conditions such as low DO (2 mg/L) and pH 13 promoted the abundance of e_{aq}^- and were hence determined to be optimal conditions for PFOA and PFOS degradation. At pH 13 and 2 mg/L DO, the pseudo-first order rate constant for degradation for PFOA and PFOS was 4×10^{-3} kGy^{-1} and 5×10^{-3} kGy^{-1}, respectively. These values agreed with previously published rate constants (1.0 -1.9× 10^{-3} kGy^{-1} for PFOS and 5×10^{-3} kGy^{-1} for PFOA).[31, 76] However, contrary to previous literature[78, 82], we did not

observe a consistent trend for the degradation of either PFOA or PFOS with increasing pH. For PFOS, degradation efficiency ranged from 45–60 % at pH 10 and from 25–70 % at pH 4. However, pH 13 yielded the highest percent degradation for both PFOA and PFOS. Consistent with previous literature, PFOS showed more resistance to degradation (77%) compared to PFOA (92%) at the same applied dose of 250 kGy. This is theorized to be due to the sulfonate functional group in PFOS being more resistant to oxidation than carboxylic group in PFOA.[78]

To test the effect of initial concentration on the degradation process, we tested PFOA and PFOS as single solute at a concentration of 100 and 500 µg/L at pH 13 and at 2 mg/L of DO. These are higher than environmentally relevant PFAS concentrations (ng/L) and were chosen to identify transformation products and to explore if e-beam technology could be used after a pre-concentration step. The degradation of PFOS and PFOA was similar for both initial concentrations tested (Figure A1). PFOA showed 93.5 ± 0.7% degradation at a dose of 250 kGy and PFOS showed 95.3 ± 5.1% degradation at a dose of 500 kGy. The overall degradation efficiencies for PFOA and PFOS at e-beam doses of 250-1000 kGy ranged from 94–99% and 68–98%, respectively. Thus, at alkaline and low DO conditions, the efficiency of e-beam treatment was similar for both PFOA and PFOS for a wide range (5X) of environmentally relevant concentrations. The water radiolysis reaction produces enough e_{aq}^- to react with PFAS molecules even at higher initial concentrations. This can be attributed to the dose rate used (1.2 kGy s^{-1}) in this study, which is amongst the lowest compared to previous studies (1.58 - 20 kGy s^{-1}) that have utilized e-beam treatment of PFAS. As e_{aq}^- are primarily responsible for PFAS degradation, a lower dose rate favors their abundance in the solution as inter-radical reactions, that can scavenge e_{aq}^- , are

reduced at lower dose rates.[40, 89] These results suggested that the degradation of PFAS at tested concentrations of up to 500 µg/L is rather limited by the competition between PFAS molecules and other water radiolysis products that act as e_{aq}^- scavengers (*e.g.*, H^+, $OH^.$ etc.). This competition is minimized by increasing the number of PFAS molecules with higher initial concentrations, favoring the reaction between e_{aq}^- and PFAS over other scavengers.[16] This can be explained by the fact that 90% removal of 100 µg/L and 500 µg/L initial concentration represents a reduction of 90 µg/L and 450 µg/L of PFAS after treatment. Thus, based on these findings, a 'concentrate and destroy' approach[16, 90] that employs a pre-concentration step followed by e-beam treatment would result in less energy consumption.

3.5.2 Mass Balance and Transformation Products of PFOA and PFOS Treatment

As e-beam doses increase, 90% degradation of PFOA was observed at doses ≥250 kGy, as shown in Figure 3.1a. The fraction of inorganic fluorine also increased with the dose applied (Figure 3.1c), with the inorganic fluorine accounting for 70% of the total fluorine content in the sample at 1000 kGy. It is important to note that the inorganic fluorine fraction can be correlated to the defluorination percentage, for these calculations. This indicates that, for PFOA, although complete degradation is observed at 250 kGy, defluorination of resulting byproducts continues to occur with increasing e-beam dose. Interestingly, 30% of the total fluorine at 1000 kGy consists of organic fluorine, suggesting the formation of recalcitrant transformation products (shorter chain PFCAs, polyfluorinated PFAS, ethers etc.) of PFOA. This is supported by the detection of short chain perfluoroalkyl carboxylates (PFCAs) such as PFHpA, PFHxA, PFPeA and PFBA by both our analytical instrument as well as previous studies[31, 78, 91] as well as attributed to formation of H-substituted

polyfluorinated byproducts detected for PFOA degradation using e-beam technology. However, for PFOA, the short chain C4-C7 PFCAs accounted for <5% of the initial PFAS mass balance although >90% degradation efficiency was obtained.
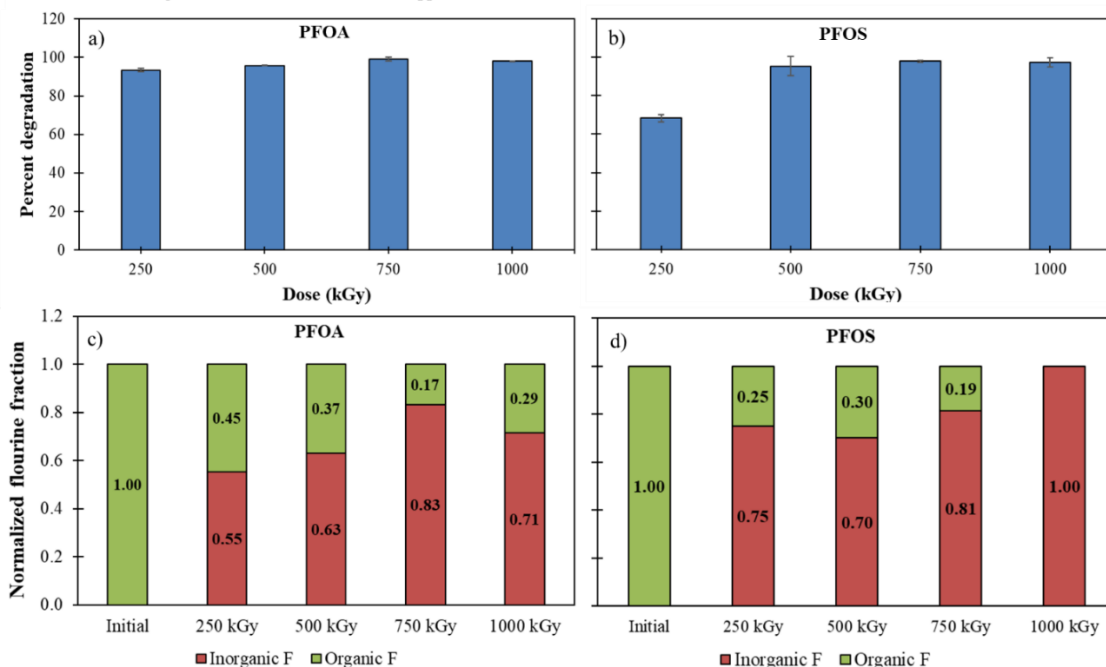
Figure 3.1 Percent degradation and normalized total fluorine fraction for PFOA (a, c) and PFOS (b, d) with increasing e-beam doses. Initial concentration: 500 µg/L, pH: 13, DO: 2mg/L. 'Initial' in panel c, d denotes untreated samples. Error bars represent variation observed from triplicate samples.

At 250 kGy the degradation efficiency of PFOS is 68%, with the inorganic fluorine fraction accounting for 75% of total fluorine. As e-beam dose increases, >90% degradation of PFOS is observed for doses ≥500 kGy. Simultaneously, the inorganic fluorine fraction increases with increasing e-beam doses, with 100% of total fluorine at 1000 kGy attributed to inorganic fluorine. This suggests that at 1000 kGy, there is complete defluorination of PFOS. This is additionally supported by the data obtained from LC-MS/MS, which did not show any detection of short chain PFAS. Compared to our results, previous studies detected measurable short chain PFCAs, alkylated and H-substituted PFOS, perfluoroalkyl

sulfonates (PFSAs) and PFOA[78, 80, 91] for PFOS degradation using gamma or e-beam irradiation. This could be attributed to the high doses (up to 1000 kGy) and low dose rate (1.2 kGy/sec) used in the current study that allowed for more e_{aq}^- -PFAS reactions, leading to a degradation of both parent compound and transformation products. This, in combination with the inorganic fluorine accounting for 100% of the total fluorine at 1000 kGy suggested that the PFOS byproducts were not as stable as PFOA byproducts.
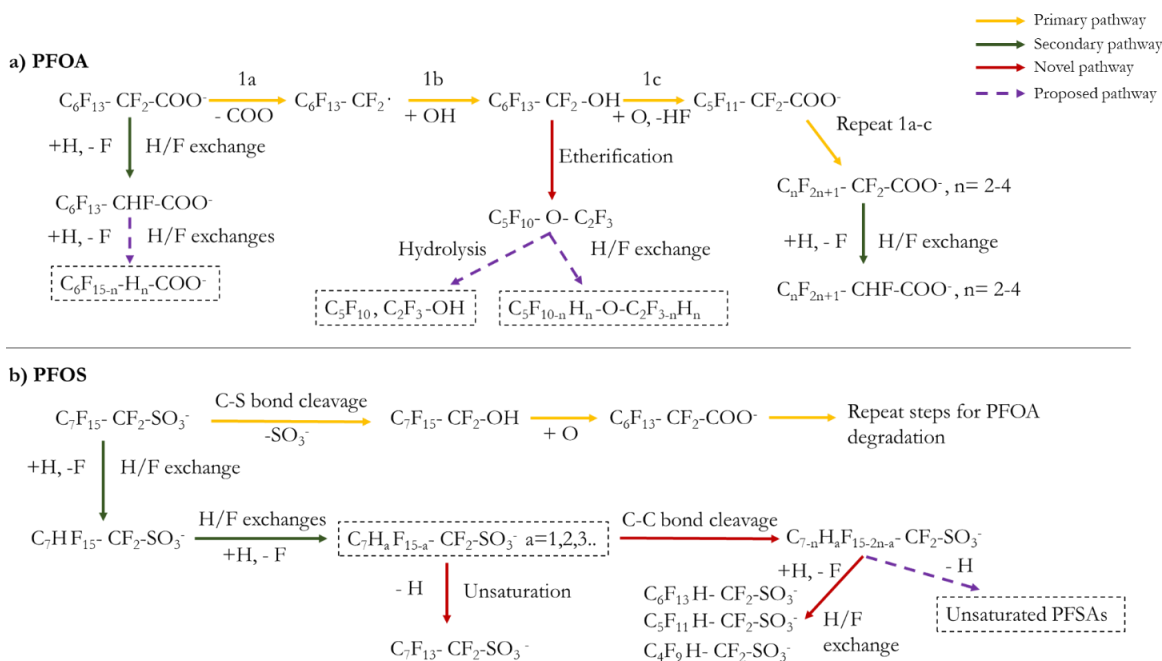
Figure 3.2 Proposed degradation pathways with detectable byproducts for (a) PFOA and (b) PFOS degradation using non-target/suspect screening. Initial concentration: 500 µg/L, pH: 13, DO: 2mg/L, dose range: 250-1000 kGy. Primary and secondary pathways yielded degradation products, consistent with previous studies; novel pathway indicates new byproducts detected in current study; proposed pathway indicates undetected products hypothesized to have formed during degradation.

To further understand the degradation mechanisms, we performed HRMS suspect screening of PFOA and PFOS treated samples. For PFOA, short chain PFCAs such as PFBA, PFPeA, PFHxA and PFHpA were detected during suspect screening, consistent with data from our targeted analysis and published in previous studies.[32, 78, 91, 92] This can

be explained by the mechanisms proposed in a recent study for PFCA degradation with e_{aq}^- using a UV system.[30, 93] This is hypothesized to occur by a stepwise reaction pathway termed decarboxylation – hydroxylation-elimination-hydrolysis (DHEH).[29, 30] During DHEH, a CO_2 moiety is cleaved, resulting in the formation of a free radical ($C_nF_{2n+1}COO^- \rightarrow C_nF_{2n+1}$·). This is the decarboxylation step (Figure 3.2), which is followed by a hydroxylation step, resulting in an addition of OH group to the free radical ($C_nF_{2n+1}-OH$). PFAS-alcohols are usually unstable and thus undergo an HF elimination to form an acyl fluoride that can undergo hydrolysis to form a shorter chain PFCA ($C_{n-1}F_{2n-1}-COO^-$).[30, 93] This cycle can repeat and can form shorter chain PFAS such as PFBA, PFPeA, and PFHxA as byproducts of PFOA degradation. Interestingly, we also tentatively identified an unequivocal molecular formula (C8 H2 F16 O4 S) that may be an H-substituted PFSA ether in PFOA samples, suggesting that post HF elimination, formation of PFAS ethers may be a possible secondary reaction (Figure 3.2). This could occur from a combination of resulting PFAS radicals with each other rather than hydroxylation in Step 1b (Figure 3.2a). It was interesting to note that increasing e-beam doses decreased the relative abundance of short chain PFCAs, indicating that with increased e-beam doses, reactions of short chain PFCAs and e_{aq}^- occurred, resulting in their degradation.

Suspect screening data also tentatively identified H-substituted PFOA, and PFPeA, suggesting a secondary degradation pathway for PFOA other than DHEH. The C-F bond on the α position for PFOA has the lowest bond-disassociation energy[30], leading to an attack by e_{aq}^-. This leads to an H/F exchange at the α position, weakening the neighboring C-F bonds and making the C-F more prone to H/F exchange. This explains the detection of multiple H-substituted PFOA, PFPeA and PFHpA by non-target analysis. However, the

lower abundance (~70–96%) of C4-C7 H-substituted PFCAs compared to the C4-C7 PFCAs indicates that DHEH is the dominant degradation mechanism that initiates PFOA degradation using e-beam. DHEH as a favorable PFOA degradation pathway was also confirmed by another study that used q-SAR data to elucidate feasible pathways for PFOA degradation.[30, 94]

For PFOS, unsaturated PFOS (U-PFOS) and subsequent C4-C7 H-PFSAs were detected in the samples post e-beam irradiation. The α C-F bonds in PFSAs do not necessarily have the lowest BDE, as indicated by a recent study[30]. This means that the H/F exchange at PFOS can occur at the lowest BDE position, away from the functional group, resulting in multiple H/F exchanges across the C-C skeleton. Multiple H/F exchanges could weaken the overall chemical stability of the parent compound, making it more susceptible to attack by both oxidative and reductive species that are abundantly formed during water radiolysis. This could lead to a C-H bond breaking for PFOS, via a chain snipping mechanism (Figure 3.2b), resulting in the formation for U-PFOS. However, it is hypothesized that for short chain PFSAs, multiple H/F exchanges away from the functional group could result in a chain zipping reaction, through an oxidative pathway, resulting in the formation of short chain PFSAs by attacking the weakened C-C bond. The H/F exchange cycle repeats and forms both H/F substituted PFSAs and short chain PFSAs subsequently. These H/F exchanges can also result in hydrolysis reaction, forming unstable telomeric alcohol $C_7F_{15} - CF_2 - OH$, which can transform to PFOA, which was detected with suspect screening. The PFOA can follow the pathway described above for PFOA degradation, resulting in the formation of H-substituted PFCAs and PFCAs, as detected by suspect screening.

3.5.3 Degradation of PFOS Isomers

Changes in the chemical structure results in variation in the physicochemical properties of PFAS isomers.[6] This can result in a variation in removal efficiencies for both sequestration and destructive technologies for linear and branched PFAS. L-PFAS are generally more sorptive but also more resistant to destructive technologies, whereas br-PFAS are more easily degraded but are less sorptive towards sequestration techniques.[6] Our analytical methods were able to differentiate between linear and different branched forms of PFOS. For this study, we combine and refer to all the branched isomers of PFOS collectively as Σbr-PFOS. Irrespective of the solution pH, Σbr-PFOS consistently showed a higher degradation percentage than L-PFOS. Interestingly, although br-PFOS showed ~90% degradation efficiency at pH 4, 10 (Figure A3), degradation of PFOS (total) is hindered due to the higher contribution and lower percent degradation of L-PFOS (Figure A3). br-PFOS is less resistant to degradation due to higher electron affinity on the tertiary carbon, making it more susceptible to e_{aq}^- attack, compared to L-PFOS.[54, 80] This is consistent with previous studies utilizing other destructive techniques[54, 95] that have observed better degradation of Σbr-PFOS than L-PFOS. However, at pH 13, presence of abundant e_{aq}^- increases the number of reactions between e_{aq}^- and L-PFOS, improving the degradation efficiency of L-PFOS (>90%) and consequently of PFOS (total). It is important to consider the isomeric impact on PFAS degradation in natural waters as this could impact the degradation efficiency of PFAS (total) due to the differences in isomeric behavior observed for destructive techniques.[6]

3.5.4 Impact of PFAS Chain Length and Functional Group on Degradation Efficiency.
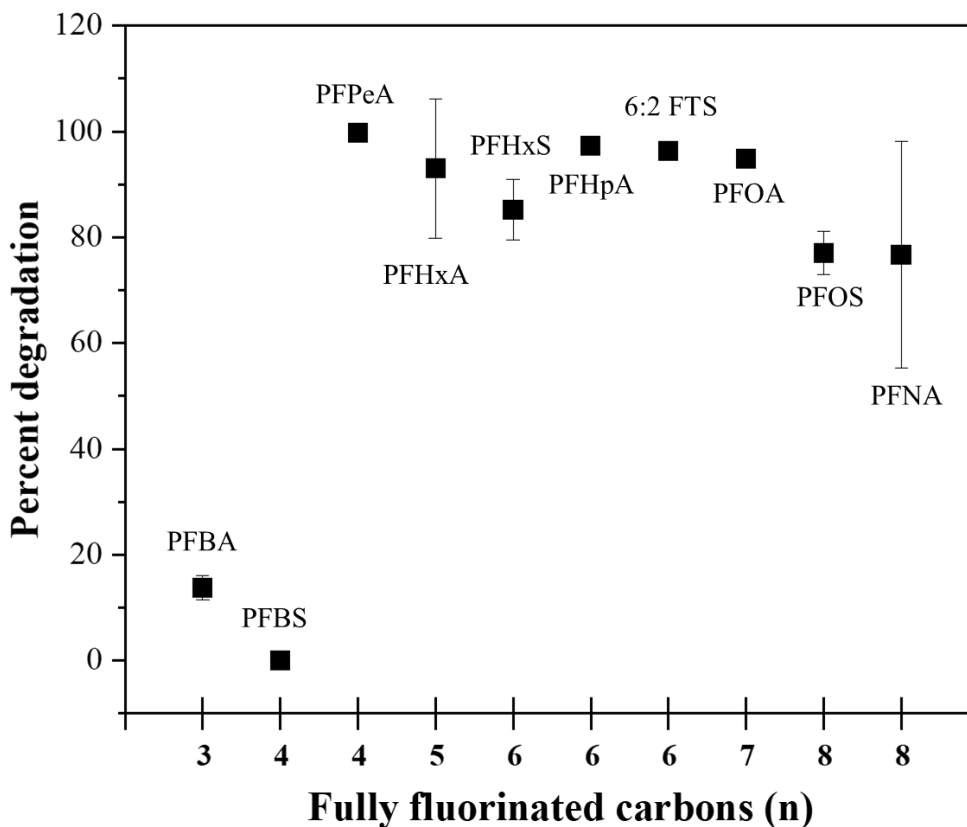
Figure 3.3 Percent degradation of PFCAs and PFSAs of different chain lengths and 6:2 FTS at a fixed dose of 250 kGy in single solute samples. Initial concentration of individual PFAS: 100 µg/L, pH = 13, DO: 2 mg/L. Error bars represent variation observed from triplicate samples and analytical replicates.

Previous studies have focused on the e-beam treatment of predominantly PFOA and PFOS under different water quality and operating parameters.[16, 31, 76, 78, 80] However, the impact of functional groups, polyfluoro compounds (*e.g.*, FTS) and chain length on the overall treatment process still remains unknown. To this regard, we tested eight other PFAS of carbon chain length ranging from 3 to 9, individually at 250 kGy and using pH (13) and DO conditions (~2 mg/L). These included PFCAs such as PFBA, PFPeA, PFHxA, PFHpA, PFNA and PFSAs such as PFBS, PFHxS and one fluorotelomer sulfonate (6:2 FTS).

In Figure 3.3, similar degradation for both PFCAs and PFSAs was observed for carbon chain length of greater than five (PFPeA, PFHxA, PFHxS, PFHpA, PFOA, PFOS and PFNA). Between the 10 PFAS studied, there was no correlation observed between PFAS degradation and the chain length, under the tested conditions (p value = 0.52). The percent degradation values for PFOA, PFHpA, PFHxA, and PFPeA were 95 ± 0.02%, 97 ± 1.1%, 93 ± 13% and 98 ± 0.02%, respectively. The average percent degradation of PFNA was slightly lower at 77% with a higher standard deviation of 21.5%. The degradation percentage observed for PFHxS and PFOS were 86 ± 5.7% and 77± 4%, respectively. 6:2 FTS showed 96% degradation although the total carbon chain length is eight (six carbons are perflourinated and two carbons are hydrogenated). This makes 6:2 FTS degradation by both e_{aq}^- and OH· possible as the simultaneously generated OH· can attack the C-H bonds, as demonstrated by previous studies that have utilized OH· radicals to degrade 6:2 FTS in a total oxidizable precursor (TOP) assay.[96,97] This further confirms that the C-F bonds are the limiting factor for the degradation via reaction with e_{aq}^-.

At 250 kGy, both PFBA and PFBS showed the lowest degradation efficiencies, with ~14% observed for PFBA and no degradation observed for PFBS. Although a clear explanation for this phenomenon is unknown, this is hypothesized to be due to the compact geometry of C4 PFCA and PFSA and higher bond dissociation energy of the C-F bonds in the short chain PFAS.[30] A similar observation was made in another study that generated e_{aq}^- using UV-sulfite process to treat AFFF mixtures. PFBS and perfluoro-1-propanesulfonate (PFPrS) remained unreactive after 4 hours of treatment compared to PFPeS, PFHxS, and PFOS.[98] This was hypothesized to be due to increased reactivity of e_{aq}^- with increasing chain length. However, in contradiction to our findings, under same conditions, reactivity

of PFCAs was observed to be similar irrespective of chain length for PFBA, PFHxA, PFHpA and PFOA.[98] To improve the degradation of PFBA and PFBS, we tested single solute samples at 100 µg/L initial concentration at an elevated e-beam dose of 1000 kGy. Samples were tested with and without the addition of 0.2 M t-butanol, an OH. radical scavenger, which was added to promote the degradation of PFBA and PFBS by increasing the abundance of e_{aq}^- in solution. We observed an average of 99% removal of PFBA and 72% removal of PFBS for samples at pH 13 without the addition of t-butanol. Contrary to previous studies[32, 80], samples with t-butanol addition performed relatively poorly with an average degradation of 34% and 13% observed for PFBA and PFBS, respectively, suggesting that more reaction time and/or energy is required to break down these short-chain molecules.

Electrical energy per order (EE/O) is a quantity defined as the energy required for one log removal (90% removal) of a contaminant in a unit volume of water. This parameter is typically used to evaluate the energy efficiency of advanced oxidation processes (AOP) to degrade a target contaminant.[46] This normalizing parameter enables comparisons between destructive techniques that have been utilized to treat contaminants. Figure 3.3 data was used to calculate the EE/O values in kWh/m^3/order according to equation derived in our previous study.[16] As the EE/O values ranged between 45 and 503 kWh/m^3/order, with 6:2 FTS showing the lowest EE/O value of 48.6 kWh/m^3/order (Table A7). For PFOA and PFOS, the calculated EE/O values ranged from 53–140 and 108–155 kWh/m^3/order respectively, which are comparable to EE/O values calculated using data from previous studies that focused on e-beam treatment.[6] EE/O values were calculated at 1000 kGy for PFBA and PFBS as no degradation of PFBS and only 13% was observed at 250 kGy (Table

A7). At 1000 kGy, the EE/O value for PFBA and PFBS was 139 and 503 kWh/m³/order, respectively. These results suggested that the levels and regulatory landscape of short chain PFAS will determine the efficiency and energy consumption of e-beam treatment of PFAS.

3.5.5 E-Beam Treatment of PFAS Mixtures

To assess competitive reactivity of PFAS in mixtures, we treated equimolar mixture of 10 PFAS (0.05 µM each) at optimized treatment conditions (pH 13, 2 mg/L DO) with varying e-beam doses ranging from 125 kGy to 1000 kGy. The corresponding mass concentrations of PFAS in the equimolar mixture were: PFBA=10.7 µg/L, PFBS=15 µg/L, PFPeA=13.2 µg/L, PFHxA=15.7 µg/L, PFHxS= 25 µg/L, PFOA=20.7 µg/L, PFOS=25 µg/L, PFNA=23.2 µg/L and 6:2 FTS=21.4 µg/L.
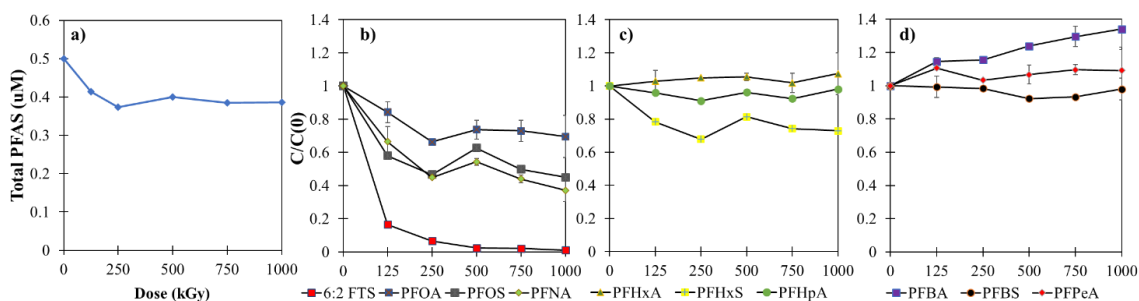
Figure 3.4 (a) Total PFAS degradation (µM) and degradation (C/C$_0$) of individual PFAS grouped according to chain length: b) 6-8; c) 5-6; d) 3-4, as a function of e-beam dose. Initial concentration of equimolar mixture of PFAS was 0.05 µM treated at pH 13 and DO of 2 mg/L. Error bars represent standard deviation of triplicate treatment.

6:2 FTS showed the highest degradation with ~ 80% degradation observed at 125 kGy (Figure 3.4b) and ~90% at 250 kGy. PFNA and PFOS showed final degradation efficiencies (at 1000 kGy) of ~60 and 50%, respectively while the degradation of PFOA was ~15 % at 250 kGy and plateaued at 30% after 500 kGy of dose. No degradation was observed for PFBS, with the C/C$_0$ remaining constant at ~1, whereas the C/C$_0$ for PFBA

increased with increasing dose and reached ~35% increase in concentration at 1000 kGy. Interestingly, C/C_0 value was ~1 at 1000 kGy for PFHxA, while ~27% degradation of PFHxS was observed at 1000 kGy, suggesting the formation of C6 carboxylates during treatment and not sulfonates.

For PFOA and PFOS, data obtained for mixture treatment was contrary to data obtained in single solute samples where both PFOS and PFOA showed >90% degradation at 500 kGy. PFOA showed a lower degradation efficiency than PFOS (~30 % for PFOA vs 55 % for PFOS at 1000 kGy). Although the exact reasons are unknown, this could be due to formation of PFOA from PFNA degradation via the DHEH mechanism. Complete degradation of 6:2 FTS compared to PFHpA suggests that polyfluorinated compounds are more reactive and undergo transformation easily compared to perfluorinated compounds. PFHxS was degraded better than PFHpA and PFHxA in equimolar mixtures (Figure 3.4c) although a similar degradation efficiency was observed for them in single solute samples (Figure 3.3). This could be due to simultaneous degradation and formation of PFHxA and PFHpA from the degradation of longer chain PFCAs. Previous studies that have utilized e_{aq}^- to degrade PFAS have detected short chain PFCAs as a byproduct of longer chain PFCA and in some cases, PFSA degradation.[30, 31, 77, 78, 80, 91] Interestingly short chain PFCAs were detected as a byproduct of PFSA degradation but the formation of short chain PFSAs was not reported. This can be elucidated by the degradation mechanisms proposed in the earlier section. For PFCAs, degradation can occur by either H/F exchange or by DHEH, the latter of which can cause the formation of short chain PFCAs. In PFSAs however, short chain PFCAs can be formed as a result of the C-S bond breakage, followed by DHEH.[30]

While looking at C4-C7 PFCAs, it is also important to consider the byproducts of 6:2 FTS degradation. The e-beam technique, being an advanced oxidation-reduction process[16], can generate both e_{aq}^- and OH$^.$ capable of transforming 6:2 FTS into short chain PFCAs. [97] In single solute samples, 6:2 FTS was completely degraded at 250 kGy of e-beam dose (Figure 3.3), forming detectable byproducts such as PFHpA, PFHxA, PFPeA and PFBA, with an overall molar yield of ~37%. This is lower than the molar yield we obtained for transformation of 6:2 FTS by OH$^.$ using TOP assay (65-75%), consistent with data reported in previous literature.[97] The depression in molar yield using e-beam, in spite of complete degradation of 6:2 FTS could be attributed to the simultaneous reactions of 6:2 FTS and its transformation byproducts (short chain PFCAs) with OH$^.$ and e_{aq}^-, formed during e-beam treatment. While utilizing TOP assay, these byproducts remain unreactive towards OH radicals as OH$^.$ is incapable of reducing them.

This lends further credence while observing the degradation of PFBA and PFPeA. C/C_o values for PFBA showed an increasing trend with increasing e-beam dose (Figure 3.4d). Compared to other PFCAs, PFBA showed significantly lower degradation efficiency in single solute mixtures. Thus, in case of PFBA and possibly PFPeA in a mixture, formation from the degradation of longer chain PFCAs and 6:2 FTS has a higher contribution than the degradation process, thus elevating the final C/C_o value observed at 1000 kGy to ~1.3 and 1.1, respectively. Unsurprisingly, for PFBS, no degradation was observed in the PFAS mixture, suggesting both competing effects of other PFAS and also the relative stability of PFBS contribute to lack of degradation. This experiment confirmed that there is competition between PFAS analytes for reaction with e_{aq}^- and reaction kinetics

may vary with perflourinated chain-length, the degree of fluorination in the carbon chain, functional group, and the presence of highly reactive intermediates.

3.5.6   E-Beam Treatment of Contaminated Groundwater Samples

Three PFAS - contaminated groundwater samples (GW1, GW2, and GW3) were collected from two different US states to treat using optimized e-beam conditions (Table A5). GW samples contained known precursors such as 4:2 FTS, 6:2 FTS and 8:2 FTS detectable but can also encompass the unknown precursors that are beyond the capability of our instrument. Thus, prior to the e-beam treatment of these GW samples, we performed TOP assay (method details can be found in Appendix A) to assess the presence of oxidizable PFAS precursors (Table A6). We observed an increase in concentrations of PFCAs as a result of TOP assay of GW samples. PFBA level increased by ~990% and 215% for GWs 1 and 3, respectively. The concentration of PFPeA (~225 and 98%) and PFHxA (~77 and 136%) showed a similar increasing trend for GWs 1 and 3 respectively , while the FTSs present in the GW samples were completely oxidized, post TOP assay. The yield of PFCAs were much higher in GW samples than the typical yield observed for FTSs after TOP assay, suggesting and confirming the presence of other unknown precursors in GW samples.

To assess if PFAS precursors were transformed during e-beam treatment, we performed TOP assay on treated GW1 and GW3 samples (dose = 250 kGy) (Figure A4). Unlike untreated GW samples, the treated samples did not yield an increase in PFCA levels, with the concentrations of PFCAs before and after TOP assay were statistically indifferent (p values = 0.6 and for GW1 at both 250,750 kGy). This confirms that e-beam technology, even at the lowest dose utilized for treatment, is capable of completely degrading PFAS precursors present in the GWs.
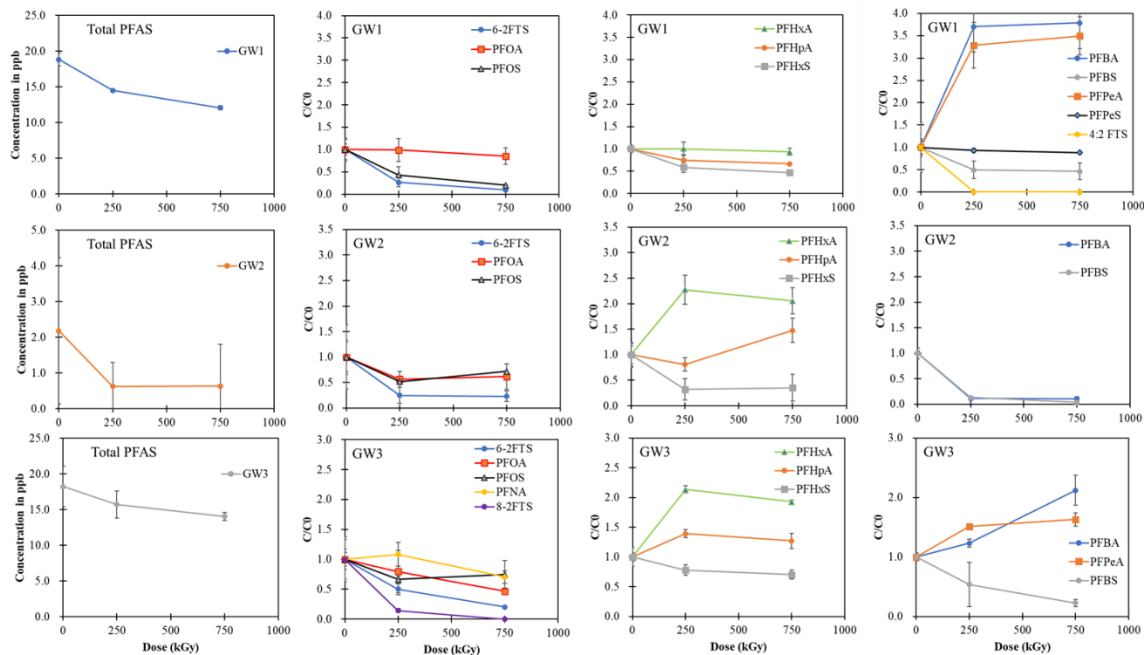
Figure 3.5 Degradation of PFAS in three different GW matrices treated at 250 and 750 kGy. Error bars represent standard deviation of triplicate treatments.

The total initial concentration of PFAS (ΣPFAS) was 18.8 µg/L for GW1 (for 14 detected PFAS), 2.2 µg/L for GW2 (for 10 detected PFAS), and 18.2 µg/L for GW3 (for 17 detected PFAS). GW1 and GW3 showed similar degradation trends with increasing e-beam dose, with 36% and 23% degradation, respectively, observed at 750 kGy (Figure 3.5). The percent degradation value for combined PFAS for GW2 matrix was ~70% at 250 kGy and remained similar at 750 kGy. The lack of complete removal of PFAS at <500 kGy in GW samples was similar to the data observed for the treatment of equimolar PFAS in DI water.

6:2 FTS consistently showed the highest removal with 75–98 % degradation observed for GW matrices. The lack of complete degradation of 6:2 FTS can be attributed to both matrix effects and competitive effects as complete degradation was observed for 6:2 FTS as single solute and in mixtures in DI water at doses <500 kGy. After 6:2 FTS, PFOS (25 – 80%), PFHxS (30 – 65%), and PFOA (15 – 54%) showed the highest

degradation and these were similar to what was observed for the treatment of equimolar mixture of PFAS in DI water. Surprisingly and contrary to our results involving DI water treatment, PFOA had a lower degradation efficiency compared to PFOS, which could be attributed to the formation due to oxidation of precursors.

We also observed 96% removal of PFBS from GW2. PFBS was also removed by 20% in GW1 and 74% in GW3 at 750 kGy. This was contrary to data reported in Figures 3.3 and 3.4, where PFBS showed no degradation compared to other PFAS. The alkalinity content of GWs 2 and 3 could play a role in the improvement of PFBS degradation. In a previous study performed to degrade PFOA using e-beam[79], the degradation at 10 kGy increased from 53.8 to 94.9% when the alkalinity was increased from 0 to 100 mg/L as $CaCO_3$. This was hypothesized that carbonate radicals can potentially react with PFOA anions, forming PFOA radicals, that can undergo further degradation.[79] The reactions of carbonate ions (79 and 430 mg/L as $CaCO_3$) in GWs 1 and 3 respectively with PFBS could likely explain the higher values of degradation efficiencies compared to GW1, that had ~79 and ~430 times lower alkalinity than GWs 2 and 3, respectively. A similar explanation for PFBA degradation could be applied with 95% removal observed for GW2. One of the factors for the increase in C/C_0 values observed for GWs 1 and 3 could be attributed to formation of PFBA by degradation of long chain PFCAs and precursors, which were abundant in GW1 and 3 compared to GW2.

3.6   Environmental Implications and Limitations

Based on the findings of the current study, e-beam technique has shown promise in treating PFAS as well as PFAS precursors. Treatment of PFAS-contaminated groundwater was

similar to controlled DI water treatment of PFAS mixtures; however, complete removal was not observed presumably due to interference of competing species present in the groundwater matrix. The calculated EE/O values in DI water ranged from 45 to 504 kWh/m^3/order in single solute samples tested at 100 μg/L of initial concentration. Based on our previous study and other recent publications, these values are comparable to other destructive technologies such as electrochemical oxidation, UV-sulfite and plasma technology[3, 16, 30, 93, 99, 100]. E-beam, similar to these technologies can be used as the final step in a concentrate and destroy approach to remediate PFAS concentrated wastes. However, as e-beam technology, advantageously, is advanced oxidation/reduction technique, it can be used to simultaneously applied to destroy other recalcitrant compounds such as 1,4-dioxane, chloroform, bromoform, sulfamethoxazole etc[16]. These will require doses significantly lower than those required for PFAS remediation, demonstrated by a recent study for 1,4-dioxane, where 5 kGy of e-beam dose completely degraded 10 mg/L of dioxane in DI water[101]. This makes e-beam technology a potential treatment approach for simultaneous remediation of a variety of recalcitrant contaminants.

E-beam can also be directly applied to solids and other complex matrices, implying a similar approach to UV/microwave irradiation[102-104]. It may be possible to directly regenerate spent GAC and IE resins with e-beam and further research is needed to study the feasibility of such applications. Results suggest improved degradation is feasible if higher doses (>1MGy) are applied to treat PFAS mixtures and real groundwater samples. In our study, delivered doses were limited to 1000 kGy due to an increase in temperature observed in our samples with increasing dose. Accelerators with higher dose rate can potentially overcome this limitation. Although good removal of C4-C8 PFAS using e-

beam was observed, the mass balance was not closed after treatment suggesting the presence of unknown transformation products. Experimental work for this study was done on an e-beam accelerator that delivers 1 kW of power only. Commercial accelerators, and the accelerator being developed at Fermilab, can deliver 100s of kWs of power. The latter systems should be capable of delivering high doses to completely defluorinate PFAS mixtures.

However, there are still limitations for the widespread use of this study and use of this technology. The EE/O values calculated as a part of the study are based on decomposition of parent PFAS calculated from the initial and final concentrations. The authors state that although complete defluorination and mass balance for the PFAS tested was not the focus of the study, incorporating conditions that will induce compete defluorination will increase the calculated EE/O values. Secondly, the EE/O values in this study were calculated using the delivered dose, without using the wall-plug efficiency. The estimated power efficiency of the utilized system is ~80% and accounting for this will increase the calculated EE/O values. E-beam technology is an energy-intensive approach and reducing power losses and compact and portable designs will be needed to implement this technology for water remediation.

Since the degradation of PFAS was similar for a wide range of environmentally-relevant initial concentrations, it is suggested from this work that the e-beam approach would be energy efficient when treating concentrated PFAS waste rather than directly treating drinking water. A combination of a concentration step followed by e-beam irradiation (end-of-train treatment) would enable large- scale applications of e-beam treatment of PFAS. This study focused on direct irradiation of contaminated water. With

the limited availability of technologies that can destroy PFAS, e-beams are attractive in the sense that it is able to achieve PFAS degradation within minutes of contact time compared to other technologies requiring several hours of treatment. The ability of e-beam to simultaneously generate both reducing and oxidizing species allows for the destruction of other toxic co-contaminants as reported in other studies[3, 16, 53]. As part of the Department of Energy's mission to get technologies developed in the national laboratories to external entities, Fermilab has designed and is in the process of building a compact, high power, high energy e-beam system that can be operated on a mobile platform. Such advancement in e-beam technologies will allow for increased applications in the water/wastewater treatment and for handling PFAS-containing waste.

3.7 Conclusion

This study successfully utilized a novel e-beam accelerator to investigate the degradation of a suite of PFAS in several aqueous matrices. In single solute samples, at a constant dose, the degradation efficiency did not increase with increasing chain length, with PFBA and PFBS showing the most resistance to degradation. A similar resistance to degradation was observed while treating equimolar mixtures and an increase in short chain PFCAs was observed due to degradation of longer chain PFAS. A negative impact of sample matrix was observed when real-world contaminated groundwater samples were treated, theorized to be due to scavenging of hydrated electrons by matrix components. Interestingly, e-beam was able to simultaneously oxidize PFAS precursors present in these samples, demonstrating its utilization as an oxidative/reductive treatment. These results and the

calculated EE/O values second the notion that e-beam technology is a promising approach to remediate PFAS from aqueous matrices.

TRANSITION 2

This chapter focused on the application of electron beam technology for the destruction of PFAS in several aqueous matrices. Through the collaboration with Fermi National Lab, it was possible to observe degradation trends for PFAS of different chain lengths and functional groups in both single solute and equimolar mixtures. For real-world samples, sample matrix had an effect on the overall PFAS degradation. Interestingly, we observed that e-beams could fully oxidize known and unknown PFAS precursors present in real-world samples, due to the production of oxidative and reductive species.

Due to the collaborative efforts between our lab, Fermi National Laboratory and with data obtained from suspect screening from McDonough lab, we were able to submit an article to Environmental Pollution for publication.

Collaboration between our lab and Fermilab also allowed us to study the degradation of 1,4-dioxane in several aqueous matrices using e-beam technology. This led to a second author publication for me titled "Low doses of electron beam irradiation effectively degrade 1,4-dioxane in water within a few seconds". This was featured in the 'Emerging investigator series but this study is not a part of this dissertation.

The next chapter focuses on the second destructive technique, electrochemical oxidation, for the degradation of PFAS in water.

CHAPTER 4

EFFECT OF CHAIN LENGTH, ELECTROLYTE COMPOSITION AND AEROSOLIZATION ON THE REMOVAL OF PER- AND POLYFLUOROALKYL SUBSTANCES DURING ELECTROCHEMICAL TREATMENT OF WATER

4.1   Introduction

Advanced oxidation processes (AOPs) have been historically utilized to treat compounds such as natural organic matter/disinfection byproduct (DBP) precursors, Volatile organic carbons (VOCs), algal toxins, and pharmaceutical and personal care products and persistent compounds such a 1,4-dioxane.[46] AOPs rely on the generation of highly reactive oxidizing species such as hydroxyl radicals (E_{redox} = 2.8 V) to degrade organic contaminants. The contaminants react with the oxidizing species in the bulk solution via the mechanism of indirect oxidation. Studies have also utilized a combination of AOP with UV light to treat persistent contaminants in groundwaters.[46] PFAS contain a number of carbon-fluorine bonds, which is thermodynamically, one of strongest bonds in the universe.[2, 7, 47] Adding to this, the high electronegativity of fluorine[105] (E_{redox} = 3.06 V) indicates that thermodynamically, it is nearly impossible to oxidize fluorine. The presence of multiple C-F bonds, lack of aromaticity of PFAS and the presence of electron withdrawing groups[106] that reduce the overall reactivity (-COOH and -SO_3H) implies that these compounds are highly resistant to oxidation even by hydroxyl radicals and ozone.[2] Hence, advanced oxidation technologies, by themselves, have shown poor performance in treating waters contaminated with PFAS.[2, 3, 16, 107] Electrochemical oxidation processes (eAOPs) fall under the category of AOPs and utilize electrical energy to potentially degrade persistent organic

compounds. The challenges with AOPs can be overcome with an additional step, direct electron transfer between PFAS molecules and the anode in eAOPs, that can make PFAS susceptible to oxidizing species.

The setup usually consists of a cathode, an electrolyte solution and an anode, with minimal auxiliary chemicals necessary and minimal waste generation.[108] As oxidation reactions take place at the anode (direct oxidation), choice of the anode material impacts the overall performance of the treatment process. In utilizing eAOPs for PFAS treatment, a direct electron transfer (DET) occurs between PFAS molecules and the inactive anodes[100]. This results in the formation of unstable PFAS radicals that can undergo further oxidation by $OH^{\cdot}$[100], formed at the anodic surface, due to water splitting. Hence, eAOPs for PFAS treatment have gained impetus with anodes such as boron-doped diamond (BDD) and titanium suboxide, doped PbO_2/SnO_2 [109, 110] favorably utilized to achieve improved degradation and defluorination efficiencies.[111] Electrochemical oxidation using these electrodes is said to follow the direct electrolysis pathway as the majority of reactions take place in the diffuse layer near the anode surface.[100, 112] Furthermore, non-active anodes such as BDD and titanium suboxide anodes require high overpotential for oxygen generation[100, 108]. This allows the water splitting reaction (Reaction 2) to take place prior to oxygen evolution. As a result, non-active metal oxide electrodes have shown higher efficiencies for oxidation of recalcitrant chemicals.[108]

$PFAS \rightarrow (PFAS^{\cdot})^{+} + e^{-}$ (Reaction 4.1)

$H_2O \rightarrow OH^{\cdot} + H^{+} + e^{-}$ (Reaction 4.2)

Table 4.1 Summary of Previous Work Utilizing eAOPs for PFAS Remediation

Parameter studied	Parameter description
Type of anode	BDD[111, 113, 114], Ti_4O_7 , mesh[115] (BDD, Ti, Ru), sponge (graphene) anodes[116], doped SnO_2 , doped[109, 110] PbO_2 , Ti/RuO_2[117]
Electrolyte used	NaCl[113, 118], Na_2SO_4[113, 119], $NaClO_4$[120], phosphate buffer[121]
Type of matrix used	Ultrapure water[119], GW[122], industrial WW[110], landfill leachate[121]
PFAS studied	C4-C18 PFCAs[113, 114] and C4-C8 PFSAs[114, 116], PFAS mixtures[123]

Amongst the inactive anodes, BDD anodes are the most commonly studied and commercially available for eAOP applications.[100] Chemical vapor deposition is commonly used to grow diamond layer on a substrate material such as niobium/silicon. Boron, a commonly used trivalent dopant impurity due to its low carrier activation energy then substitutes for carbon atoms, giving rise to a p-type semiconductor. This means that there are excess holes created in the matrix, with a hole-hopping mechanism occurring at low doping levels.[100]

Contrary to an AOP system that works by oxidation in the bulk phase, the reactions in an eAOP system take place on/near the surface of the anode.[100, 112] PFAS are generally resistant to advanced oxidation processes due to the presence of multiple C-F bonds on the C-C- skeleton. eAOPs overcome this by including another step, the DET, where an electron is transferred from the PFAS molecule onto the surface of the inactive anode. The first step for the degradation of PFAS in eAOP system is the adsorption step. This is an important step as in an inactive anode, most of the reactions, including the formation of oxidative

species take place near the anode surface. This is followed by the DET step, as shown in Figure 1 between the PFAS anion and the active sites present on the anode surface.[100, 112] It is important to note that while the PFAS-anode interactions occur, a simultaneous water splitting reaction, forming OH· also occurs near the anode surface.

This transfer of an electron from the PFAS molecule to the anode results in the formation of a PFAS radical, as shown in Figure 1. The OH· are incapable of reacting with and degrading PFAS, similar to reactions in an AOP system for PFAS degradation[2, 3] ,prior to Step 2, which is the formation of a PFAS radical. However, post DET, OH· radicals are capable of oxidizing the PFAS radicals with a standard redox potential of 2.8 eV.[124] This results in the formation of degradation byproducts[100, 125], which are further susceptible to OH radical attack.
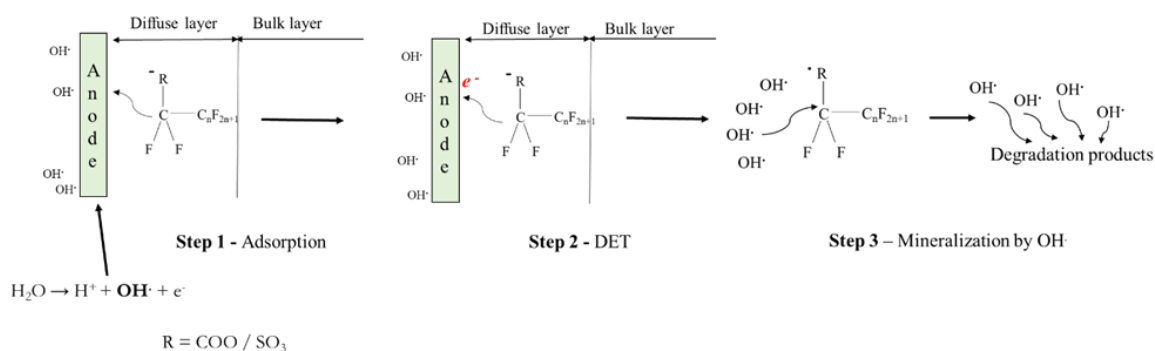
Figure 4.1 Proposed steps for degradation of PFCAs in an eAOP system. Figure adapted from Chaplin et al; 2014 and Radjenovic et al.; 2015, 2020.[100, 108, 112]

As shown in Table 4.1, there have been numerous studies that have designed and utilized electrochemical oxidation to study PFAS degradation.[68, 116, 117, 120, 126-130] These studies have utilized several inactive anodes to study degradation of a suite of PFAS under various water quality and operating parameters (Table 4.1). Although the steps for PFAS degradation using an eAOP system (Figure 4.1) are fairly agreed upon, there is still

contradictory literature on the effect of the supporting electrolyte on the PFAS degradation process. The role of the supporting electrolyte on both the resulting potential at the anode and the participation of supporting anions on the direct oxidation of PFAS radicals is unclear and needs further investigation. Further, it is necessary to identify the factors limiting the degradation of PFAS (such as PFBA, PFBS)[113, 114, 116], post DET step. PFAS tend to accumulate at the air-water interface due to their surface activity and hydrophobic nature. The generation of gas bubbles in eAOP systems have the potential to entrap PFAS, transporting them to the water surface, which can lead to PFAS aerosolization when the bubble bursts. This process can lead to a loss in concentration of PFAS from the solution, which if unaccounted for, can be miscalculated as a part of degradation by the eAOP system. This phenomenon and its effects on the efficacy of the treatment process need immediate investigation.

In this study, we designed and assembled a laboratory-scale batch electrochemical system for the treatment of PFAS in water. We utilized a commercially available BDD anode and a stainless steel cathode as the two electrodes. The main objectives of this study were to:

i.   test the impacts of supporting electrolyte on the PFAS removal and anodic potential

ii. evaluate the effect of varying chain length and functional group of PFAS at various a range of higher than environmentally relevant concentrations (μg/L-mg/L),

iii. assessed the role of aerosolization in the removal of PFAS from eAOP systems, and

iv. elucidate removal pathways by performing a F$^-$ mass balance.

4.2   Research Questions

1. What are the initiating steps in the degradation of PFAS in eAOP systems?

2. What is the role of the supporting electrolyte in the degradation process?

3. How does the PFAS chain length and functional group impact performance?

4. How does the presence of OH radical scavengers in the solution impact the performance of eAOP system?

4.3   Research Hypotheses

1. The degradation of PFAS will occur by i) adsorption onto the anode surface, ii) DET between the anode and PFAS and iii) mineralization by OH radicals.

2. Under similar EC and voltage/current density, the supporting electrolyte will play no role in the overall degradation process, with the degradation efficiencies independent of the anions present in the solution

3. Long chain PFAS will perform better in an eAOP system due to higher hydrophobicity. Similarly, for PFAS with the same chain length, more hydrophobic PFAS (PFOS vs PFOA) will show higher degradation efficiencies.

4. As most of the reactions occur near the anode surface, presence of radical scavengers in the bulk solution will not significantly impact the treatment of PFAS

4.4   Materials and Methods

All chemicals and solvents used in this research were of either certified ACS reagent grade or LC/MS with high purity and were purchased from Sigma-Aldrich (USA) and Fisher Scientific (USA). For the bench scale eAOP system, one liter glass beaker was chosen as the reactor vessel with the sample volume kept constant between 875-900 mL. A circular

glass disk was chosen as the lid material, and it was appropriately sanded down to ensure a shrug fit onto the top of the beaker. A sampling port was drilled on the lid surface in such a way that it ensured a 5 ml Eppendorf pipette tip to smoothly slide in for sample collection.

A commercially available BDD anode was purchased from Hunan Boromond EPT Co Ltd , China and used for the experiments. This anode has a boron doping level between 5000-6000 ppm with an electrical conductivity of 5-15mΩ·cm. The boron doping significantly improves the conductivity of diamond and reduces the resistivity of diamond film to 0.01 ~ 100 Ω cm, which is beneficial for electrochemical reactions. The dimensions of BDD anode are 100 x 20 x 2.0 mm and the upper limit of current density to be applied is 100mA/cm^2 . The stainless steel cathode was purchased from ScienceKitStore, with the dimensions of 125 x 20 mm, An Ag/AgCl reference electrode was purchased from Fisher Scientific. Finally, a 30 V, 5A DC power supply was purchased from Newegg. This is a regulated DC Bench Linear Power Supply with 4-Digits LED Power Display with a readout for voltage, current and power.

Samples were prepared by filling the glass beaker with DIW, with the solution volume kept constant. A known amount of electrolyte (Na_2SO_4, $NaCl$, $CaSO_4$ etc.) was added with the conductivity, pH, ORP, and temperature constantly monitored with a portable Hach multimeter. Through the sampling port, DIW mixed with the supporting electrolyte was spiked from a 10 ppm stock solution of PFAS created in DIW. The electrodes were connected to the power supply cables using alligator clips and the power supply was turned on and the voltage/current was appropriately adjusted. Samples were collected from the sample port in duplicates for PFAS and inorganic fluorine analysis.

Treated samples were diluted (1:1) with methanol to prevent any sorption prior to PFAS analysis. An aliquot of the diluted sample was taken out for further dilution (to fall within the calibration) and the pH was adjusted to near neutral using 10% acetic acid. 10 µL of 100 µg/L isotopically-labeled standards (M2PFOA, MPFOS) were added prior to analysis to provide recovery corrected PFAS concentrations. Samples were analyzed using an Agilent 6495B triple quadrupole liquid chromatography tandem mass spectrometer (LC-MS/MS) equipped with electron spray ionization (ESI). Details about the MRM transitions, analyte recovery, LC-MS/MS conditions are provided as supporting information (Table A4). Sample aliquots taken for inorganic fluorine (F^-) were analyzed by using a portable Hach HQ440d fluorine meter, without any methanol dilution.

4.5   Results and Discussions

4.5.1   Effect of Supporting Electrolyte on PFAS Degradation

To test the effect of supporting anions due to the presence of electrolyte, we performed a controlled set of experiments with PFOA as a model contaminant at an initial concentration of 50 µg/L. The sample volume was fixed at ~875 mL and the starting conductivity was fixed at 1000 µS/cm. The DIW conductivity was adjusted with six different salts, namely NaCl, Na_2SO_4, $NaNO_3$, $Al_2(SO_4)_3$ and KNO_3, with the amount required to achieve the conductivity of 1000 µS/cm, varying with each salt. The removal of PFOA was observed with different electrolytes, with sampling done after every 30 minutes.

As seen in Figure 4.2, the final removal values for PFOA in NaCl and Na_2SO_4 were ~ 84 and 81%, respectively (Figure 4.2a), with the statistical difference being insignificant

in the removal trends (p value = 0.99). This suggested that while the electrical conductivity was the same, presence of supporting anions, SO_4^{2-} and Cl^- did not have an impact on the overall removal process. This was contrary to previous studies involving PFAS removal using BDD anodes[113, 114], which suggested an improvement in PFAS removal in Na_2SO_4 over NaCl as the generated SO_4^{2-} radicals could better oxidize PFAS over the Cl radicals. Our results were also contrary to another study that suggested that addition of Cl^- to a solution of Na_2SO_4 improved the PFAS removal by ~15%, due to Cl radical formation, with excess Cl^- inhibiting the water oxidation[131], with a ~6% reduction in anodic potential reported with Cl^- addition. Although $OH^.$ are considered to be the primary species responsible for direct oxidation of PFAS radicals, previous studies have hypothesized that the supporting electrolytes used during electrolysis such as NaCl, Na_2SO_4 can produce reactive species that can aid in PFAS oxidation. It was theorized that species such as sulfate radical ($SO_4^{2- .}$), and reactive chlorine species (HOCl and $Cl^.$) can aid $OH^.$ in PFAS oxidation, leading to an overall improvement in PFAS removal.[113, 114, 131]

For $NaNO_3$, $Al_2(SO_4)_3$ and KNO_3 (Figure 4.2a), the final removal efficiencies obtained were 53, 51 and 53% respectively with no statistical differences between the removal trends (p value = 0.82). Under the tested conditions, for the five salts chosen as the supporting electrolytes, the statistical differences in the removal trends were not significant (p value = 0.62) although NaCl and Na_2SO_4 did outperform the other electrolytes. This indicates that although anions such as NO_3^-, SO_4^{2-} and Cl^- present in the solution could produce radical species during electrolysis, varying the supporting electrolyte at the tested conductivity and applied voltage did not significantly impact the PFOA removal.

We also investigated the impact of supporting anions of the obtained anodic voltage, at the same starting conductivity fixed at 1000 μS/cm using NaCl, Na_2SO_4 and $NaNO_3$. This was done by using a three electrode system with Ag/AgCl as the reference electrode and BDD anode as the working electrode. Our results also suggested that for NaCl, Na_2SO_4 and $NaNO_3$ for a tested applied voltage range of 5-28 V and at a constant starting conductivity of 1000 μS/cm, the potential at the anode did not significantly vary amongst the three tested electrolytes (SI Table 1) (p value = 0.9).
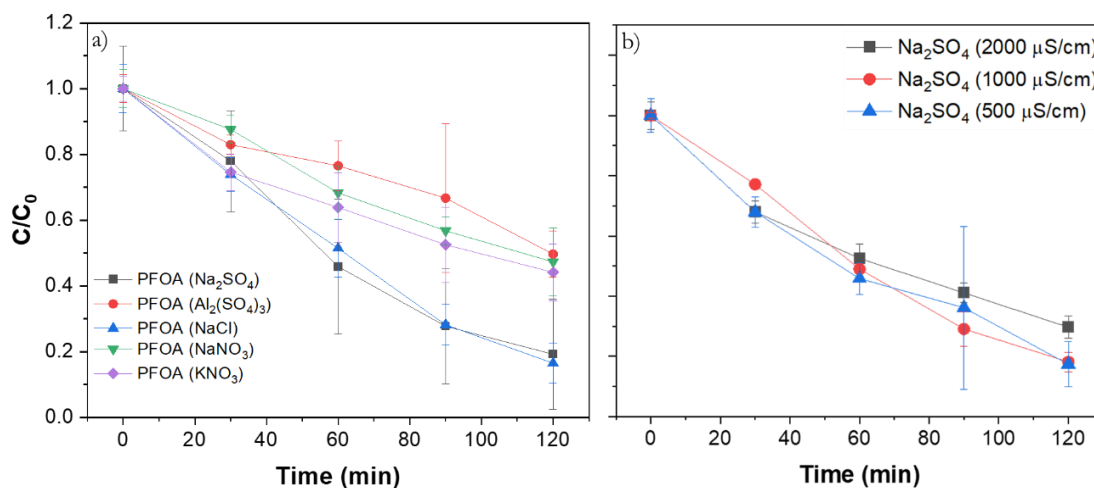
Figure 4.2 a) Removal of PFOA with a) fixed electrical conductivity (1000 μS/cm) attained with different electrolytes. Applied voltage: 12 V (fixed), obtained current density: ~17 mA/cm^2 and b) different conductivities attenuated with Na_2SO_4 . Applied current density: 17 mA/cm^2 (fixed).

This suggests that the anodic potential was not impacted by the presence of supporting anions in the solution, under the tested conditions. As the anodic potential directly can impact the DET mechanism, this shows that the efficacy of the DET between PFOA and the anode was consistent with varying supporting electrolytes.

To further test the effect of supporting anions on PFOA removal, we tested the removal in three different conductivities of 500, 1000 and 2000 μS/cm obtained by Na_2SO_4, with the starting current density of 17 mA/cm^2 (Figure 4.2). Unsurprisingly, to achieve the

desired current density, at 500 μS/cm, the average system voltage was 21 V, while it reduced to 9.1 V at 2000 μS/cm. It is important to note that although the obtained voltage varied across the three solutions, the applied current was kept constant. The final C/C_0 values for solutions with 500, 1000 and 2000 μS/cm of starting conductivity were 0.17, 0.18 and 0.29, respectively with no statistical differences observed in the removal trends (*p* value = 0.96). This indicated that although the amount of sulfate ions increased in the bulk solution from 500 μS/cm to 2000 μS/cm of conductivity, the removal of PFOA was unaffected.

The lack of impact of supporting anions on PFAS removal could be due to a combination of two factors: firstly, the OH· are produced due to water splitting near the surface of the BDD anode while the electrolyte anions are in the bulk phase. This means that they would have to undergo electrolysis to produce radicals such as sulfate and chlorine, migrate to the anode surface to participate in PFAS radical oxidation. This multi-step process potentially reduces the number of anion radicals that are present in the diffuse layer, compared to the OH· radicals. Secondly, the standard reduction potential of OH· radical is 2.8 eV, which is one of the highest redox potentials amongst radical species[124] such as chlorine (2.4 eV) and sulfate (2.4 eV)[124]. Hence, OH· radicals will both preferentially and more effectively be able to oxidize PFAS radicals than other oxidizers in the solution. Thus, based on the obtained data and the above hypothesis, it can be concluded that the supporting electrolyte, under the tested conditions, had no significant impact on the PFOA removal.

4.5.2 Impact of PFAS Chain Length and Functional Group on Removal Efficiency

We tested six PFAS (three perfluorinated sulfonic acids (PFSAs), two carboxylic acids (PFCAs), and one fluorotelomer sulfonate (FTS)) to observe the impact of chain length and functional group on the overall parent PFAS removal. Single solute experiments were conducted with Na_2SO_4 (1000 µS/cm) chosen as the supporting electrolyte with the starting PFAS concentration of 50 µg/L. Figure 4.3 describes the change of C/C_0 at a fixed voltage of 12 V for the PFAS tested in the eAOP system.
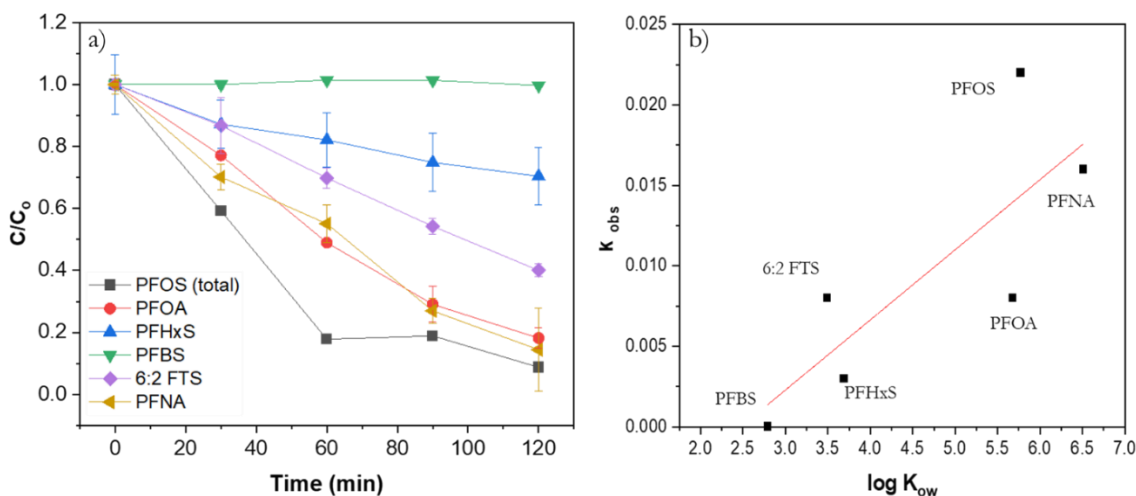
Figure 4.3 a) C/C_0 of PFAS of different chain length and functional group as a function of time. Applied voltage: 12 V, Obtained current density: ~17 mA/cm^2, EC : 1000 µS/cm (Na_2SO_4) b) Correlation plot of k_{obs} as a function of PFAS's log k_{ow}.

As shown in Figure 4.3a, similar removal was observed for long chain PFNA, PFOS (total) and PFOA (p value = 0.78) indicating ~86, 93 and 82% removal respectively. 6:2 FTS displayed ~60% removal, with the final C/C_0 value being 0.4 whereas the removal efficiency for PFHxS (total, *i.e.*, linear + branched forms) was ~30%. For the tested conditions, no removal of short chain PFBS was observed. The data is consistent with previous studies on eAOP treatment of PFAS, where the long chain PFAS have displayed better removal efficiencies than the shorter chain PFAS such as PFBA and PFBS (~50-90%

for PFOA and PFOS vs ~ 5-40% for PFBA and PFBS, under similar conditions)[68, 113, 114, 116].

One of the factors that can affect the DET is E_{anion}^0 defined as the 'anode potential at which a DET can be initiated between the PFAS anion and the anode', calculated by a recent study[112]. As DET essentially involves a direct electron transfer, from the PFAS to the anode, this is essentially an oxidation step. Thus, while looking at E_{anion}^0 values, the lower the value, the easier it is for the PFAS to donate the electron to the anode. Interestingly, the calculated E_{anion}^0 values for PFOS, PFHxS and PFBS were similar at ~3.7 V vs SHE, while the C/C_0 values showed an increasing trend with chain length. 6:2 FTS and PFOA had similar values of 3.03 and 2.91 V vs SHE, while showing 60 and 82% removal in our system, respectively. For the system tested, the anodic potential for an applied voltage of 12 V was ~9 V, higher than E_{anion}^0 required for DET of PFSAs tested. This means that there was sufficient voltage at the anode under the tested conditions, to initiate DET for all of the PFAS tested, assuming the migration of PFAS in the diffuse layer of the anode. Thus, DET was not thought of as the rate limiting step, that affected the PFAS performance in the eAOP system. Thus, for our experimental setup, the E_{anion}^0 was determined to not be a limiting factor affecting the performance of eAOP system in PFAS removal.

We then focused on PFAS properties such as hydrophobicity and solubility that could vary with functional group and chain length. This can affect the performance of PFAS in an eAOP system, where the first step of the electrochemical treatment process is the adsorption of PFAS to the anode surface. To test this, we first calculated the first order rate constants for the different PFAS tested. We then plotted the first order decay constants for

the tested PFAS against their respective octanol-water partitioning coefficient (Figure 3b). The pseudo first order rate constant (k) was calculated by taking the slope of the curve of log (C/C_0) versus time while the log K_{OW} values were obtained from the EPA's CompTox dashboard (predicted average values utilized). Figure 3b displays the plot of k_{obs} and log K_{OW} for the tested conditions with a strong correlation observed (r = 0.80). This indicates that the PFAS hydrophobicity was strongly related to the first order rate constant for the corresponding PFAS in the eAOP system. Thus, the PFAS hydrophobicity was determined to be the limiting factor for PFAS treatment using eAOP system.

Previous studies have reported similar performance of the eAOP systems in treating PFOS isomers.[6, 68, 115] Consistent with these studies, the k_{obs} for L-PFOS, br-PFOS and PFOS (total), were all ~ 2 x 10^{-2} s^{-1} showing no significant difference. However, for PFHxS, the k_{obs} for L-PFHxS was 3.2 x 10^{-3} s^{-1} , ~2.3 times the k_{obs} for br-PFHxS at 1.4 x 10^{-3} s^{-1}. This is hypothesized due to a greater variation in the log K_{OW} values between PFHxS isomers, compared to PFOS isomers. However, as the PFHxS isomers are not as well studied as PFOS isomers, our observation needs further investigation and testing. Based on the variation of k_{obs} for PFHxS, this strengthens the point made by a previous study[6] that while using eAOPs as well as other destructive techniques for PFAS treatment, it is essential to account for the isomeric behavior of PFAS towards the removal mechanism of the treatment technique used.

4.5.3   PFAS Removal Influenced by Gas Bubbles Generated in eAOP System

The water splitting below the oxygen evolution potential can still lead to H_2 gas formation, leading to bubble formation, in which the gas can be trapped. These bubbles can entrap the surface-active PFAS carrying it on the air-water interface, enabling the hydrophobic PFAS

to a surface for adsorption. As the bubbles reach this interface, their surface activity causes them to burst, leading to PFAS aerosolization and removal from the system. This was evident in our eAOP system by an observable condensation on the beaker rim and the lid formed during the treatment process. Post eAOP treatment (2 hours) of PFAS studied in section 3.2, we attempted to quantify the PFAS enrichment by first transferring the treated solution carefully into an HDPE bottle. Utilizing a spray bottle, we collected PFAS enriched on the beaker rim and the lid with methanol. We transferred the methanol with PFAS condensate into a 50 mL polypropylene tube, measured the volume collected, and analyzed it on the LC-MS/MS after appropriate dilution. Similar to sea-spray aerosol enrichment, the eAOP system has the potential to enrich PFAS at the air-water interface.[132] This is due to the surfactant properties of PFAS and the formation of bubbles due to H_2 formation at the cathode surface, that can aid in PFAS enrichment.[100, 132, 133]
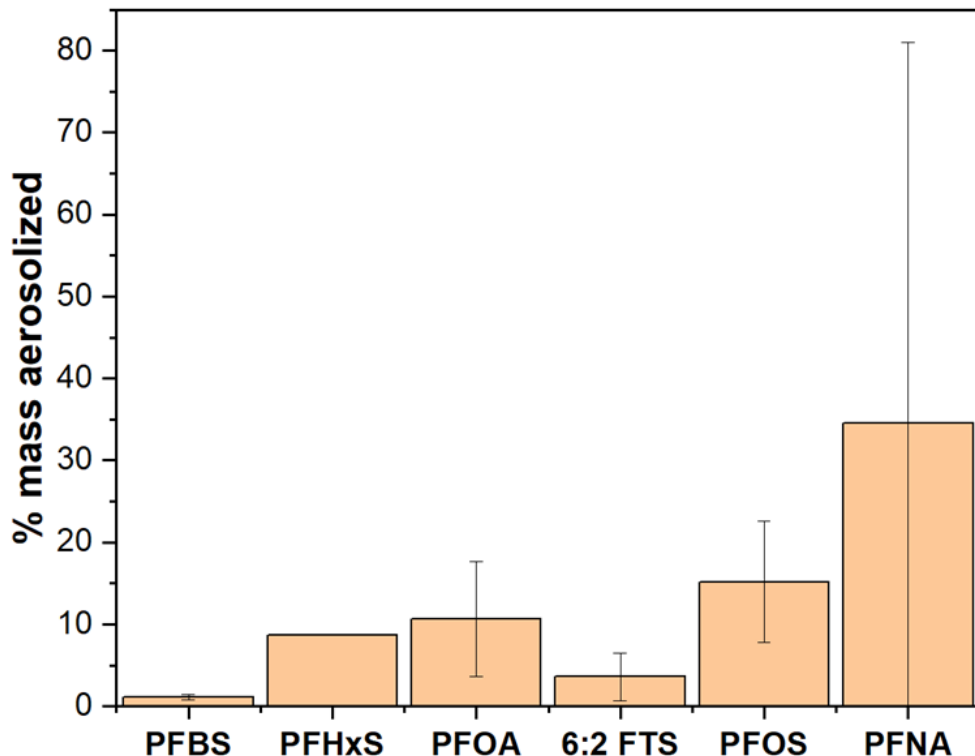
Figure 4.4 Percentage of mass of PFAS aerosolized by electrochemical aerosol formation. Initial single solute PFAS concentration: 50 ppb. Applied voltage: 12 V, anodic voltage: 9.2 V, Electrical conductivity: 1000 µS/cm (Na_2SO_4).

PFNA showed the highest removal due to aerosolization, with an average of ~40% of the initial mass aerosolized and captured on the reactor lid. However, in one of the experimental runs, ~85% of PFNA was aerosolized when the initial concentration was ~5 µg/L. Average removal of PFOS and PFOA by aerosolization were ~ 15±7 and 11±7%, while ~10% removal was observed by PFHxS. The removal of and PFOA showed similar removal by aerosolization, with ~12.5 and 15 % mass aerosolized, while PFHxS showed ~10 % enrichment. It is important to note that PFOS, PFOA and PFNA showed >80% removal while PFHxS showed only ~30% during the eAOP treatment. The enrichment data is consistent with previous study focusing on electrochemical aerosol formation that indicated an increase in enrichment with an increase in chain length attributed due to higher surface activity.[132] It is important to note that the aforementioned study was designed to

pre-concentrate PFAS as a sample preparation technique[132]and was not a treatment study. The lower removal by aerosolization of 6:2 FTS in spite of its similar chain length as PFOS could be associated with lower surface activity induced by its polyfluorinated chain compared.[134] PFBS, due to its low surface activity, displayed almost no enrichment (<2%), while also undergoing no removal in the eAOP system. Results from the current study showed that while degradation of PFAS using the eAOP system was the ultimate goal, PFAS removal by aerosolization can occur during the treatment. If unaccounted for, this would lead to i) overestimation of the treatment efficiency if the percent degradation was calculated based on the initial and final concentration and ii) risk of contamination and health risks to the surrounding environment and individuals.

Thus, due to the phenomenon of enrichment, it is important to note that the removal referred to in this study, denotes a 'loss in concentration', a combination of PFAS degradation and aerosolization, that combined to reduce the initial concentration of PFAS. Our setup was not optimized to capture all of the PFAS aerosolized by the eAOP system, and it may be possible that the condensate on the lid may have re-entered the solution, and thus underestimating our calculation of the mass of PFAS aerosolized. Based on the results of this study, we recommend previous studies that utilized eAOP processes for PFAS removal to revisit their data to calculate the 'true' degradation happening in their system accounting for PFAS aerosolization. Although the current study focuses on using BDD anodes, this would apply to all eAOP systems for PFAS remediation, that produce H_2/gas bubbles due to cathodic reactions. For future studies, while performing the reactor and experimental design, it is important to factor in the loss in PFAS, due to the aerosol

formation to both avoid overestimating the performance of the eAOP system tested and preventing > ppm levels of PFAS contamination in the reaction setup.

4.5.4 Fluorine Mass Balance for PFAS Removal

Some studies have proposed degradation mechanisms for PFCAs and PFSAs by pathways involving $OH^{\cdot}$, H_2O and O_2 cycles, while acknowledging that the exact degradation mechanisms still remain unknown.[100, 112, 135] A recent study utilized kinetic modeling to illustrate the degradation mechanism of PFOA by using eAOP.[125] Although this study gave an insight about PFOA degradation, this was based on DFT calculations and the mechanisms of other PFAS classes still remain unknown. In this study, we attempted to perform a mass balance of total fluorine in the system both before and after eAOP treatment. We tested single solute samples for four PFAS (PFOA, PFOS, PFNA and 6:2 FTS) at an initial concentration of 1 mg/L. The applied voltage/current density was fixed at 12V/17 mA/cm^2 and the solutions were run for a period of 6 h with aliquots periodically taken for both PFAS and inorganic fluorine analysis. After treatment, the PFAS loss via aerosolization was accounted for as described in the previous section.

Similar to single solute samples at 50 ppb (Section 3.3), PFNA showed the highest loss in concentration with almost complete removal observed at ~240 minutes. PFOS also showed compete removal in six hours while the final percent removal for PFOA and 6:2 FTS was ~80 and 70%, respectively. These results were similar to single solute samples at 50 ppb initial concentration samples where 6:2 FTS showed the lowest removal amongst the four compounds tested. However, the trends for inorganic fluorine detected in the solution after treatment are different than removal trends. Assuming complete defluorination, the maximum fluorine detectable for 1 ppm for PFOA, PFOS, 6:2 FTS and

PFNA would be 0.69, 0.64, 0.57 and 0.69 mg/L. Based on these values, the percent defluorination for PFOA, PFOS, 6:2 FTS and PFNA were obtained as 48, 20, 41 and 25 %, respectively while the percent removal values were ~ 80, 100, 70 and 100 %, respectively.
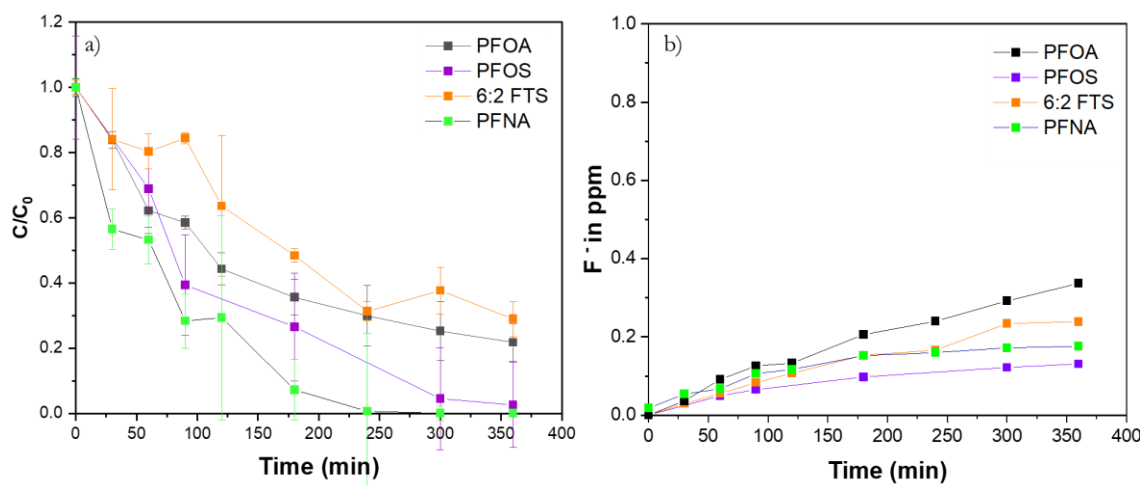
Figure 4.5 a) C/C$_0$ of PFAS of different chain length and functional group and b) mg/L fluorine released as a function of time. Applied voltage: 12 V, EC : 1000 µS/cm (Na$_2$SO$_4$), initial concentration: 1 ppm.

Although no short chain PFCAs/PFSAs were detected post PFOS treatment, there was an increase in short chain PFCAs namely PFHpA, PFHxA and PFPeA post treatment of PFOA and 6:2 FTS. This was consistent with previous studies that observed an increase in PFCAs post PFOA removal[119, 125], however, the formation of short chain PFCAs accounted for <10 % of the total PFAS initially present in the solution for both PFOA and 6:2 FTS. This is contradictory to other destructive techniques (UV-ARP, e-beam, plasma)[3, 6, 30, 136], where chain shortening by DHEH was the dominant removal mechanism for PFCAs. Other byproducts measurable within our instrument capabilities were not detected in the system after treatment. Based on the parent PFAS and its byproducts detected, measurement of inorganic fluorine and kinetic modeling proposed in previous studies[112, 125], the following steps are proposed as the dominant mechanism for PFOA removal.

$$C_7F_{15}COOH \rightarrow C_7F_{15}COO^- + H^+ \qquad \text{(Reaction 4.3)}$$

$$C_7F_{15}COO^- + h^+ \rightarrow C_7F_{15}COO^\cdot \qquad \text{(Reaction 4.4)}$$

$$C_7F_{15}COO^\cdot \rightarrow C_7F_{15}^\cdot + CO_2 \qquad \text{(Reaction 4.5)}$$

$$C_7F_{15}^\cdot + OH^\cdot \rightarrow C_7F_{15}OH \qquad \text{(Reaction 4.6)}$$

$$C_7F_{15}OH - H^+ \rightarrow C_7F_{15}O^- \qquad \text{(Reaction 4.7)}$$

$$C_7F_{15}O^- + h^+ \rightarrow C_7F_{15}O^\cdot \qquad \text{(Reaction 4.8)}$$

$$C_7F_{15}O^\cdot \rightarrow C_6F_{13}^\cdot + COF_2 \text{ (repeat steps 17-23)} \qquad \text{(Reaction 4.9)}$$

$$COF_2 + H_2O \rightarrow CO_2 + 2\ HF \qquad \text{(Reaction 4.10)}$$
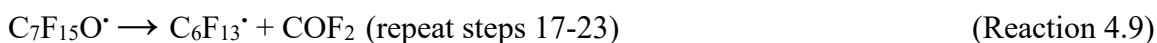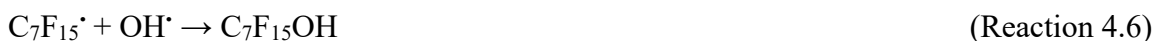
PFAS will generally exist in its anionic form as per reaction 1 at the highly acidic boundary layer near the anode surface.[100] Post the loss of an electron (DET), the anionic form is transformed into a PFAS radical, which, in the case of PFOA, loses its carboxylic acid group[100, 112, 137], forming a $C_7F_{15}^\cdot$. Although reactions 4-6 result in the formation of $C_7F_{15}O^\cdot$ determined to be thermodynamically stable by DFT modelling[125, 137], another mechanism termed as the O_2 cycle may also occur yielding the same product. This pathway involves the reaction of $C_7F_{15}^\cdot$ with O_2 forming a $C_7F_{15}OO^\cdot$, which eventually dissociates to yield $C_6F_{13}^\cdot$. This dissociation yields COF_2 as a byproduct which can further hydrolyze to yield inorganic fluorine as per reactions 7 and 8. Depending on the reaction cycle, the byproducts could be CO_2, F^-, PFAS alcohols and short-chain PFCAs, that can undergo further reactions.[100, 119, 135, 138, 139] Generation of short chain PFCAs and inorganic fluorine could not account for 100% of the total mass balance, indicating that there are other pathways/removal processes (*e.g.*, aerosolization) that need further investigation. This is, however, beyond the analytical capabilities of our instrument and beyond the scope of this study. The lack of short chain PFCAs and PFSAs detected for PFOS during eAOP treatment

as opposed to reductive destructive treatments such as e-beam[80] and UV-sulfite[30] suggests that a similar removal mechanism may occur to the one proposed for PFOA. However, similar to PFOA, more research that focuses on removal mechanisms and thermodynamic modeling are needed.

We additionally performed a fluorine mass balance for PFOA and 6:2 FTS at initial concentration of 1 ppm. After spiking the parent PFAS in the electrolyte solution, the fluorine can compartmentalize into (i) organic fluorine in the solution (parent PFAS and transformation products); (ii) organic fluorine loss from aerosolization; (iii) inorganic fluorine generated from defluorination of PFAS; and (iv) irreversible adsorption and/or precipitation of organic/inorganic F onto the anode surface. For PFOA and 6:2 FTS, the total fluorine recovery, calculated on a molar basis was 68 and 69%, respectively. The inorganic fluorine released during the eAOP treatment accounted for the highest fluorine fraction, with 41 and 33 %, respectively for PFOA and 6:2 FTS. The organic fluorine fraction due to short chain PFCA formation accounted for <5%, while the parent PFAS still present in the solution accounted for ~21 and 28%, respectively, for PFOA and 6:2 FTS. Although both PFOA and 6:2 FTS were detected via enrichment, their contribution to the total fluorine was <3 %, due to the higher initial concentration utilized for this study. The incomplete fluorine mass balance indicates that there are more factors that should be accounted for.

One of these is the adsorption of fluorine onto the anode surface. A previous study[140] using BDD anodes for PFOA treatment (8 mM) performed an XPS analysis on the anode surface post treatment. A clear F1s peak was observed on the BDD anode surface after eAOP treatment, indicating that fluorine adsorption could occur during the eAOP

treatment of PFAS. To test this, we performed energy dispersive spectroscopy (EDS) for the submerged and non-anode surface to test for presence of fluorine on the anode surface. Post treatment, there was no F1s peak observed on the anode surface, indicating that either the adsorbed fluoride was below the detection limit of the instrument or that minimal adsorption of fluoride on the anode occurs. Thus, it is hypothesized that the rest of the mass balance can be closed by analyzing the organic fluorine, post treatment of the solution and to entrap any volatiles that are generated during the eAOP process. Suspect screening could also elucidate degradation pathways and byproducts, leading to a near complete fluorine recovery.

4.6   Conclusion

This study demonstrated the effectiveness of electrochemical oxidation as a treatment approach for PFAS remediation. Using commercially available BDD anode and a stainless steel cathode, we were able to design and utilize a bench-scale electrochemical system to study PFAS removal. At a constant electrical conductivity, this study demonstrated that the supporting anions, introduced by changing the supporting electrolyte did participate in PFAS degradation. This was further supported by a lack of variation in the anodic voltage, which was measured for the tested supporting electrolytes by varying the applied voltage. A fluorine mass balance, post treatment, revealed inorganic fluorine as the major transformation product for PFOA and 6:2 FTS. Although short chain PFCAs were detected, post treatment, a lack of complete mass balance shows the formation of unknown transformation byproducts that requires further examination.

This was the first study to demonstrate that the gas bubbles produced at the cathode could transport and aerosolize PFAS out of the solution for eAOP treatment of PFAS. It differentiated between PFAS removal and degradation and emphasized the need to account for PFAS aerosolization to prevent overestimation of the treatment efficiency and performance. Accounting for PFAS aerosolization would reveal 'true' degradation efficiency and can be used by future researchers to report PFAS compartmentalization, post treatment by eAOPs. This work resulted in an article submitted to 'Environmental Science: Water Research & Technology', which is currently in review (December 2023).

TRANSITION 3

Until now, I focused on utilizing two destructive technologies for PFAS remediation. While comparing the data I obtained with previous studies that focus on treatment of PFAS, either by sequestration or destruction approaches, I noticed that they combine branched and linear isomers of PFAS to report it as PFAS-total. This is also true regarding the current regulations (October 2023) that combine the branched and isomeric forms as total PFAS to design drinking water regulations and advisory limits.

However, it was interesting to see that PFAS isomers behaved differently in the two treatment technologies studied. Branched isomers of PFOS and PFHxS showed near complete degradation at the lowest e-beam doses tested, compared to the linear isomers, that showed varying degradation efficiencies. In the eAOP reactor, degradation trends of the branched isomers were either almost identical or poorer compared to the linear forms. We then performed a literature review to see if there were studies focusing on isomeric distribution of PFAS and the consequences on treatment technologies.

To our surprise, there was no review paper that summarizes the effects of isomeric distribution on the various treatment approaches. Hence, Chapter 5 is a critical review paper titled "The need for testing isomer profiles of perfluoroalkyl substances (PFAS) to evaluate treatment processes". This was published in Environmental Science and Technology in October 2022.

CHAPTER 5

THE NEED FOR TESTING ISOMER PROFILES OF PERFLUOROALKYL SUBSTANCES (PFAS) TO EVALUATE TREATMENT PROCESSES

5.1   Introduction

Two of the most used and studied PFASs are perfluorooctanoic acid (PFOA) and perfluorooctane sulfonic acid (PFOS). Although the intent is to manufacture linear forms of PFOA and PFOS for various applications, the type of manufacturing process used can result in the formation of different chain lengths and structural isomers of PFASs as impurities[7, 141, 142]. Electrochemical fluorination (ECF) and telomerization are the major manufacturing processes for PFOA.[141] As the ECF process is of a free-radical nature, it leads to the rearrangement and breakage of the carbon chain. This leads to the production of linear and branched isomers, mainly perfluorinated as well as homologues of the raw material[7]. The 3M Co. was the major manufacturer of PFOA from the 1950s until 2002, after which perfluorooctyl chemistries were phased out. The 3M Co. PFOA, measured in 18 production lots over 20 years was found to be approximately 78% linear and 22% branched.[7, 141, 143] Since 2002, large scale production of linear PFOA has continued by telomerization process and is considered to be the predominant perfluoroalkyl carboxylic acid (PFCA) manufacturing process. The telomerization process is one that involves addition of a free radical to a starting telogen with a taxogen that is usually unsaturated. This results in a chain lengthening by units of CF_2-CF_2, which when subjected to oleum oxidation, can yield PFOA.[144] The result of the telomerization process is a product (*e.g.*, PFOA) that is isomerically pure, but can contain chain length impurities.

In contrast, ECF can result in greater numbers of byproducts, including branched and linear isomers that can have odd and even chain lengths.[144] PFOS has predominantly been manufactured by ECF, while telomerization sources for PFOS are unknown. The 3M Co. produced PFOS from the 1950s to 2002 with a distribution of approximately 70% linear and 30% branched.[141, 143] Since the phase out of PFOS by 3M Co. in 2002, production of perfluorooctane sulfonyl fluoride (POSF) and its derivatives has continued in developing countries.[141] The residual impurities, generated as byproducts of PFAS manufacturing processes, can influence the isomeric distribution of PFASs in the environment. In addition to PFOA and PFOS, other PFASs can also exhibit isomerism, including several PFCAs such as PFBA/perfluorobutanoic acid (C4), PFPeA/perfluoropentanoic acid (C5), PFHxA/perfluorohexanoic acid (C6), PFHpA/perfluoroheptanoic acid (C7), PFNA/perfluorononanoic acid (C9), PFUnA/perfluoroundecanoic acid (C11) [144, 145], perfluorosulfonic acids (PFSAs) such as PFPeS (C5), PFHxS (C6)[86, 144, 146], POSF[144, 147]and perfluorooctane sulfonamide (FOSA).[148]

In the past two decades, although many pieces of literature have reported multiple PFASs in diverse aquatic environments, PFAS isomers (*i.e.*, branched or br-PFAS vs. linear or L-PFAS forms) have received relatively little attention, probably due to analytical difficulty and the relatively low abundance of branched isomers compared to their linear counterparts in the environment.[86, 148, 149] The structural difference between linear and branched PFAS isomers would determine their physical and chemical properties, such as hydrophobicity, leading to differing fate and transport mechanisms of PFAS isomers in the environment. In some instances, the concentration of branched isomers may surpass linear isomers in source waters. [86, 150] This may have an impact on the overall treatment efficiency

of PFASs as a few studies have highlighted the variation in the treatment efficiency between linear and branched isomers of PFASs.[54, 80, 151-155] For example, early breakthrough of branched isomer from granular activated carbon (GAC) filtration system[155, 156] and preferential degradation of branched isomers over linear form in destructive approaches[54, 80, 157] have been reported. In this paper, we highlight the need for differentiating the isomers of PFASs during treatment/remediation approaches as the branched-to-linear ratio in source waters can influence the overall treatment efficiency of the selected approach. The specific objectives of this critical review paper were to (i) summarize the environmental occurrence of branched and linear isomers of PFASs; (ii) highlight isomer-dependent physicochemical properties and toxicokinetics of PFASs, (iii) provide the current understanding of the variability in treatment efficacy between PFAS isomers, and (iv) highlight the impact of isomer profile on PFAS treatability.

5.2 Research Questions

1. What is the variation in distribution of PFAS isomers in different natural environmental compartments?

2. What is the variability in physicochemical properties of PFAS isomers?

3. How can the variation in physicochemical properties impact the selection and efficiency of treatment techniques?

4. What are some of the analytical challenges that occur during quantification of PFAS isomers?

5.3   Isomeric Distribution of PFAS in the Environment

Source waters can have large variations in the isomeric distribution of PFASs. One of the factors contributing to this is the proximity and type of PFAS manufacturing industry, that can greatly influence the type of PFASs released into the environment. The isomeric distribution in natural waters can also be influenced by the inherent properties of linear and branched forms. A recent study[86] summarized the global distribution of linear and branched forms of PFASs in surface water, groundwater, and seawater. They found that ratio of br-PFAS to L-PFAS in certain surface waters was higher than expected. This was attributed to the higher normalized organic carbon to water partition coefficient[148] of L-PFAS compared to the branched forms, elaborated more in the later sections. They further theorized that this could lead to stagnant water bodies such as lakes having a reduced percentage of L-PFAS than flowing bodies such as rivers, as river currents might reduce adsorption further from equilibrium conditions. Linear isomers accounted for 42–87% in lake waters and for 24–89.5% in river waters, with the distribution highly dependent on the location and water source. Similar to behavior in sediments, L-PFAS sorb better to soils than the br-PFAS, leading to relatively higher concentrations of br-PFAS in groundwaters.[86, 141] The br-PFAS are less retarded during subsurface transport, leading to a possible enrichment of br-PFAS in groundwater with distance.[158] [85] This was also observed in a recent study conducted in El Paso County, Colorado, when PFOS isomer concentration was analyzed at locations near and further away from the source. The average br-PFOS contribution (br-PFOS to PFOS-total) was ~26% near the source but increased to ~46 % at the location furthest from the source[10]. It is also important to note that biotransformation could enhance the concentration of L-PFAS in the environment due to

the preferential degradation of br-PFAS.[158] However, the preferential transformation of br-PFAS precursors over L-PFAS precursors[159, 160] could increase the br-PFAS/L-PFAS ratio in the environment, making concentration estimations and predictions entirely based on source tracking in environmental samples difficult.
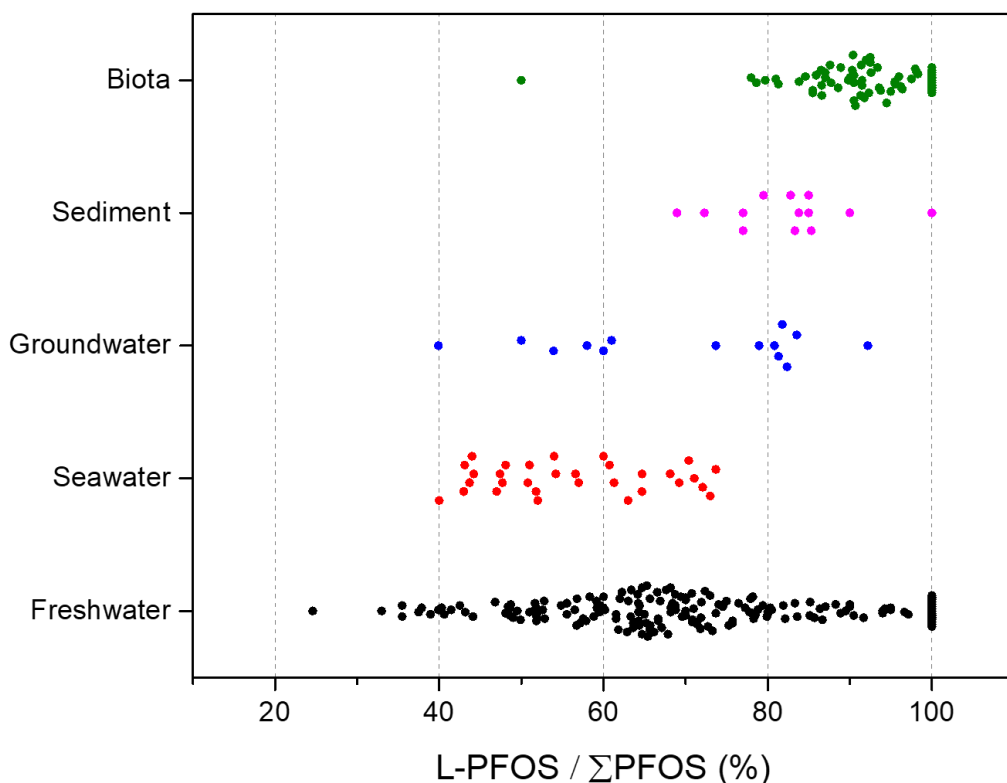
Figure 5.1 Representation of percentage of L-PFOS present in various environmental matrices.[4, 56, 57, 85-87, 141, 144, 145, 148-150, 158, 161-181] Dots represent ratios calculated at multiple data points using average L-PFOS and br-PFOS values.

Figure 5.1 summarizes the percentage of linear PFOS (L-PFOS) out of total PFOS in the environment reported in the literature. The ratio (L-PFOS/∑PFOS), represented as %L-PFOS, varies significantly between the aqueous phase, abiotic solids (sediment and suspended particles), and biota and is also influenced by different locations and studies. The largest variation of the L-PFASs was observed in freshwater systems, ranging from 25% to 100%. In contrast, %L-PFOS showed a more compact distribution in sediment and

biota samples, ranging from ~70% to 100%. These distributions seem to be impacted by the differences in the sorption properties of linear and branched isomers of PFOS. For PFOA, the L-PFOA accounted for 50% to 100% in water and 80% to 100% in sediment and biota samples.[4, 165] For PFHxS, the linear L-PFHxS accounted for 64% to 99% in water and 85% to 96% in sediment and biota samples. PFOS exhibited a more considerable variation in terms of the isomeric fractionation than PFOA and PFHxS. Because of the nature of the longer chain-length of PFOS, the outcome of isomeric fractionation of L-PFOS from br-PFOS would be more distinct after a series of natural and anthropogenic processes, possibly due to the greater variation in physicochemical properties reported between the isomeric forms with increasing chain length.[146]

Several factors are known to govern the composition of PFAS isomers in water. First of all, the release from manufacturing processes (*e.g.*, ECF and telomerization processes) can directly determine the isomeric distribution of PFASs in water. Natural and anthropogenic processes can further modify the ratio between linear and branched isomers. For natural processes in water, L-PFAS would preferentially sorb to suspended particles, sediments, and phytoplankton cells, therefore leading to scavenging of L-PFAS from the aqueous phase and the enrichment of L-PFAS in abiotic solids[148] and algal cells. Floating foam formed by natural organic matter could also take up more L-PFAS than br-PFAS, leaving more br-PFAS in the bulk of water. Preferential degradation of branched over the linear precursors can increase the concentration of br-PFAS in the environment. The distribution amongst the branched isomer products can also differ due to the difference in biotransformation rates of br-PFAS precursors.[160] In organisms, L-PFAS is known to be

more bioaccumulative and br-PFAS can be eliminated faster, explaining why L-PFASs are often highly enriched in biota (Figure 5.1).

5.4 Variation in Physicochemical Properties of Different PFAS Isomers

There are only a few studies that report the variation in physicochemical properties of PFAS isomers as summarized in Table 5.1.[146, 147, 182-184] In a study done by Chen et al. (2015), the field-based water sediment distribution coefficients (K_d) were used to calculate the organic carbon-water partitioning coefficient (K_{OC}) values[148]. For PFOA, the L-PFOA had a log K_{oc} value of 3.11 ± 0.38 cm^3/g whereas the iso, 4m and 5m (br-PFOA) forms had relatively lower log K_{oc} values of 2.96 ± 0.48, 2.77 ± 0.53, and 2.82 ± 0.51 cm^3/g, respectively.

Table 5.1 Reported and Predicted Physicochemical Properties of PFAS Isomers in Literature Along with Their Significance

PFAS analyte	Property	Reported values	Difference in value for br-PFAS relative to L-PFAS	Significance
L-PFOS[183]	CCC bond angle	~115°	~ 4.3 – 5.2 % ↓	Distortion in molecular structure impacts molecule stability
br-PFOS[183]		~109 – 110°		
L-PFOS[183]	Relative ΔG of the acidic form (normalized)	0 kJ/mol	-	More positive ΔG indicates higher reactivity
br-PFOS[183]		1.4 – 14.6 kJ/mol		
L-PFOS[148]	Sediment derived log K_{oc}	~3.38 cm^3/g	~ 6.2 – 34 % ↓	Higher K_{oc} values indicate higher partitioning onto sediment phase
br-PFOS[148]		~2.22– 3.17 cm^3/g		
L-PFOA[148]		~3.11 cm^3/g	~ 4.8 – 10.9 % ↓	
br-PFOA[148]		~2.77 – 2.96 cm^3/g		
L-PFOSA[148]		~4.41 cm^3/g	~ 17.6 % ↓	
br-PFOSA[148]		~3.63 cm^3/g		
L-PFOSA[160]	Dynamic bioconcentration factor (BCF) in carp	~ 134 L/kg	~ 92 % ↓	Higher BCF indicates longer retention in the body
br-PFOSA[160]		10.7 L/kg		
B vs L-PFOS[185]	Retention in rats	NA	-	Branched isomers are preferentially excreted in rats compared to linear forms
L-PFNA[186]	Growth-corrected elimination rate constants in male rats	0.012–0.018	~ 50 % ↑ (average)	Branched isomers are preferentially excreted in rats compared to linear forms
Br-PFNA[186]		0.019–0.026		
L-PFOS[184]	Human population average half-life *	2.91 years	~ 77.3 – 81.7 % ↓	Branched isomers are preferentially excreted in humans compared to linear forms
1m-PFOS[184]		0.55 years		
3/4/5m-PFOS[184]		0.64 years		
2/6m-PFOS[184]		0.66 years		

Table 5.1 (Continued) Reported and Predicted Physicochemical Properties of PFAS Isomers in Literature Along with Their Significance				
L-PFOS[187]	K_d (dissociation constant for human serum albumin)	$8(\pm4)\times10^{-8}$		Linear isomer preferentially binds to human serum albumin
3m-PFOS		$4(\pm2)\times10^{-4}$		
4m-PFOS		$8(\pm1)\times10^{-5}$		
5m-PFOS		$9(\pm5)\times10^{-5}$		
L-PFOA		$1(\pm9)\times10^{-4}$		
3m-PFOA		$4(\pm2)\times10^{-4}$		
4m-PFOA		$3(\pm2)\times10^{-4}$		
L-PFOS[188]	Drinking water equivalent levels (DWELs) in µg/L[53]	0.29	206 – 637 % ↑	Higher DWEL levels suggest less effectiveness in reducing thyroid hormonal blood levels
1 m-PFOS[188]		1.26		
2 m-PFOS [188]		1.84		
3 m-PFOS[188]		1.40		
4 m-PFOS[188]		1.75		
5 m-PFOS[188]		2.14		
6 m-PFOS[188]		0.89		
br-PFPeA[146]	Predicted octanol-water partitioning coefficient, dry (log $K_{OW, dry}$)	3.24 – 3.42	0.29 – 5.5 % ↓	Higher K_{OW} values indicate higher potential for bioaccumulation
L-PFPeA[146]		3.43		
br-PFHxA[146]		3.54 – 4.01	1.2 – 12.8 % ↓	
L-PFHxA[146]		4.06		
br-PFHpA[146]		3.61 – 4.64	0.64 – 22.6 % ↓	
L-PFHpA[146]		4.67		

* Model considers original serum levels in humans. ↑ and ↓ indicate increase and decrease respectively in the percentage value of the property being considered.

A similar trend was observed for PFOS where the L-PFOS had the highest log K_{oc} value of 3.38 ± 0.43 cm^3/g and the values for br-PFOS ranged from $2.65 - 3.17$ cm^3/g.[148] These values suggest that the L-PFASs are more likely to be preferentially distributed (~16% more) in the particulate phase than the br-PFASs. This could explain the lower-than-expected concentrations of the L-PFOS in surface and groundwaters (as shown in Figure 5.1) as the preferential adsorption would enrich the br-PFOS/L-PFOS ratios in the aqueous phase.

Although L-PFAS have higher K_{ow} values compared to br-PFAS, bioaccumulation factors for PFAS generally don't correlate well with K_{ow} and are better predicted using protein binding coefficients. This is because PFAS do not follow a lipophilic persistent organic pollutant's traditional bioaccumulation pattern. Composition of branched and linear PFOS in human serum and their association with adverse health outcomes were recently reviewed[86]. Branched PFOS isomers tend to have shorter half-lives in the human body than linear PFOS, likely due to the variation in affinity for lipids and transporter proteins, including varying binding affinities for human serum albumin and organic anion transport proteins[184, 189]. The average half-lives for L-PFOS were found to be $4.4 - 5.3$ times higher than that of br-PFOS in a cohort with AFFF-impacted drinking water.[184] This may have implications for remediation targets and safe drinking water levels that are defined for branched versus linear isomers. Differences in toxicokinetics have been considered when developing Drinking Water Equivalent Levels (DWELs), resulting in lower values for L-PFOS (0.26 µg/L) versus br-PFOS isomers ($0.89 - 2.14$ µg/L) in this case suggesting that the linear isomers pose a greater risk for lowering thyroid hormonal blood levels.[188] For the most part, current regulatory levels do not differentiate between

branched and linear isomers. In cases where branched isomers make up a significant portion of total drinking water contamination, this may mean that recommended levels would become more conservative. At this time there are not sufficient data related to differences in relative source contributions and reference doses for branched versus linear isomers to safely define distinct isomer-specific drinking water guidelines.

Despite their faster elimination rates, branched PFOSs are found at similar levels to linear isomers in serum from some populations, with typical %br-PFOS ranging from 30%– 50% .[86] In contrast, most wildlife studies report lower contributions from branched isomers (Figure 5.1). This may indicate greater exposure of humans to PFAS precursors, which are transformed *in vivo* to form perfluoroalkyl acids (PFAAs), with preferential formation of branched isomers. While much remains to be learned about relative source contributions, it is likely that among the general population, human exposure to metabolically labile precursors originates primarily from sources other than drinking water, such as certain foods, paper products, textiles, and other consumer products.[11, 190, 191]

The structural and thermodynamic properties of the PFAS isomers can provide insights into their overall stability and susceptibility to degradation. It was found that all the carbon-carbon-carbon (CCC) angles for L-PFOA were approximately 115° whereas in br-PFOS, the CCC angles where the -CF$_3$ group was bonded, were approximately 109-110°. [183] This distortion in the CCC angle in the backbone structure can affect the stability of the br-PFAS[183], making them less stable and more susceptible to degradation. This can be further elucidated by comparing the Gibbs free energy (ΔG) of the PFOS isomers by setting the least positive value to zero for relative comparison. It was observed that for the acidic forms, L-PFOS had the least positive value of ΔG and was set to zero while 1-CF$_3$–

PFOS, 2-CF$_3$–PFOS, 3-CF$_3$–PFOS, 4-CF$_3$–PFOS, 5-CF$_3$–PFOS and 6-CF$_3$–PFOS had ΔG values ranging from 1.4 – 14.6 kJ/mol, where n-CF$_3$-PFOS indicates branching at the carbon position 'n'.[183] A more positive ΔG value for br-PFAS indicates that these isomers are more likely to be reactive and degraded by reactions with species such as hydrated electrons or hydroxyl radicals[183] than their linear counterparts. However, it is important to note that the study done by Rayne et al (2010) using different models to predict the ΔG values of isomers of PFOS and PFOA pointed out the lack of utility of using thermodynamic data for PFAS isomeric distribution studies. When the authors studied the thermodynamic stability of isomeric forms of alkanes such as hexane and heptane, the modelling data agreed with the experimental data in stating that the linear form of alkanes was the least stable thermodynamically. The model predicted similar results for PFASs, where the L-PFOS and L-PFOA were predicted to be the least stable, with stability increasing with branching. The authors attributed this to a lack of thermodynamic data available for PFCAs and stated that improved models might be essential for accurate datasets[147], that could bridge the gap between predicted and experimental data, where L-PFAS have been found to be the dominant isomers. As a result, although certain models may predict L-PFAS as the most stable form under certain conditions, more information is needed to accurately predict stability of various PFAS isomers from mere thermodynamic data.

A similar conclusion, favoring the stability of the L-PFASs, however, can also be drawn based on the bond dissociation energies (BDE) of L-PFAS and br-PFAS. Previous studies have reported that the BDE values ranked in the order of tertiary<secondary<primary bonds.[192] This means that the initial C-F bond cleavage occurs

at the bond with the lowest BDE, *i.e.*, the tertiary C-C bond.[192] Thus, it can be expected for br-PFASs to behave differently during various physical and chemical treatment processes impacting the overall PFAS treatment efficiency.

5.5   Impact of Isomeric Properties on Treatment Performance

Difference in the physicochemical properties between PFAS isomers and their relative levels in source waters can influence the overall treatment efficiency of PFAS. In the case of adsorption techniques such as GAC filtration, where the dominant mechanism is hydrophobic interaction with contaminants, the L-PFASs tend to show better removal than the br-PFASs. This has been reported in previous studies[151-153, 155] using GACs as well as materials such as Geothite.[193] A study involving a pilot scale GAC system indicated that the br-PFAS showed earlier breakthrough than their respective linear isomer, attributed to better interactions between L-PFAS and GAC.[156] In another study involving 2-stage carbon filters, the relative percentage of br-PFOS kept increasing in treated waters as water passed through the filters.[152] This would also imply that the br-PFAS would exhibit an earlier breakthrough from GAC columns than L-PFAS.

In case of adsorption processes involving charged interactions as the dominant mechanism, there would be minimal effect on the final L-PFAS : br-PFAS ratio after treatment.[153, 154] In a previous study that utilized anion exchange resins (AIX) and GAC to remove PFCAs, PFSAs and FOSA, similar removals were observed for PFOS, PFHxS, and FOSA isomers using AIX, but branched isomers showed lower removals using GAC.[153] In another study to remove PFCAs and PFSAs utilizing magnetic AIX, identical uptake was observed for br-PFAS and L-PFAS.[154] As br-PFAS and L-PFAS will have similar

electrostatic interactions, we hypothesize that treatment techniques that rely on charged interactions with PFAS will not have an observable impact on the isomeric distribution of PFASs in treated water.

The ΔG and the BDE will play a crucial role when considering the interactions of PFAS isomers with reactive species during chemical treatment processes. As mentioned previously, in certain cases, the br-PFAS possess more positive ΔG (thus more reactive) and a lower BDE than L-PFAS. This makes them more prone to an attack by reducing species and susceptible to degradation. In a study done to evaluate reductive defluorination of PFOS, br-PFOS showed more susceptibility to reductive dehalogenation than L-PFOS[157]. When PFOS degradation was performed by electron beam, br-PFOS preferentially degraded over L-PFOS attributed to higher electron affinity of branched isomers.[80] Similar results were observed for PFOS using a UV-sulfite system and using photodegradation[95] where the br-PFOS degraded faster than L-PFOS due to the tertiary – CF_3 group being more susceptible to degradation.[54] In another study done by using UV-sulfite to degrade PFASs of different chain length and functional group, rate constants for degradation for branched forms (>2 h^{-1}) of PFOS, PFHpA, PFHpS, PFHxS and PFOA were an order of magnitude higher than the corresponding linear forms (0.018 – 0.440 h^{-1}). [98] Thus, it can be concurred that contrary to adsorption techniques, destructive treatment will enrich the L-PFAS-to-br-PFAS ratio due to the preferential degradation of branched isomers. However, this may not be valid in certain destructive techniques such as electrochemical oxidation that employ a two-step mechanism. This technique consists of inactive electrodes such as boron-doped diamond or Magneli-phase titanium suboxide anodes, where the first step is the adsorption of PFAS on the surface of the electrodes,

followed by a direct electron transfer[68, 100, 108, 193, 194] (DET) reaction and mineralization of the PFAS radical by hydroxyl radicals. As the first step of this technique involves a sorption step, the linear isomers would be preferentially adsorbed and partake in the DET and get degraded in the process. This may lead to a scenario where more L-PFAS are degraded than br-PFAS leading to a possible enrichment in the br-PFAS in the treated water. Thus, as more and more destructive techniques involving multi-step mechanisms are looked at for PFAS treatment, it is essential to understand the behavior and monitor the final concentrations of PFAS isomers.

5.6   Analytical Challenges in Quantifying Isomers of PFAS
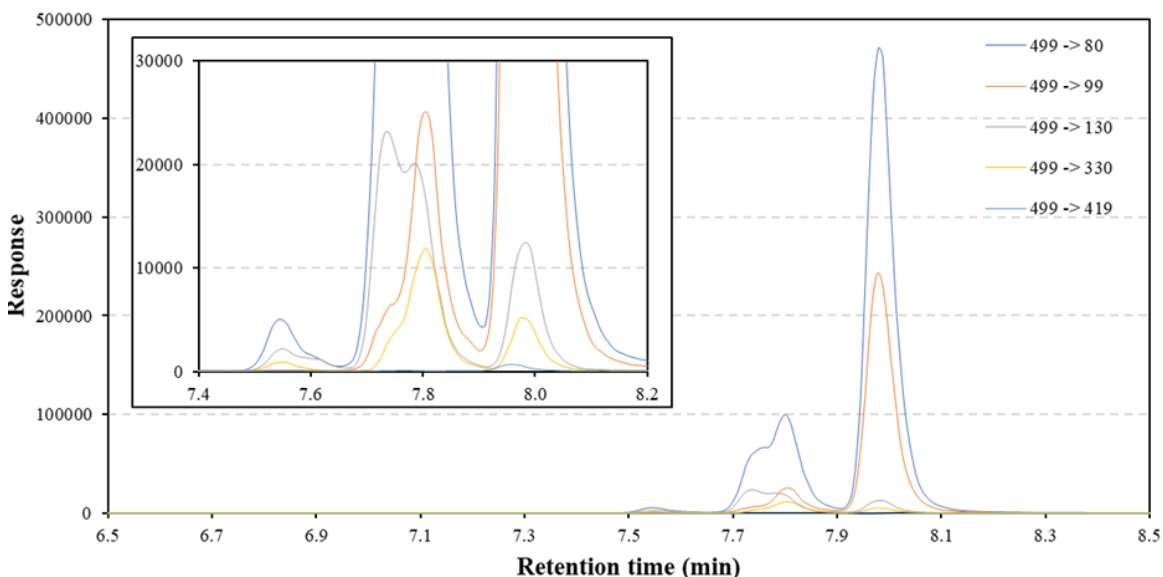
Figure 5.2 LC-MS/MS chromatogram representing linear and branched forms of PFOS isomers. The response is from a 5 pg injection.

EPA Methods 537.1 and 533 are commonly used by research and commercial laboratories for PFAS measurements in water matrices. However, the fraction of linear and branched isomers for the same compound can vary based on the supplier for the analytical standards.

This was clearly shown by Vyas et al (2007) that for potassium perfluorooctane sulfonate (K-PFOS) from different manufacturers, the percentage of linear form varied from 76.0 ± 1.9% to 82.2 ± 0.9%.[195] Similarly, for perfluorooctane sulfonyl fluoride, linear form accounted for 71.8 ± 1.3 to 74 ± 1.6, based on the manufacturer.[195] In the majority of commercially available PFAS standards and neat materials, the relative mass or concentration of linear and branched PFAS is often not reported. ^{19}F NMR is required to accurately determine the fraction of the isomeric composition. Although liquid chromatography tandem mass spectrometer (LC-MS/MS) can differentiate branched and linear PFAS (for PFOS, PFHxS, etc.), the EPA methods require the users to integrate both peaks together and report total concentration rather than isomeric-specific concentrations. Ideally, the assumption is that the peak area can reflect the mass of the uncharacterized isomers in samples. However, the instrument sensitivity, the collision energy, and the abundant ion transitions of each isomer is different and therefore can potentially lead to a bias in quantification of total PFAS levels. A summary of analytical techniques including column specifications, reagents utilized etc. to identify different PFAS isomers by previous studies can be found in Table 5.2.

Table 5.2 Summary of Analytical Techniques Used for Differentiating Branched and Linear Isomers

Column	Column dimensions	Analytical reagents	Injection volume	Instrument	PFAS isomers (with count) studied[*]	Study
FluoroSep-RP Octyl column	150 × 2.1 mm, 3 μm particle size	methanol and water (3 mM formic acid in water, adjusted to pH 4.0 with ammonia)	10 μL	LC-MS/MS	PFOA (4), PFOS (6), PFOSA (2)	Chen et al; 2015[148]
FluoroSep RP Octyl column	150 × 2.1 mm, 3 μm particle size	methanol and water (adjusted to pH 4.0 with ammonium formate)	20 μL	HPLC−MS/MS	N-EtFOSA(12), FOSA (6), PFHpA (4), PFHxA (8), PFOA (10), PFOS (11), PFNA (11), PFDA (3), PFUnA (7), PFDoA (18)	Benskin et al; 2007[196]
BEH C18 column	2.1 × 50 mm, 1.7 μm particle size	methanol and 2 mM ammonium acetate	1 μL	UPLC MS-MS	PFOS (2)	Gu et al; 2016[54]
Hypersil Gold pre-column + Betasil C18 column	10 × 2.1 mm, 5 μm particle size + 50 × 2.1 mm, 5 μm particle size respectively	methanol and water (both with 10 mM aqueous ammonium acetate	10 μL	HPLC	PFHxS (2), PFOS (2)	Belkouteb et al; 2020[151], Ahrens et al; 2016[197]
Zorbax Extend-C18 column	2.1 × 50 mm, 1.8 μm particle size	methanol and ammonium acetate in water (pH 6)	10 μL	HPLC + Q-TOF	PFOS (8)	Trojanowicz et al; 2019[31]
Zorbax RRHD Eclipse Plus C18 column	100 mm x 2.1 mm, 1.8 μm particle size	methanol and 5 mM ammonium acetate in water	-	LC-MS/MS	PFOS (2)	Park et al; 2020 [155]
Zorbax Eclipse Plus C18 column	4.6 mm x 100 mm, 3.5 μm particle size	3% methanol in water and 10 mM ammonium acetate in methanol	-	HPLC + MS/MS	PFPeA, PFHxA, PFHpA, PFOA, PFNA, PFBS, PFPeS, PFHxS, PFHpS PFOS, FPeSA, FHxSA, FOSA, N-TAmP, FHxSA (2 for each)	Rodowa et al; 2020[156], Barzen-Hanson et al; 2017[198]

Table 5.2 (Continued) Summary of Analytical Techniques Used for Differentiating Branched and Linear Isomers

C18, analytical column	100 × 3.0 mm, 5 µm particle size	methanol and 20 mM ammonium acetate in water	1 mL	QTOF	PFOS, PFHpS, PFHxS, PFOA, and PFHpA (2 for each)	Tenorio et al; 2020[98]
Perfluorinated phenyl (PFP) phase + X-Terra C18 phase	150 × 2.1 mm, 5 µm particle size 100 Å pore size + 100 × 3.0 mm, 3.5 µm particle size, 125 Å pore size respectively	methanol and 4 mM ammonium acetate in water	-	ion trap mass spectrometer (LCQ	PFOS (7)	Langlois et al; 2006[199]
Thermo Acclaim 120 C18 column + FluoroSep RP Octyl column (3 mm, 2.1mm150 mm	4.6 × 150 mm, 5 µm particle size + 2.1× 150 mm, 3 µm particle size	Acetonitrile and 10 mM ammonium acetate in water	-	HPLC + MS/MS	PFHxS (2), PFOS (6), PFOA (6)	Gao et al; 2019[85]

*Note: 2 indicates br (grouped together/single isomer studied) and L-PFAS

Previous researchers have also observed in case of PFOS isomers that if the isomer profile in the sample and the quantification standards were not identical, this could lead to an analytical bias of unknown proportion.[144, 200] This was further quantified by a latter study that used individual, purified PFAS isomers to compare the response factors, albeit relative to the linear isomer. The 1-CF$_3$ PFOS was monitored using a mass to charge (m/z) ratio of 80 whereas 4,4-CF$_3$ m2- and 4,5CF$_3$-PFOS (br-PFOS) were monitored using a ratio of 99. It was observed that at least one PFOS isomer was missing from the final chromatogram, irrespective of the product ion used.[141, 201] This could lead to underreporting of certain isomers, leading to an analytical bias being introduced during quantification. An example chromatogram featuring br-PFAS and L-PFAS with different precursor-product pairs is shown in Figure 5.2. It is challenging to separate and quantify every single branched isomer and therefore it is understandable that EPA Methods 537.1 and 533 only require determining linear and "bulk" branched isomers. Transitions 499→80 and 499→99 are chosen for PFOS quantification and qualification because m/z 80 and m/z 90 are the most common products among all PFOS isomers and m/z 80 gives great sensitivity. A systematic bias could also be introduced during analysis if the concentration of branched isomers in samples reaches the detection limit. This could lead to the contribution of linear form for PFAS to be incorrectly reported as 100%. This bias can be eliminated by reporting the ratio of each individually detected branched isomer to the linear isomer.[141]

To demonstrate the uncertainty that can occur with different calibration methods, as an example here we use K-PFOS standard purchased from Wellington Lab Inc. with %L-PFOS of 78.8%. Calibration method 1 involved the addition of peak areas of linear and branched isomers, creating one calibration curve to calculate the total PFOS

concentration and then calculating linear and branched PFOS concentrations separately based on the fraction of the peak area. Calibration method 2 involved the generation of two calibration curves based on the peak areas for linear and branched PFOS individually with the well-characterized standard, calculating their concentrations separately and then summing the values to determine the total PFOS concentration. Both linear and quadratic regressions were used for creating calibration curves (Figure 5.3). To simulate the uncertainty in these two methods, we fixed the total peak area equivalent to 1 μg-total PFOS/L but varied the percentage of the linear isomer's peak from 0% to 100% to calculate total PFOS concentrations using Methods 1 and 2. The simulated result is shown in Figure 5.3. Because the total peak area (linear plus branched) is fixed, the calculated total PFOS concentrations by Method 1 was the same regardless of the fraction of L-PFOS (Figure 5.3(ii) a and b, blue lines). In contrast, the calculated total PFOS concentrations by Method 2 (Figure 5.3(ii) a and b, red lines) showed a clear deviation from Method 1. Two methods have a similar result only if the fraction of L-PFOS in the sample is very close to the calibration standard (where the blue and red lines cross, L-PFOS/total-PFOS = ~0.75). The deviation becomes greater as the L-PFOS fraction declines or increases. The relative percentage deviation (Figure 5.3(ii) a and b, green lines) between two methods can be up to 15% in certain cases, and the deviation is primarily contributed by branched isomers. It should be noted that such deviation can vary a lot from one analytical batch to another, depending on the quality of the calibration curves established. This simulation demonstrates that biases could occur merely due to the selection of calibration methods and PFAS standards. As a result, the concentrations of L-PFAS and br-PFAS reported in the literature and summarized in Figure 5.3 can differ based on the method employed. Thus,

for accurate quantitative of PFAS isomers in samples, it is not only important to select correct analytical techniques mentioned in Table 5.2 but also the PFAS standards and the methods that can distinguish different PFAS isomers.
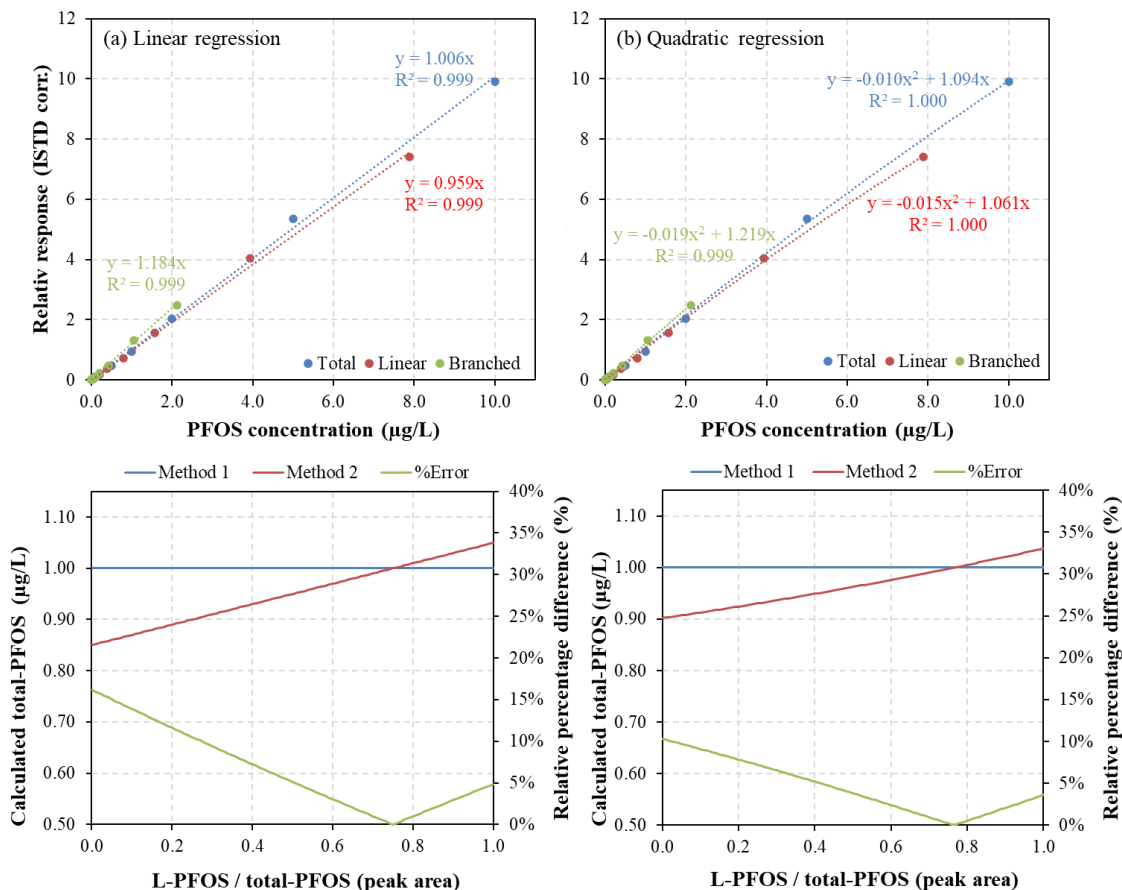
Figure 5.3 Calibration curves of K-PFOS using (a) linear and (b) quadratic regressions. The calibration ranges from 0.010 to 10.0 µg/L. The intercept is forced to zero. Simulation of the calculated total PFOS concentration using Methods 1 and 2 with (c) linear regression and (d) quadratic regression, as a function of the peak area of L-PFOS/total-PFOS. Green lines represent the relative percentage difference (RPD) between two values calculated by Methods 1 and 2, respectively.

5.7   The Need for Testing PFAS Isomers in Source Waters and Treatment Processes

The scientific community has not recognized the need to differentiate PFAS isomers during development and testing of treatment technologies. This is partly due to the absence of any differentiation in the regulation of PFAS isomers and limitations with available analytical methods as highlighted above. Many U.S. states have proposed stringent drinking water limits for selected PFASs in drinking water at concentrations lower than 10 ng/L.[202-205] Changes in the isomeric profile in source water can lead to preferential treatment of L- or br-PFAS and depending on the type of technologies used, and some scenarios may lead to concentrations exceeding the regulatory limit in treated water. Although the differences in properties and the resulting fate of different PFAS isomers during treatment may seem to be small, at such low regulatory limits, these differences could influence the overall treatment efficiency. For example, the presence of higher levels of br-PFAS in source waters can impact GAC performance by reducing the life of the carbon requiring frequent changeouts and thus increasing the cost of treatment. For many destructive approaches, like advanced oxidation processes (AOPs), the treatment conditions are optimized in laboratory settings prior to full-scale operation. If the PFAS isomer profile in the source water utilized for the optimization process is different from actual field conditions, the treatment technology may not perform ideally to achieve treatment goals.

This can be elucidated by Figure 5.4 that simulates the PFOS (total) concentration after treatment utilizing destructive techniques (Figure 5.4a) and sequestration techniques (Figure 5.4b) as a function of L-PFOS in source water. The model considers initial concentrations of PFOS in source water to range from 50 ppt to 100 ppt. The extreme scenarios are defined by the treatment of PFOS from 100 ppt with the lowest degradation

efficiency reported in the literature (black curve) and by the treatment of PFOS from 50 ppt with the highest degradation efficiency reported in the literature for br-PFOS and L-PFOS (red curve). The upper and lower limits of the curve are chosen based on analysis of EPA's UCMR3 data that reported a mean PFOS concentration of 77 ppt in source water. [206] For destructive techniques the model considers efficiencies of 100% (br-PFOS) and 45% (L-PFOS) reported for UV-sulfite technique[54] to generate the line of highest degradation and of 90% (br-PFOS) and 13% (L-PFOS) reported using e-beam technique as line of lowest degradation.[80] Similarly, the model considers removal efficiencies of 90% (L-PFOS) and 80% (br-PFOS) using GACs[153] and 35 % (L-PFOS) and 25 % (br-PFOS) estimated for treatment using coagulation[2, 207] as lines of highest and lowest removal, respectively. The shaded regions below the corresponding curve represent violation of state regulations or federal limits as a function of L-PFOS fraction.

For destructive techniques (Figure 5.4a), it can be noted that the total PFOS concentration post-treatment increases with the increase in %L-PFOS. This can result in a violation of California reporting limit (6.5 ppt, notification limit) first and eventually the New York State limit (10 ppt) at a L-PFOS fraction of 0.21 for the high degradation scenario. As the fraction of L-PFOS increases, the final PFOS concentration (total) can violate NJ limit (13 ppt) and NH limit (15 ppt) at L-PFOS fractions of 0.35 and 0.46, respectively. A similar trend occurs for the line with lowest removal observed in Figure 5.4a, however the individual US state violations occur at a much lower fraction of L-PFOS in the water, shown by numbers adjacent to the fraction of L-PFOS at which the violation occurs, eventually violating the EPA drinking water limit (70 ppt) at L-PFOS fraction of 0.81. For sequestration techniques, CA state regulation is violated using coagulation

approach to treat 50 ppt of initial concentration of PFAS (Figure 5.4a) but as the fraction

L-PFOS increase, the system performance improves below CA limit at a fraction of ~0.7.

It is important to note that this model does not include the interim updated health advisory

limit of 20 parts per quadrillion or 0.02 ppt published by the EPA[208]. However, even at the

lowest initial PFOS concentrations used in the model of 50 ppt and at highest removal

efficiencies of 90 and 80 % for L-PFOS and br-PFOS respectively, the lowest value attained

of total PFOS is still ~5.5 ppt, approximately 275 times higher than the interim health

advisory limit proposed for PFOS of 0.02 ppt.[208]
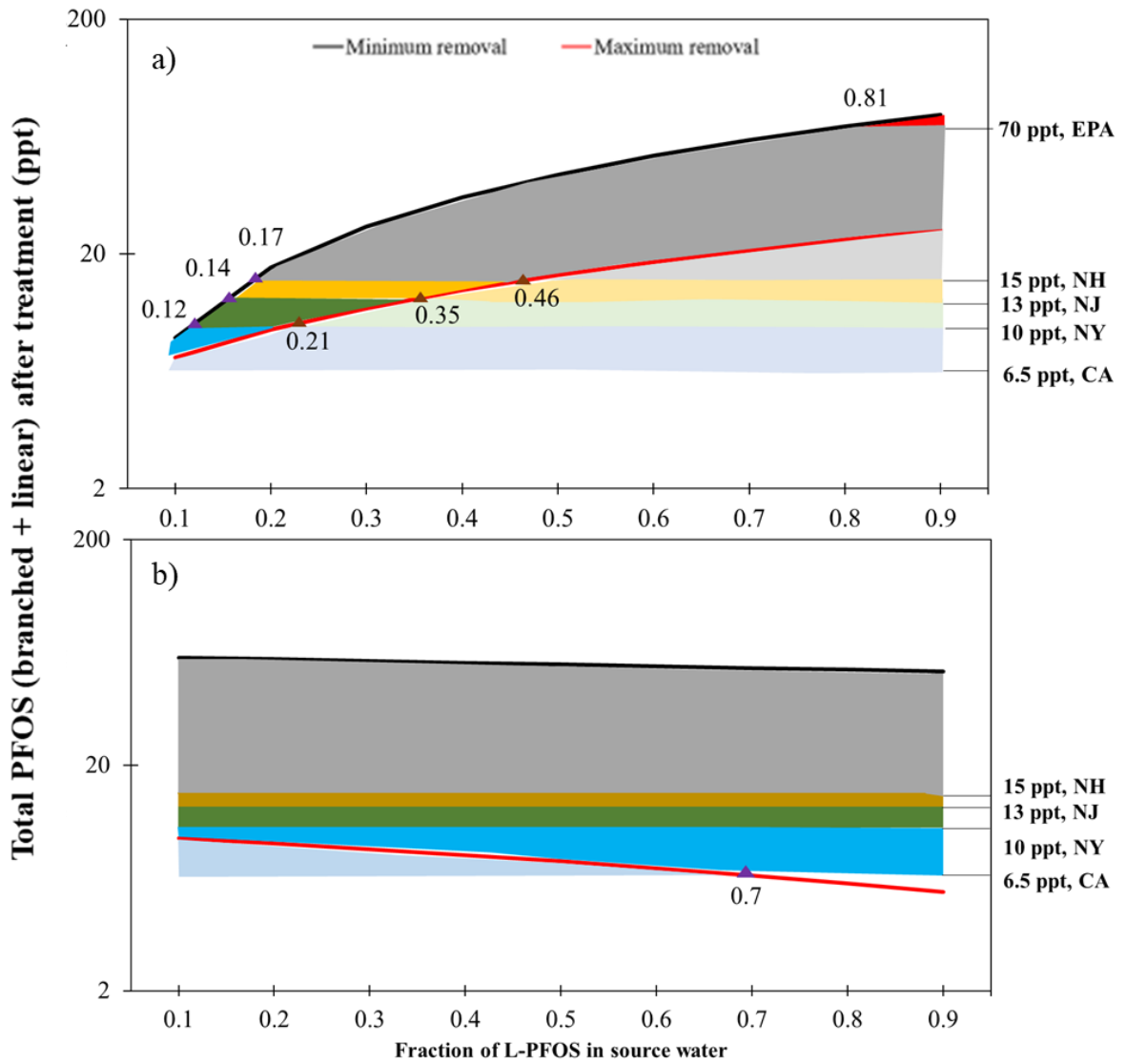
Figure 5.4 Simulation of total PFOS after treatment using (a) destructive techniques and (b) sequestration techniques as a function of fraction of L-PFOS in the source water. Upper black curve represents a scenario featuring minimum removal percent efficiencies for L-PFOS and br-PFOS at (a) 13 and 90%[54] and (b) 35 and 25%[207], respectively when treating a source water with initial total PFOS concentration of 100 ppt. Bottom red curve represents a scenario featuring maximum removal percent efficiencies for L-PFOS and br-PFOS at (a) 45 and 100%[80] and (b) 90 and 80%[153], respectively when treating a source water with initial total PFOS concentration of 50 ppt. Shaded regions below the curve represents scenarios showing violation of individual state and federal PFOS limits after treatment. Numbers adjacent to the curves indicate fraction of L-PFOS at which a particular violation occur.

This simulation demonstrates that the same treatment system can violate or abide by a regulation limit if the isomeric composition of the source water changes over time. This simulation highlights the need for considering the isomeric distribution of PFAS in source waters and during the design/selection of treatment approaches for PFAS. This critical review highlights the need to consider the following when studying PFASs that exhibit isomers:

1) Standardized analytical methods are needed to differentiate and quantify the isomeric forms of PFASs in the source waters.

2) Violation of federal and state regulatory limits may occur due to inaccurate data processing and exclusion of branched isomers from analysis.

3) Selection and optimization of treatment technologies are contingent on the isomeric distribution of PFASs in source waters;

4) Research needs on degradation rates, reaction mechanisms, and competitive sorption of specific isomers in environmentally realistic mixtures; and

5) Consideration of the behavior and transformation of different isomers of PFAS precursors and their impact on the final results of different water treatment

TRANSITION 4

In this dissertation, Chapters 2, 3 and 4 focused on e-beam and electrochemical oxidation as destructive approaches to breakdown PFAS into less toxic, more manageable byproducts. Findings from these studies and the general consensus, based on the current literature, revealed that destructive technologies would be more energy efficient if combined with a pre-concentration step such as GAC, IX, NF or foam fractionation techniques. As a part of a 'concentrate and destroy' approach, PFAS concentrations would be elevated from ng/L to mg/L or even g/L, with the concentrate treated with a destructive technology such as e-beam/DC plasma, UV-ARP technology. By reducing the sample volume and the number of treatments necessary, it would make the treatment train approach energy efficient and economically feasible.

Thus far for my PhD dissertation, I focused on remediation of PFAS in aqueous matrices. Although PFAS were primarily considered aqueous contaminants, soil as a compartment for PFAS accumulation should not be overlooked. The organic matter in soils can provide adsorption sites for the accumulation of PFAS. PFAS can then leach from the soil into aqueous matrices such as groundwater and surface water, making the treatment of these soils essential to study. Hence, the next chapter of this dissertation focuses on remediation of PFAS in contaminated soils.

CHAPTER 6

AIR-BUBBLING ASSISTED SOIL WASHING APPROACHES FOR PFAS CONTAMINATED SOILS

6.1   Introduction

The importance of soils as a potential global PFAS reservoir was first highlighted by a study in 2012[209, 210] that looked at the concentrations of 13 PFAS in surface soil samples. This was an extensive study, with samples collected from 60 locations from 6 countries. Interestingly, the samples were collected from locations far from known PFAS-contaminated locations and estimated the global soil loadings of PFOA and PFOS to be 1860 and >7000 metric tons respectively.[209, 210] A follow up study utilized data from previous findings and estimated the average load of PFOA and PFOS to be 1000 metric tons.[210] These results stated the importance of the vadose zone as a major reservoir for PFAS. PFAS accumulated in this zone can serve as a long-term contamination source to groundwater, surface water and eventually the atmosphere and biota.

The term 'soil remediation' can be viewed as the management of the contaminant as a particular site that aims to minimize or mitigate the damage to health of humans and/or the environment. The first step involves the identification of the soils that require remediation and evaluation of the contamination and their concentrations. The next stage includes setting the remediation objectives, development of remedial strategies and the risk evaluation. Remediation strategies are chosen based on the treatment goals, nature and concentrations of the contaminants, with the protection of human life and environment, considered as key elements.[211] Broadly, soil treatment technologies can be classified into three categories: (i) physicochemical, (ii) biological, and (iii) thermal.

The approaches for soil remediation can be classified as either *in situ* or *ex situ*. Gas fractionation is an approach that was demonstrated in a recent study to increase the PFAS removal nine times compared to other soil remediation approaches[212]. This was an in-situ approach that was impacted by the gas type, the flowrate and the fractionation time[212]. Similarly, more *in situ* approaches have been recently investigated for PFAS contaminated soils. A recent study showed successful extraction of an undisturbed, 3 m deep, sandy vadose zone soil contaminated with aqueous film forming foam (AFFF) by gas fractionation enhanced soil washing in Norway, with removal efficiencies ranging from 11-73%[213]. However, the efficacy of an *in situ* process is affected by the soil permeability, affected by the undisturbed soil structure[214]. PFAS tend to preferentially adsorb to air-water interfaces in soil pores or micropores and thus, this process can unintentionally permeate PFAS beyond the remediation zone and in the surrounding matrix.[214]

Soil washing is an *ex situ* physicochemical technology that has been historically used to remove organic and inorganic contaminants such as metals, polycyclic aromatic hydrocarbons and polychlorinated biphenyls.[214-217] Soil washing can be viewed as the removal of contaminants from soil usually by physical and/or chemical separation to reduce the volume going to waste or incineration. Compared to *in situ* approaches, this approach offers better handling and control and can limit migration of contaminants into the surrounding matrix. For a contaminated site, post excavation. attrition, a wash solution is used to aid in extraction of contaminants from the soil phase. The waste solution gets concentrated with the chemical of interest and the treated soil can potentially be transferred back to the original site.

The research on identifying soil washing techniques for PFAS removal from contaminated soils is limited.[210, 214, 218-220] A study investigated the soil from Eielson Air Force Base in Fairbanks, Alaska, which was treated in bench-scale and full-scale studies. This was done by collecting three 20 L soil samples and then treating it in three subsequent stages; 1) size separation; 2) attrition and 3) chemical extraction using water in a 5:1 liquid: soil slurry.[219] The soil was mainly contaminated with PFOA, PFOS and PFBS and post treatment, enrichment of mainly PFOS and also PFOA was observed on the fines (<0.074 mm).[219] A recent study treated soil contaminated with AFFFs using soil washing and studied the influence of grain size, organic carbon and organic matter residue (decomposable part of soil) content on PFAS sorption. The K_d values increased in the following order: PFCAs<PFSAs<FTS<FOSA, with the fine grained silt and clay fractions demonstrating the highest sorption potential due to their high organic carbon content (OC).[221] The retardation for PFAS of the same chain length increased in the order PFCAs<PFSAs<FTS<FOSA, which was directly related to the K_d values of the compounds.[221] Another study combined soil washing with foam fractionation with electrochemical treatment as a three step process to desorb and treat PFAS from contaminated soils.[222] Soils with <0.4% organic carbon content, contaminated predominantly with PFOS were treated and the effect of soil particle size, pH and soil: liquid ratios were evaluated. ~95% PFOS was removed by soil washing, ~95-99% through foam fractionation and aeration and ~97% removal was achieved using electrochemical oxidation, via the three stage treatment. [222] A simulation study modeled the adsorption of PFCAs and PFSAs in soils and found a strong correlation between their K_d values based only on the soil OC and silt and clay contents and PFAS chain length.[223] Organic carbon

content of soils was found to the primary factor affecting sorption, while sorption at mineral sites, especially for short chain PFAS had as an important contribution for soils with low OC and high silt and clay content.[223]

It is important to note that these studies identified the organic carbon matter in these soils as the primary adsorption sites for PFAS. The organic content (OC) in the previous studies ranges from 0-3%[214, 219-222], classifying these soils as non-organic/sandy. PFAS exhibit the potential to adsorb in organic carbon rich soils, more commonly referred to as 'organic soils' with the approximate OC content>18%. We hypothesized that this could lead to a potential strong/irreversible adsorption of PFAS onto the soil, with soil washing, alone as a remediation approach, proving potentially insufficient to extract PFAS from soil. Hence, in this study, we aim to combine soil washing with aeration/air-bubbling approach to reduce the number of treatment steps and to simultaneously extract PFAS from contaminated soils. Generated air bubbles can interact with and desorb hard to extract PFAS from contaminated organic soils, synergically improving the efficiency of soil washing. As demonstrated in Chapter 4, air bubbles can entrap PFAS in the solution onto their surface, migrate to the air-water interface and enrich (similar to foam fractionation)[98, 132, 224-226] /aerosolize PFAS. The current study aims to combine air-bubbling with soil-washing techniques to investigate removal of PFAS from contaminated soils. The flexibility of this approach allows it to be used as a stand-alone pre-concentration or a treatment in series with other destructive technologies (*e.g.*, e-beam and eAOP treatment). Commercially available soil was mixed with sand/gravel, spiked with PFAS and treated by the soil washing-air bubbling system, using an aqueous wash solution. The primary aim of

this work was to combine air-bubbling with soil washing to extract PFAS of varying

hydrophobicity in organic soils. The main objectives of this study were:

1) Evaluating the effect of bubbling on the extraction of PFAS from soil under varying soil-to-water and sand-to-soil ratios (organic carbon content).

2) Performing a PFAS mass balance to investigate the compartmentalization of PFAS, post soil treatment.

3) Investigate the impact of wash solution pH and cationic surfactants on PFAS compartmentalization

6.2 Research Questions

1) How does the extraction efficiency into the solution phase vary with PFAS structure?

2) Does air-bubbling affect PFAS compartmentalization and improve PFAS extraction?

3) How do the sand: soil ratios (organic carbon content) and solution pH affect PFAS partitioning into the aqueous phase?

4) Does addition of cationic surfactants impact PFAS extraction efficiency from high OC soil?

6.3 Research Hypothesis

1) Less hydrophobic and more water-soluble PFAS will migrate better into aqueous phase.

2) Air bubbles can help in the desorption of PFAS from soil due to their surface activity, leading to better extraction of PFAS during soil washing process.

3) Increasing mass of soil will increase organic content, which could induce competition and reduce migration of PFAS into the aqueous phase.

6.4   Materials and Methods

6.4.1   Preparation of PFAS-Contaminated Soil

Commercial premium topsoil (lawn and garden soil conditioner) was purchased from Home Depot and sand (C33, no OC, specific gravity of 2.5-2.7) was obtained from wastewater research and innovation facility at Stony Brook, NY. Sand and soil were dried in an oven at 70°C and grinded using a mortar and pestle and the stones, branches, coarse chunks were removed. Sand and soil were mixed in a pre-fixed ratio (75:25 or 25:75) in an HDPE container and a known amount (200-300 mL) of DIW was added to form a slurry. PFAS was spiked in the slurry from a stock solution (in methanol) and the container was placed on an orbital shaker overnight. Post mixing, the container was placed in an oven overnight to dry at 70°C. This procedure was followed to uniformly distribute PFAS in the test soil. The drying process was not expected to alter the chemistry of the soil as indicated in Table 1. The increase in nutrients and OC was likely due to a reduction in moisture content after drying.

Table 6.1 Characterization of Tested Sand: Soil Mixtures and Comparison with Typical Soil Values and Values Utilized by Studies for PFAS Contaminated Soils[218-220, 222, 227]. * low lying, extremely marshy soil. ADL indicates above detection limit

Sample composition			75 soil, 25 sand- Non Dried	75 soil, 25 sand- Dried	25 soil, 75 sand- Non Dried	25 soil, 75 sand- Dried	Typical values	Typical values (PFAS studies)
Analyte concentration/ parameters	pH		7.47	7.27	7.4	7.39		4-8.2
	P	lb/acre	305	770	166	264	0-137	
	K		ADL	ADL	1011	1461	0-277	
	Mg		1169	1749	532	691	0-295	
	Ca		5271	ADL	2740	3615	0-1790	1800-2000
	Zn	parts per million	13.11	26.18	5.76	7.82	1-50	
	Cu		1.77	3.95	0.93	1.13	0.5-20	
	Mn		20.56	65.24	21.3	33.24	25-100	200-300
	B		3.08	5.35	2.27	2.62	0.5-20	
	Fe		195.19	265.9	140.4	150.19	50-100	14500-15000
	S		11.9	506.75	12.68	62.48		
	EC	mmho/cm	1.13	2.59	0.66	0.99		
	Organic matter		18.6%	20.6%	3.6%	4.8%	0.1-90*%	0-3%
	Gravel content	>2 mm	16%	13.5%	16%	13.6%		0-5 %
	Sand		89%	90%	91%	93%		0.3-96.5%
	Silt		8%	6%	5%	4%		3-56%
	Clay		3%	4%	4%	3%		0-50%
	CEC	meq/100g	18.63	21.37	10.3	13.8	5-25	

6.4.2   Soil Washing Process

Prior to utilizing air bubbling combined with soil washing, the operating and treatment conditions were optimized to select the ideal conditions for soil washing. The soil: liquid (S:L) ratio is an important treatment parameter that can impact the removal efficiency. Preliminary experiments were conducted to identify the ideal S:L ratio to ensure i) that the soil-water solution level is above the bubbling and sampling port and ii) that the soil-water solution does not clog the sampling port/interfere with extraction steps, highlighted in 6.4.3, iii) the stir paddles made contact with the solution. S:L ratios of 1:5, 1:10, 1:20, 1:50 and 1:100 were tested and it was observed that at ratios below 1:20, the paddles were unable to mix the solution. Previous studies that have utilized soil washing for PFAS remediation have used S:L ratios ranging from 1:5 – 1:25[218, 219, 221, 222] and hence, for this study, S:L ratio of 1:20 was chosen as the favored ratio for soil washing. For the soil, two ratios of organic soil: sand were chosen (75:25 and 25:75) to simulate the contamination of PFAS in i) an organic soil with high OC (18-21%) and ii) sandy soils, consistent with previous studies, with OC <5%. Thus, the results from this study can be applied to treat PFAS contaminated soils (either near a manufacturing/discharge source or soils in proximity of use of AFFFs) that are classified as low OC/sandy as well as for high OC/organic soils.

Fixed mass of dried sand-soil mixture was placed in separate HDPE containers and known amount of wash solution was added to keep constant soil: water ratios (1:20). The containers were placed on a Phipps and Bird's PB-900™ series programmable jar tester setup (Figure 6.1b) and the paddles were carefully connected to the stir rod. Holes were drilled in the HDPE bottle and a cylindrical stone diffuser was attached at the bottom, bubbling tubes were connected to the ports at the bottom of the container and air-bubbler

apparatus was turned on. The mixing speed was set to 100 rpm and the air flow rate was set at 0.5 L/min to generate microbubbles and the experiment was run for one hour. Duplicates were run for each sample condition and a control (no mixing, no bubbling) was also run in duplicates for each batch of operation.
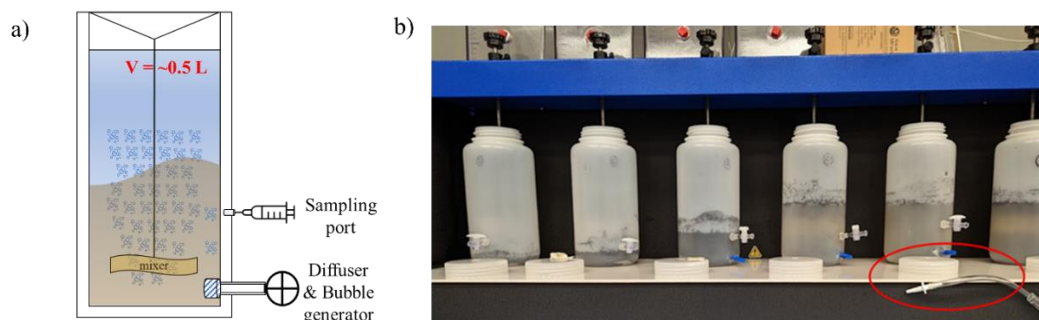
Figure 6.1 a) Schematic and b) actual batch column set-up for air-bubbling extraction of PFAS from soil. Red circle highlights the connector tube for bubbling.

6.4.3 Sample Processing

After treatment, 3 mL of the aqueous wash solution was drawn using a syringe and transferred to a 5 mL PP tube. A known amount of surrogate was injected into the sample and the sample was centrifuged at 3000 rpms for 3 minutes. The supernatant was carefully transferred to a syringe and passed through a 0.22 μm Regenerated Cellulose (RC) membrane filter. The final solution was collected in a separate PP tube, diluted 1:1 with methanol stored, prior to analysis at 4°C

The paddles and stir rods were disconnected and the wash solution was carefully decanted into separate containers. The remaining soil at the bottom was rinsed with DIW and scooped out using a disposable spatula into 50 mL PP tubes and the resulting treated soil-water was dried in the oven at 70°C. Post drying, both the dry treated and untreated soil was extracted following a modified EPA 1633 method. Briefly, this involved extraction

of 0.25 grams of soil (surrogate spiked) using 0.3% methanolic ammonium hydroxide at different volumes, followed by water addition to bring up the volume to ~35 mL. To remove the methanol, a N_2 blowdown was performed until the final volume reached ~10 mL, after which ~40 mL water was added. The pH of the solution was verified to be ~6-7 and a solid phase extraction was performed, using Oasis wax cartridges and the final eluate was collected in PP tubes and stored for analysis.

The HDPE containers were washed using water and air dried. Respective paddles were inserted and stir rods were connected to the empty containers and methanol was used to elute any PFAS absorbed to any surface. The eluate was collected and stored for further analysis.

Finally, the aqueous solution that was transferred into a separate container, was passed through a 0.45 μm nitrocellulose filter to filter out non-settleable organic carbon, also referred to as 'fines' in previous studies. The filter was weighed before and after to account for the gain in mass, post filtration. The filter papers were then extracted using EPA's 1633 method, similar to that used for untreated and treated soil. Post SPE, the eluate was stored for further analysis.

6.4.4 Sample Analysis

An aliquot of the samples was taken out for further dilution (to fall within the calibration) and the pH was adjusted to near neutral using 10 % acetic acid (if needed). 10 μL of 100 μg/L isotopically-labeled standards (M2PFOA, MPFOS) were added prior to analysis to provide recovery-corrected PFAS concentrations. Samples were analyzed using an Agilent 6495B triple quadrupole liquid chromatography tandem mass spectrometer (LC-MS/MS) equipped with electron spray ionization (ESI). Details about the MRM

transitions, analyte recovery, LC-MS/MS conditions, and analyte recoveries are provided in Appendix A,C.

6.5 Results and Discussions

6.5.1 Treatment of Soil Contaminated with Single Solute PFAS

Soils spiked with a single PFAS were prepared at a topsoil: sand ratio of 75:25, according to methods described in section 4. DIW, as wash solution, was added to maintain a final soil: water ratio of 1:20. The concentration of PFAS (single solute) on the untreated soil was set at 0.1 µg PFAS/g soil and was measured using the EPA 1633 method as described in section 6.4.3.
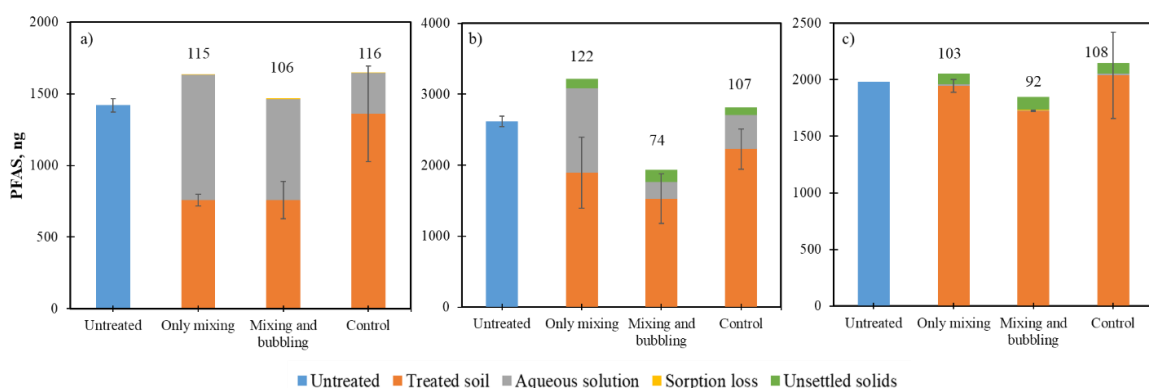
Figure 6.2 Compartmentalization of PFAS in untreated and treated soils containing 0.1 µg/g as a single solute of a) PFOA, b) PFOS and c) PFDA after 60 minutes of soil washing. Error bars represent variation in duplicate samples. Numbers above the bars represent the average percentage of PFAS accounted for, after treatment.

As seen in Figure 6.2, for PFOA, ~4 ± 23% was extracted from the soil to the aqueous phase for the control sample. The extraction efficiencies from the soil phase to the aqueous phase for the 'only mixing' and 'mixing and bubbling' conditions were higher at 46.5 ± 3% and 46.4 ± 9.3%. Interestingly, bubbling did not improve the extraction

efficiency for PFOA. For the tested conditions, the contribution of PFOA from sorption loss and unsettled solids was <1% each. For PFOS, mixing alone led to ~27.5 ± 19.2% of PFOS extracted from the soil phase into the aqueous phase and this value rose to 41.6 ± 13.4% for samples that were mixed and bubbled. Bubbling along with mixing led to ~26% of PFOS mass which was unaccounted for and is hypothesized to be due to aerosolization of PFOS from the aqueous system due to the generated air bubbles. Under similar conditions, after one hour of treatment, <1% PFDA compartmentalized in the aqueous phase and this number was ~ 1.8 ± 2.9% with only mixing and ~13 ± 0.3% for the mixing and bubbling condition. Thus, bubbling did positively impact the extraction of hydrophobic PFOS and PFDA into the aqueous phase, compared to the control samples and samples that were simply mixed.

The difference in the extraction efficiencies for the soils contaminated with single solute PFAS can be attributed to their adsorption to the organic matter in the soil phase. This is represented either by the K_d or the K_{oc} values and is related to the PFAS hydrophobicity. The hydrophobicity for the three PFAS studied is PFOA<PFOS<PFDA, indicating that PFDA displays higher sorption to organic matter, while PFOA displays the least.[134, 223] This was confirmed experimentally by a recent study investigating soils contaminated due to AFFFs, where the K_d values for PFOA, PFOS and PFDA were ~ 1.2, 6.5 and 22 L/kg, respectively. The higher the K_d value, stronger is the adsorption to the organic phase, resulting in reduced compartmentalization to the aqueous phase.

We assessed three conditions to improve the extraction of PFDA into the aqueous phase; varying the wash solution pH, sand: soil ratio and adding cationic surfactant, cetyltrimethylammonium chloride (CTAC). As seen in Figure 6.3b, varying the wash

solution pH did not improve PFDA extraction efficiencies with ~85% PFDA still present in the soil and ~15% unaccounted for the three conditions tested. This is contrary data obtained by previous studies[218, 222], where the percentage of PFOA, PFOS and PFDA bound to multiple soil samples decreased as the solution pH was increased. This was attributed to the electrostatic interactions between the PFAS and the soil, which decreased as the solution basicity increased. In one of the studies (OC 0.3-3.1%), PFDA loading on the soil in this study was 33 ± 7.5 μg/kg or ~ 0.03 μg/g, 70 % lower compared to 0.1 μg/g, used as a part of the current study. In the other study, although the PFAS loading for the two soils testes were ~0.78 μg/g and 0.27 μg/g, the total organic content of the soils was 0 and 0.2%.[222] The reaction times used in two studies were 7 days at 45 rpms[218] and 24 hours at constant mixing[222], compared to one hour at 100 rpms, used in the current study. Thus, the higher PFAS loadings, presence of organic carbon and lower mixing time is likely to cause a lack of impact of variable pH of the wash solution on PFDA extraction from soil.
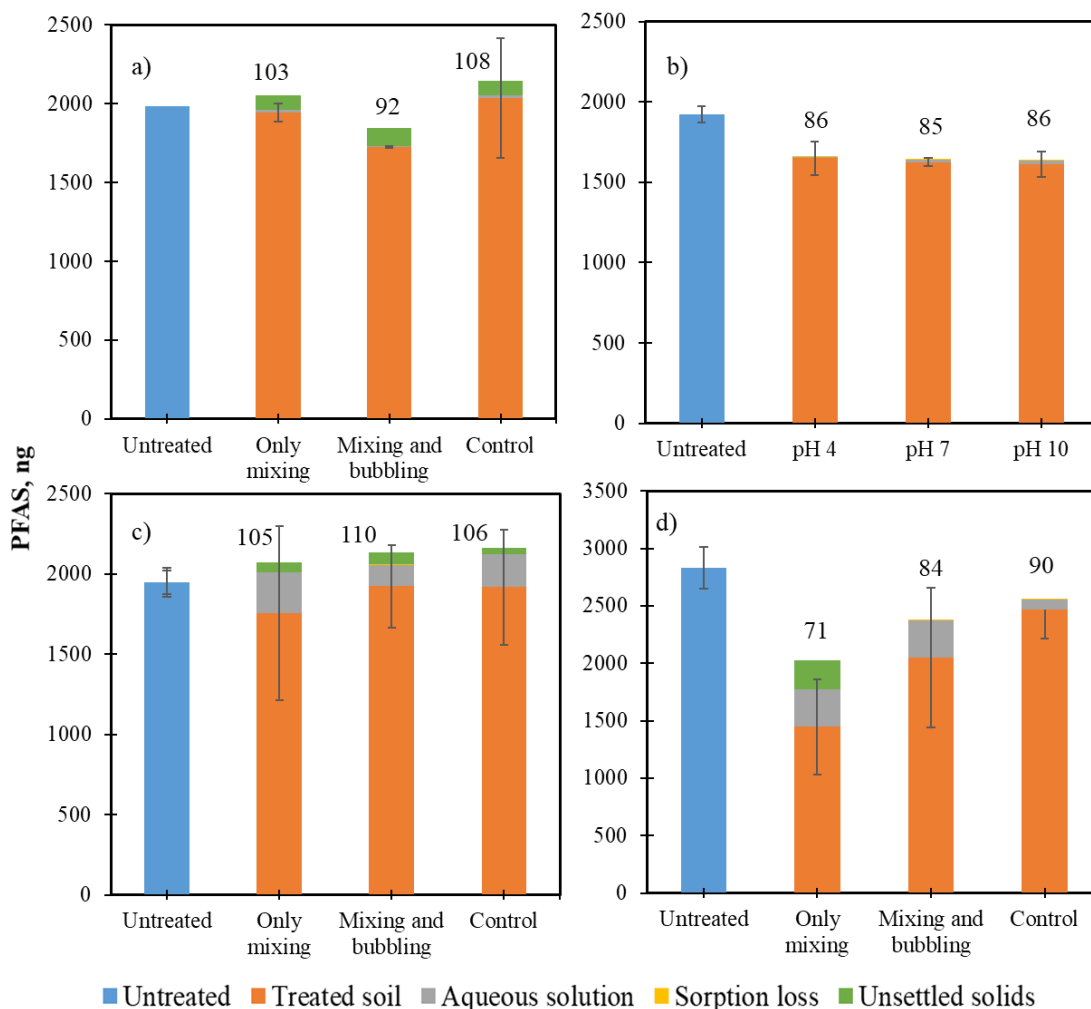
Figure 6.3 Compartmentalization of PFDA contaminated soils for a) no additives, b) varying pH for the wash solution, c) 1 mg/L CTAC addition under no pH variation (pH 7.3) and d) at reduced OC content of soil (soil: sand ratio of 25:75), pH 7.3. Error bars represent variation in duplicate samples. Numbers above the bars represent the average percentage of PFAS accounted for, after treatment.

We also added 1 mg/L of CTAC to the wash solution (DIW, no pH adjustment) to observe the effect on PFDA extraction. As seen in Figure 6.3c, extraction efficiency for the control sample was ~1.6 ± 19%, which increased to ~11 ± 28% with mixing. The extraction efficiency for the samples that were mixed and bubbled was ~1.3 ± 14%. Interestingly, we detected PFDA in the wash solution, with ~ 13, 7 and 10% of the initial PFDA compartmentalized in samples that were simply mixed, mixed and bubbled, and for the control sample. Although, addition of CTAC did not lead to a complete extraction of PFDA,

134

it demonstrated a slight increase in migration of PFDA to the aqueous phase. This is attributed to the competition between the long chain (C16) surfactant molecule: CTAC and PFDA (C10), which could lead to substitution and adsorption of CTAC onto sites containing PFDA.[228] This was elucidated in a recent study using GAC that showed that the adsorbed short-chain PFAS were prone to displacement, upon addition of long-chain PFAS.[229] Formation of a ion pairs between CTAC and PFAS could also likely improve extraction from soil. This latter explanation is speculative and more research is needed to promote the PFAS compartmentalization into the aqueous phase to confirm effects of cationic surfactant, for the tested conditions. Thus, addition of a more hydrophobic surfactant could lead to the displacement of PFAS absorbed onto contaminated soils. However, depending on the toxicity of the chosen additive, it may not be possible to transfer the soil back to the source, requiring subsequent remediation.

Finally, we tested the addition of sand to contaminated soil to reduce the organic content of the soil. 6.25 grams of soil (0.4 µg PFDA/g soil) was mixed with 18.75 grams of sand, to which 500 mL DIW was added, without any additives. This was to maintain concentration of PFDA in the topsoil: sand (25:75 ratio) mixture as 0.1 µg/g. As shown in Figure 6.3d, compartmentalization of PFDA in the wash solution/aqueous phase was ~11 ± 4.6 % and ~11 ± 3.2 % for samples only mixed and mixed and bubbled respectively and <3% for the control samples. Thus, varying the soil: sand ratio showed slight improvement in the extraction efficiency in the wash solution. These results were similar to the previously tested condition (CTAC addition), where ~10% PFDA compartmentalized into the aqueous phase. Thus, under the tested conditions, we did not observe a significant

improvement by i) addition of cationic surfactant, CTAC, b) varying the sand: soil ratios and c) combining mixing with air bubbling for PFDA contaminated soils.

6.6 Treatment of Soil Spiked with Equimolar PFAS as a Mixture
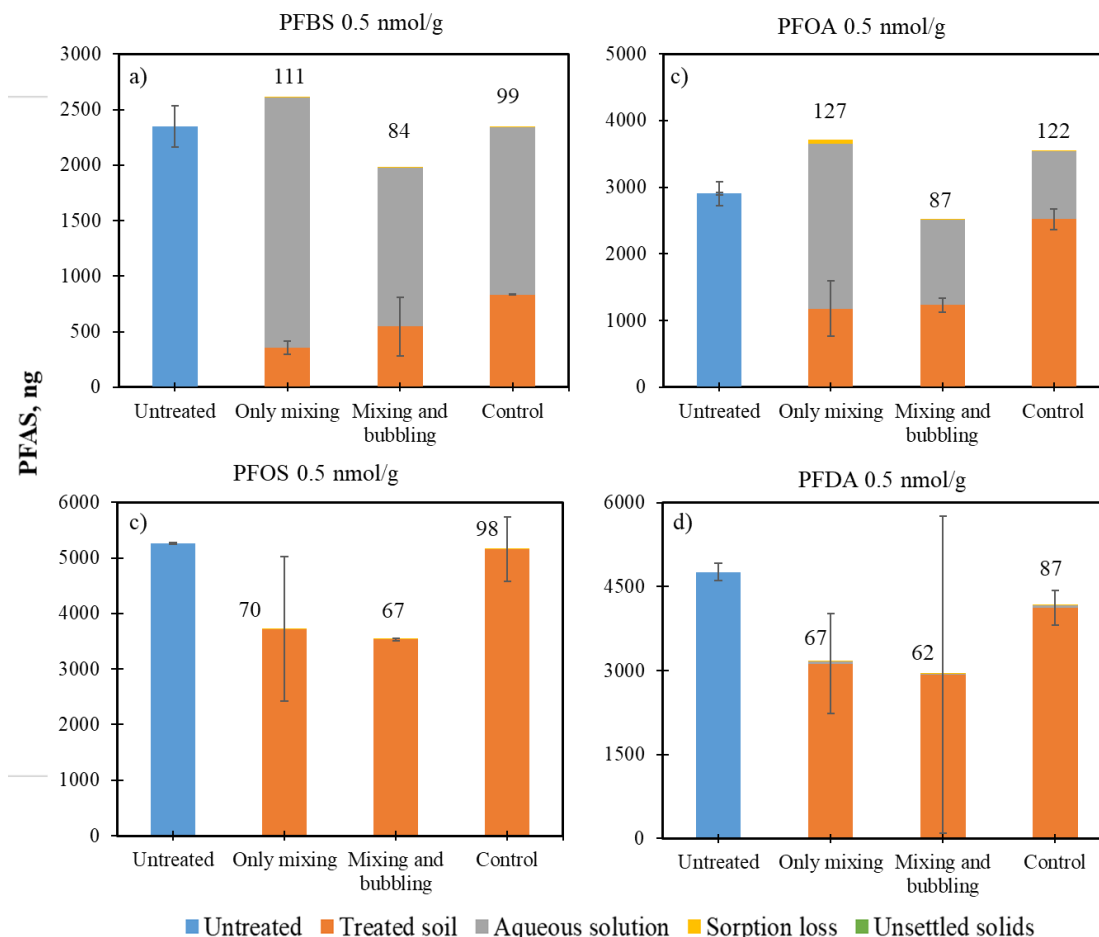
Figure 6.4 Compartmentalization of a) PFBS, b) PFOA, c) PFOS and d) PFDA, pre- and post-treatment from soil spiked with 0.5 nmol/g of each PFAS. Error bars represent variation in duplicate samples. Numbers above the bars represent the average percentage of PFAS accounted for, after treatment.

We also tested the extraction efficiency of soil (75 soil, 25 sand) spiked with 0.5 nmol/g of PFBS, PFOA, PFOS and PFDA each, without any additives or variation to the wash solution pH (DIW, pH ~6). The spiked mass concentrations for PFBS, PFOA, PFOS and

PFDA were 0.15, 0.20, 0.25 and 0.26 µg/g respectively. As seen in Figure 6.4a, the extraction efficiency of PFBS into the aqueous phase was 64 ± 2.8 % for the control sample. This increased to $\sim 84.8 \pm 2.7\%$, when mixed and was $\sim 76.7 \pm 11.3\%$ when mixed and bubbled. For PFOA, without any mixing and bubbling (control), $\sim 13.2 \pm 7.4$ was extracted into the aqueous phase and this number increased to $\sim 60\%$ for samples that were only mixed and samples that were mixed and bubbled. It is noted that these numbers were calculated based on PFOA concentrations in treated and untreated soil as the mass balance for samples only mixed was overestimated by $\sim 18\%$. Similarly, the extraction efficiency for PFOS and PFDA for samples only mixed and mixed and bubbled was $\sim 30\%$. However, $\sim 30-40\%$ of PFOS and PFDA was unaccounted for, after the treatment and we did not detect either of those PFAS in the aqueous solution. This could be either due to aerosolization of hydrophobic PFOS and PFDA during the treatment, adsorption on the RC filter or the lack of a representative soil aliquot sample processed and analyzed, post treatment.

The results for both single solute and equimolar PFAS contaminated soil experiments demonstrate that under similar conditions, the extraction of PFAS from soil into the aqueous phase inversely correlated to their hydrophobicity/K_d values. Compounds such as PFDA, with the highest K_d value amongst those tested, did not display significant extraction from soil, even with variation in wash solution pH and CTAC addition. This is contrary to our results (unpublished) for both long and short chain PFAS in contaminated waters, where addition of CTAC showed near complete removal of both PFBS and PFDA via foam fractionation. This experiment was performed for waters spiked with PFAS, with no organic medium (soil) available for sorption. We also observed a significant

improvement in PFAS removal in contaminated waters (unpublished) when bubbling was introduced, which was not observed for contaminated soils. This could be attributed to a) poor extraction from soil phase, suppressing the effects of bubbling via an air-flotation mechanism and b) resorption of PFAS onto readily available organic matter present during treatment of contaminated soils.

6.7   Conclusion

The current study aimed to utilize soil washing assisted with air bubbling as a technique to remove PFAS from contaminated, high OC (organic) soils. This was done by spiking commercially available topsoil with PFAS, followed by soil washing assisted with air bubbling at a constant soil: sand ratio. Results from this study indicated that for PFOA, air bubbling did not have an effect on the overall compartmentalization. There was a loss in concentration for samples that were mixed and bubbled for PFOS, indicating that aerosolization of PFOS extracted from the soil took place. The current setup was unable to successfully extract PFDA from the contaminated soil, under similar conditions, with a majority of the spiked PFDA still adsorbed onto the soil post treatment. Slight improvement (6-13%) in the migration to the aqueous phase was observed with the addition of CTAC and by mixing nonorganic sand to contaminated soil prior to soil washing. This was due to induction of a competitive effect by CTAC addition for PFAS migration and due to decrease in overall organic content of the soil: sand mixture, preventing the possibility of resorption of desorbed PFDA respectively. The addition of bubbling along with mixing to interact with the soil did not improve PFDA extraction even with addition of CTAC or sand.

However, this effect is expected to be more pronounced if the desorption of PFDA from the soil was made possible, by changing the PFAS loadings onto the soil or by addition of an anionic surfactant to compete for the adsorption sites onto organic carbon present in the soil. Results from the study will inform future researchers about the challenges of extracting a range of hydrophobic PFAS strongly adsorbed onto high organic content soil, with the aim of developing strategies that can successfully remediate soils affected by PFAS contamination. Thus, future or recommended work on soil remediation will focus on i) reducing the organic carbon content to observe the effect of solution pH, and additives such as cationic/anionic/non-ionic surfactants in the presence of air bubbles, ii) observing the compartmentalization and competition effects of a wider suite of PFAS in real world AFFF impacted soils, and iii) varying the clay content of the soils to evaluate the impact of soil composition on the removal trends.

SUMMARY AND LESSONS LEARNT

The primary objective of this dissertation was to focus on the application of destructive technologies for the remediation of PFAS from aqueous and soil matrices. The first technique I investigated was electron beam technology, which utilizes an irradiation source to generate a beam of electrons that interact with water to generate oxidizing and reducing radicals. I found that the e_{aq}^- can react with and breakdown recalcitrant PFAS in the solution and this process is dependent on the water quality (solution pH, dissolved oxygen) and operating parameters (dose, dose rate). It was also demonstrated that the solution matrix can affect the treatment by scavenging the hydrated electrons and reducing the reactions with PFAS molecules and also that short chain PFAS (PFBA, PFBS) show the highest resistance to degradation, compared to the longer chain PFOA, PFOS and PFNA. Importantly, this study demonstrated a complete transformation of PFAS precursors in real world samples, through the oxidative pathway. With so many encouraging results, an obvious question is the lack of application of this technique on a more widespread basis. This technology is highly energy intensive, as demonstrated in chapter 1, when the wall to plug efficiencies are accounted for. This technology cannot be utilized on a bench scale or in a flow through system and as it is utilizing a radioactive source, lacks the freedom to be freely researched upon. It is true that certain applications of e-beam technology have been utilized for full scale treatment of wastewater, considering the energy requirements for PFAS treatment, this is not a currently viable option. The ideal way to utilize this technology would be to concentrate the PFAS from ng/L to g/L or even higher and treat this stream at high e-beam doses (>1000 kGy), reducing the sample volume and number of necessary treatments. This can be made more efficient by combining waste streams of

multiple contaminants to utilize the oxidative/reductive nature of this technology, enabling the ultimate destruction of a suite of contaminants simultaneously.

Compared to e-beam technology, PFAS destruction by eAOPs has been more widely investigated. The current study aimed to identify and fill in the knowledge gaps by utilizing a simple two electrode system with a BDD anode and a stainless steel cathode. PFAS can migrate to the anode surface, undergo a direct electron transfer, forming PFAS radicals. These radicals can be degraded into degradation products, that can potentially undergo DET or further degradation. This study demonstrated that the solution anions, due to the addition of the supporting electrolyte, do not impact the PFAS removal. The PFAS removal was also found to be strongly correlated with hydrophobicity, with short chain PFAS showing the poorest removal efficiencies. This is one of the limitations of using eAOPs to treat PFAS that needs further investigation. One of the current research directions in this field is to improve the removal efficiencies of short chain PFAS is functionalizing the anode to improve the electrostatic interactions with PFAS anions. Another approach is to modify the solution with additives that can bind with PFAS, migrate to the anode surface and undergo degradation as an ion pair. Another limitation is the high capital costs, associated with the specially fabricated electrodes, that can increase the overall costs of utilizing this technology. The lack of auxiliary chemicals and high temperatures, ease of setup, operation and modification and comparatively lower energy requirements still make eAOPs one of the most viable technologies currently for PFAS removal.

While utilizing these destructive technologies, the percentage degradation was calculated based on the initial and final concentrations of the parent compound. While the ultimate objective of a destructive approach is to completely transform the PFAS into

inorganic fluorine and CO_2, this was not achieved for the two approaches studied. This means that although a complete degradation of a parent compound occurred, generated byproducts still exist in the treated solution as either perfluoro or polyfluoroalkyl substances, These daughter products can be equally as persistent and toxic as the parent compound and thus, prove a challenge firstly for correctly identifying them through non-target screening and secondly, treating them effectively. Destructive approaches have an advantage over sequestration techniques in that they actually aim to destroy PFAS rather than remove it. The question of whether we are solving a single problem or creating a hundred new ones can only be answered by further research and careful PFAS screening.

The concluding chapter provided interesting insights into the mechanisms of PFAS sorption onto soils and the process of soil washing. Firstly, the rationale behind this work was to improve the soil washing process by addition of an air bubbling component. The hypothesis behind this was that the generated air bubbles would collide and interact with PFAS adsorbed on soil, leading to a more efficient extraction process. Furthermore, the bubbles could entrap PFAS, migrate to the air-water interface, resulting in PFAS enrichment. This concentrated PFAS solution at the top could be simply removed, wash solution could be reused and the soil could be transferred back to the source. However, under the tested conditions, the air bubbling did not significantly improve the extraction efficiency. This could be due to the limitations in design of the bubbling setup (bubbles generated above the soil layer) or poor interactions between bubbles and PFAS as mixing the samples could lead to a bursting of bubbles. The lack of improvement, especially for long chain PFAS, with the addition of bubbling needs further investigation.

PFDA displayed the poorest extraction efficiency amongst the PFAS evaluated, owing to the strong sorption onto the organic matter in soil. The tested conditions did not yield a significant extraction of PFDA, post treatment, with most of it still accounted for in the organic-rich treated soil. It is necessary to overcome this PFDA adsorption by either addition of an anionic surfactant or by changing the PFAS loading onto the soil. Although this may prove challenging due to the high K_d value for PFDA, the tested conditions may yield significantly variable data if PFDA was extracted from the soil phase. The current study used a methanol rinse to elute the PFAS adsorbed on the container and paddles. This was done by carefully using a methanol squeeze bottle to rinse the container walks, paddle and stir rod. This may prove insufficient if PFAS is strongly bound and a better elution approach can be utilized by filling the container with methanol, followed by sonication.

This dissertation demonstrates the multitude of challenges associated with PFAS remediation. Irrespective of whether a destructive or a sequestration approach is taken to resolve a particular problem, the unique physicochemical properties of PFAS, which can vary significantly with the chain length and functional group, make a 'one solution fits all' approach largely ineffective. With a more collective approach, careful research and novel pathways, I strongly believe that the issue of PFAS contamination can be managed, in the near future. As a part of an overall summary of the knowledge gained during the PhD journey, I would like to propose Figure 7.1. This is a qualitative figure that can inform regulatory agencies, researchers, consultants and utility companies about the treatment options available and provide an initial understanding of the stepwise treatment approaches needed to achieve PFAS remediation.
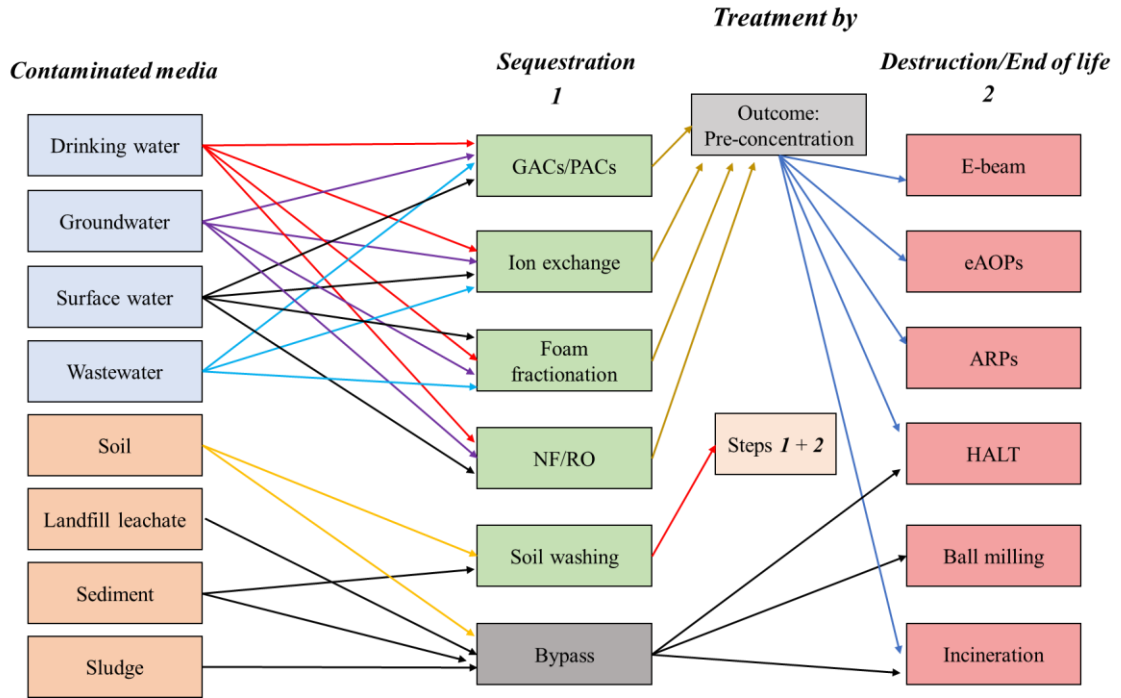
Figure 7.1 Recommended treatment train for the remediation of PFAS-contaminated media.

Note: '1+2' for soil washing implies that a combination of sequestration followed by destruction need to be applied.

APPENDIX A

APPLICATION OF ELECTRON BEAM TECHNOLOGY TO DECOMPOSE PER- AND POLYFLUOROALKYL SUBSTANCES IN WATER

The following sections, figures and tables are supporting information published with the manuscript.

A1. Optimization of Sample Container and Volume.

Preliminary tests were conducted to identify the ideal sample containers for e-beam treatment. Three different container materials were tested to assess its interaction with the contaminants and treatment efficiency: borosilicate glass, soda lime glass, and polypropylene jars. At high e-beam doses (>500 kGy), the soda lime glass became fragile post treatment. For both borosilicate glass and polypropylene, we did not observe any significant loss of contaminants in our control jars due to adsorption for a period of 14 days. Four different sample volumes were treated depending on the dimensions of the jars: 15 mL, 90 mL, 130 mL, and 160 mL. The goal was to maintain a constant sample depth of 3 cm to match the penetration depth of the electron beam radiation. Preliminary results revealed a similar treatment efficiency amongst samples that had different sample volumes but the same penetration depth. This is consistent with previous literature that confirms that the depth of the water was the determining factor for treatment as long as the irradiation is uniform throughout the cross section of the sample container[16, 22, 42].

A2. E-Beam Accelerator and Dosing

Fermilab houses a demonstration accelerator (Accelerator Application Development and Demonstration, A2D2) that enables proof-of-concept studies. A2D2 is a 9 MeV electron accelerator and is provided by a repurposed teletherapy linac. It is a normal conducting multi-cell 2.85 GHz accelerator structure. Electrons are generated by a thermionic electron gun and is powered by a classic Klystron amplifier. Once the electrons are accelerated, they are collimated by thin slits and a 270-degree bending magnet. When combined, these electrons have a narrow momentum spread and are well focused leaving the vacuum window. With variable settings the machine can provide a maximum of 1.2 kW of beam power and electron kinetic energy of 9 MeV. Dosimetry is provided by a NIST certified dosimetry system that is available to measure/verify the amount of total dose given to each sample. For all samples to be placed in the electron beam, an optical density film is placed alongside the sample to measure the dose received by the sample. The dosimetry method used to measure absorbed dose for e-beam irradiations was Far West Film dosimetry (FWT-60, Far West Technology, Inc., Goleta, CA). These 44.5 µM thin radiochromic films are derivatives of the family of aminotriphenyl-methane dyes that gradually change from colorless to a deeply colored state as a function of absorbed dose.

A3. TOP Assay

Total Oxidizable Precursor (TOP) assay was performed for contaminated groundwater samples using a modified method outlined in previous studies[97, 230, 231]. Briefly, 5 mL of GW was mixed with 5 mL of reagent stock (600 mM NaOH + 200 mM Potassium persulfate ($K_2S_2O_8$)) with the NaOH: $K_2S_2O_8$ ratio of 1:3 in samples. Final pH of samples was verified to be >13. Samples were gently mixed and placed in a water bath maintained

at ~86 °C for 8 hours. Post TOP assay, tubes were placed in a water bath, maintained at room temperature for cooling and were stored at 4°C for further processing. Samples were then processed via solid phase extraction (SPE) using Oasis WAX Plus cartridges and analyzed using LC-MS/MS.

A4. Q-TOF Methods and Sample Analysis

q-TOF via methods adapted from previous work[10]. Briefly, samples were concentrated ten times under a gentle stream of nitrogen and 50 uL was injected onto the LC. Separation was performed with flow rate 0.6 mL min^{-1} using 100% Optima LCMS-grade methanol and 20 mM ammonium acetate in Optima LCMS-grade water as the organic and aqueous mobile phases, respectively. Detection was carried out in data dependent acquisition (DDA) mode screening all mass-to-charge (m/z) ratios from 100 – 1200 Da. Resulting data was screened using Agilent Profinder software and the NIST Suspect List of Possible PFAS[232] v 1.6.0. Peaks were filtered by peak height (> 400 counts), mass error (< 10 ppm), match score (70 or greater using the Profinder algorithm based on exact mass match and isotope pattern), detection frequency (must appear in at least two of three replicate sample injections), and comparison to solvent blanks (peak area must be > 10x a blank solvent injection). The remaining 27 features were assigned confidence levels as recommended by data published in a recent study[233]. based on parameters including exact mass match, mass spectra, MS/MS fragmentation spectra (when available), retention times, and presence of sub-class homologues.

A5. True TOF® Methods and Sample Analysis

True TOF® is a capability that involves the use of a novel combustion ion chromatography (CIC) platform developed by Metrohm . The technology involves a built for purpose CIC (Profiler F) that was developed solely for organofluorine testing. The advantage of this method is it can simultaneously quantify total fluorine, or TF (combusted at high temperature) and inorganic fluoride (IF) using two parallel IC modules. Subtracting the TF from the IF gives you the True TOF® value. The percentage recovery falls within 80 and 120% and the precision is within 5 - 10%.

A6. Optimizing Sample Dissolved Oxygen and pH to Achieve Highest Degradation Efficiency

To test the effect of DO concentration, we purged the samples with nitrogen gas prior to treatment of PFOA and PFOS at an initial concentration of 100 µg/L and an e-beam dose of 200 kGy. Two target DO concentrations of 4 mg/L and 2 mg/L were tested along with no purge condition. Both PFOA and PFOS degradation improved with decreasing DO concentration. An improvement of 47% and 23% was observed for PFOA and PFOS, respectively, for samples with 2 mg/L DO levels as compared to samples with no purging. For samples at 4 mg/L of DO post purging, the improvement was ~12 and 13% for PFOA and PFOS, respectively. This is consistent with previous studies that have reported an improvement in the degradation of PFAS by purging with N_2 or Ar gas[31, 77, 78].

Along with reactive species, water quality parameters such as DO can reduce the abundance of e_{aq}^- according to Reaction A1. As a result, reducing the DO, improved the abundance of e_{aq}^- , and thus enhanced PFAS degradation.

$$e_{aq}^- + O_2 \rightarrow O_2^-$$ (Reaction A1 (k = 1.9 x 10^{10} $M^{-1}s^{-1}$))

To identify the optimum pH for treatment, we tested pH 4, 10, and 13 for PFOA and PFOS as single solute at 100 µg/L initial concentration and e-beam doses ranging from 250 to 1000 kGy (Figure SI1). Samples were purged with nitrogen gas prior to treatment to attain a DO concentration of 2 mg/L. The highest degradation efficiencies for PFOA (92 – 99%) and PFOS (77 – 99%) were observed for samples at pH 13, with increasing e-beam doses (Figure SI1). e_{aq}^- can be scavenged by radical-radical combinations with other species such as OH·, H^+ and H· radicals amongst others[41]. These radicals are formed as a result of water radiolysis[89] and can reduce the abundance of e_{aq}^- in aqueous solutions, according to Reactions A2-5. e_{aq}^- can also react with itself, although at a slower rate, as shown below by Reaction 7.

$$e_{aq}^- + OH· \rightarrow OH^- \qquad \text{(Reaction A2 } (k = 3 \times 10^{10}\, M^{-1}s^{-1}))$$

$$e_{aq}^- + H^+ \rightarrow H· \qquad \text{(Reaction A3 } (k = 2.2 \times 10^{10}\, M^{-1}s^{-1}))$$

$$e_{aq}^- + H· \rightarrow H_2 + OH^- \qquad \text{(Reaction A4 } (k = 2.5 \times 10^{10}\, M^{-1}s^{-1}))$$

$$e_{aq}^- + e_{aq}^- \rightarrow H_2 + OH^- + OH· \qquad \text{(Reaction A5 } (k = 5 \times 10^{9}\, M^{-1}s^{-1}))$$

At pH 4, H^+ ions present in the samples can react with and scavenge e_{aq}^- from the solution according to reaction 5. Due to lower H^+ ions present in the solution at pH 13, their scavenging effect is reduced, leading to an abundance of e_{aq}^-. As a result, more PFAS- e_{aq}^- reactions can occur at alkaline conditions, leading to significant improvement in the degradation efficiencies as shown in Figure A1. This is consistent with previous studies that have used gamma radiation[91], hydrothermal alkaline treatment[234] and advanced reduction processes involving UV[235] and have identified alkaline conditions to be optimum to initiate PFAS degradation using e_{aq}^-. At alkaline conditions, there is a greater

concentration of OH⁻ than H⁺. These OH⁻ can react with e_{aq}^- scavengers such as OH· and DO as per Reactions 8 and 9[16], increasing the reactions between e_{aq}^- and PFAS molecules.

$$OH· + OH^- \rightarrow O·^- + H_2O \qquad \text{(Reaction A6 (k = 1.2 x 10}^{10}\,\text{M}^{-1}\text{s}^{-1}\text{))}$$

$$O·^- + O_2 \rightarrow O_3·^- \qquad \text{(Reaction A7 (k = 3 x 10}^9\,\text{M}^{-1}\text{s}^{-1}\text{))}$$
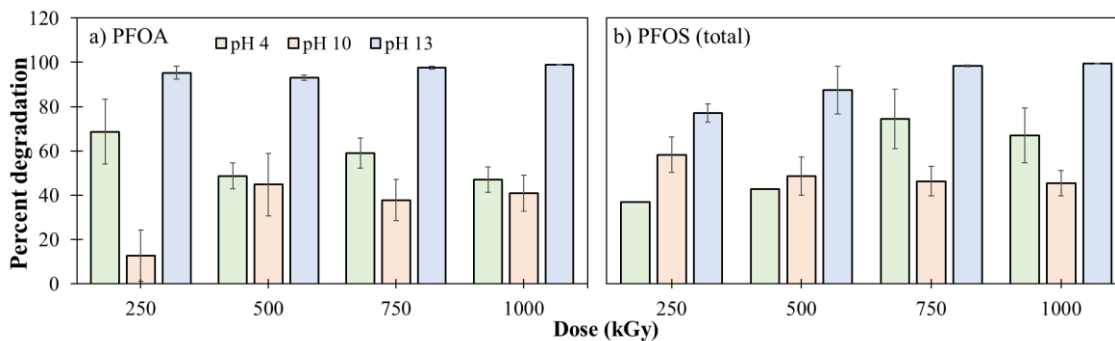
Figure A.1 Percent degradation of a) PFOA and b) PFOS (total) at different pH conditions as a function of e-beam dose. Initial concentration: 100 µg/L. Error bars represent standard deviation for triplicate treatments.
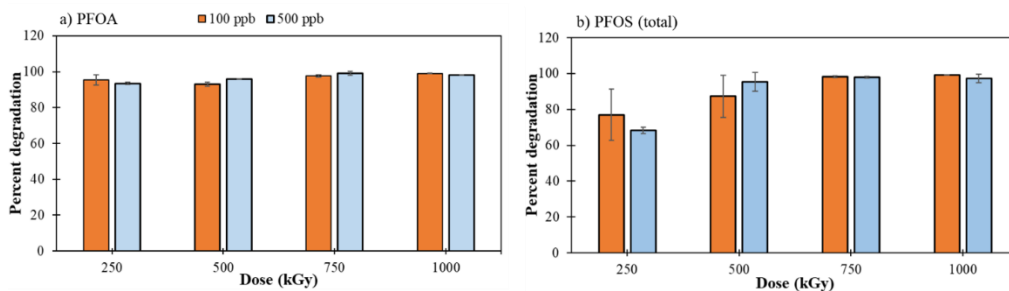
Figure A.2 Percent degradation of a) PFOA and b) PFOS (total) with increasing e-beam doses at pH 13 and 2mg/L of DO. Error bars represent duplicate samples.
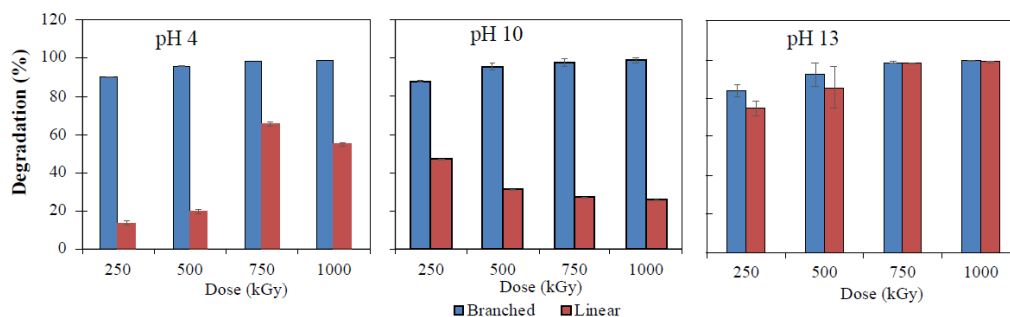
Figure A.3 Comparison of degradation efficiencies of L-PFOS and br-PFOS at different pH and e-beam doses. DO: 2 mg/L. Error bars represent standard deviation of triplicate samples.

.
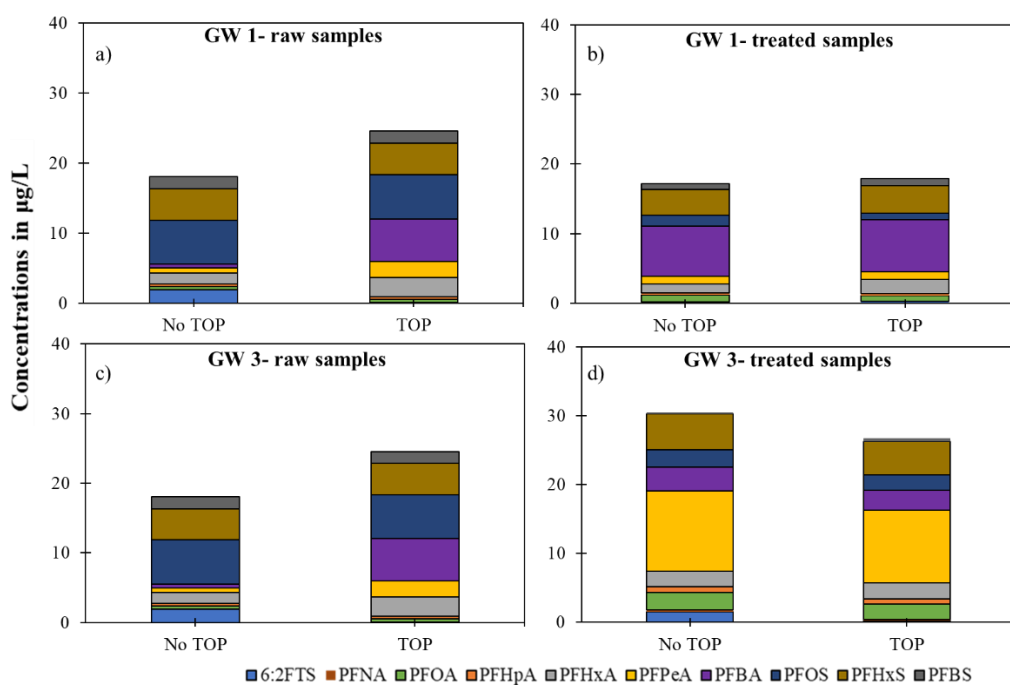
Figure A.4 PFAS concentrations for raw a) GW1 and b) GW1 treated with e-beam, c) raw GW2 and d) GW2 samples treated at 250kGy, with and without TOP assay.

Table A.1 Analytical Method Performance

Batch#	PFAS analyzed	RPD * (%)	Standard addition recovery (%)
5	PFOS	0.3	86
	PFOS	1.6	92
	PFOS	3.0	97
6	PFOA	2.3	109
	PFOA	1.7	97
	PFOA	0.4	127
7	PFOA	2.0	85
	PFOS	0.3	104
	PFHxS	2.9	85
8	PFPeA	2.5	96
	6:2FTS	6.8	90
	6:2 FTS	0.2	-
9	PFNA	3.2	151[#]
	PFBS	0.2	58[#]
	PFBS	1.0	99
10	PFHxA	7.0	97
	PFPeA	17.9	81
	PFOS	1.3	80
11	PFAS mix	3.4	99
	PFAS mix	2.5	96
	Average	3.0	95
	stdev	4.0	11

*RPD = relative percentage difference of duplicate samples

[#]These samples were not used in interpretation of results

Table A.2 MRM Transitions and Full Forms for All Compounds Studied

Analyte	Full name	Internal standard	Precursor (m/z)	Product 1 (m/z)*	Product 2 (m/z)*
Perfluoroalkyl carboxylates (PFCAs)					
PFBA	Perfluorobutanoic acid	^{13}C4-PFBA	213	169	-
PFPeA	Perfluoropentanoic acid	^{13}C5-PFHxA	263	219	-
PFHxA	Perfluorohexanoic acid	^{13}C5-PFHxA	313	269	119
PFHpA	Perfluoroheptanoic acid	^{13}C8-PFOA	363	319	169
PFOA	Perfluorooctanoic acid	^{13}C8-PFOA	413	369	169
PFNA	Perfluorononanoic acid	^{13}C8-PFOA	463	419	169
Perfluoroalkyl sulfonates (PFSAs)					
PFBS	Perfluorobutanesulfonic acid	^{13}C3-PFBS	299	80	99
PFHxS	Perfluorohexanesulfonic acid	^{13}C3-PFHxS	399	80	99
PFOS	Perfluorooctanesulfonic acid	^{13}C8-PFOS	499	80	99
Fluorotelomer sulfonate (FTS)					
6:2FTS	1H,1H, 2H, 2H-Perfluorooctane sulfonic acid	^{13}C8-PFOS	427	407	81

*Products 1 and 2 serve as quantifier and qualifier, respectively.

Table A.3 Summary of Treatment Conditions Tested for PFAS

Parameter Studied	Contaminant(s)	Value Range
pH	PFAS	pH 4, 10 ,13
Initial concentration	PFAS	100, 500 µg/L
Dissolved oxygen (DO)	PFAS,	2 mg/L – 8.5 mg/L
E-beam dose	PFAS	25 – 1000 kGy
Co-contaminants	PFAS mixture	-
	PFOS, PFOA	
Groundwater matrix	PFAS mix,	

Table A.4 LC-MS/MS Conditions

LC Instrument conditions	
Parameter	**Value**
LC	Agilent G7120A 1290 Binary Pump Agilent G7116A 1260 Multicolumn Thermostat Agilent G7167A 1260 Multisampler
Analytical column	Agilent ZOBRAX Eclipse Plus C18 3.0 x 50 mm, 1.8 micron
Delayed column	Agilent ZOBRAX Eclipse Plus C18 4.6 x 50 mm, 3.5 micron
Column temperature	50 °C
Injection volume	5 µL
Mobile phase	A) 5 mM Ammonium acetate in water B) Methanol
Flow rate	0.4 mL/min
Gradient	Time (min) %B
	0.0 10
	0.5 10
	2.0 30
	14.0 95
	14.5 100
Stop time	16.5 minutes
Post time	6 minutes
MS Instrument conditions	
Parameter	**Value**
MS	Agilent 6495 Triple Quadrupole MS/MS Agilent Jet Stream ESI source
Drying gas temperature	175 °C
Drying gas flow	17 L/min
Nebulizer	20 psi
Sheath gas temperature	275 °C
Sheath gas flow	11 L/min
Capillary voltage (Neg)	2500 V
Nozzle voltage (Neg)	0 V
iFunnel High pressure RF (Neg) Low pressure RF (Neg)	90 V 40 V

Table A.5 Characterization of Water Quality Parameters for The GW Samples

Matrix	Ammonia (mg N/L)	TKN (mg N/L)	Nitrate + Nitrite (mg N/L)	Nitrite (mg N/L)	TOC (mg N/L)	Alkalinity (mg/L as CaCO$_3$)	Conductivity (μS/cm)
GW1	0.03	<0.5	0.57	0.01	2.59	1	25.8
GW2	0.06	<0.5	0.77	0.01	2.80	78.8	90.7
GW3	1.29	1.7	0.01	0.01	5.50	429.6	208.0

Table A.6 Groundwater PFAS Concentration and Increase in PFAS Concentration After TOP Assay in Untreated and E-Beam Treated Samples.

Note: E-Beam Dose: 250 kGy BDL Denotes Below Detection Limit.

Matrix	PFAS	Background PFAS concentration (ppt)	PFAS concentration post TOP assay of untreated sample (ppt)	Percentage increase in concentration post TOP assay in untreated sample (%)	Percentage change in concentration on post TOP assay in e-beam treated sample (%)
GW1	PFBA	550	6040	988	<10
	PFPeA	710	2310	225	<10
	PFHpA	390	400	<10	<10
	PFHxA	1548	2738	77	49
	PFOA	1830	2080	13	-15
	6:2FTS	1890	90	-95	-
	4:2 FTS	80	BDL	-100	-
GW2	PFBA	110	90	-18	TOP assay was not performed.
	PFPeA	90	80	-11	
	PFHxA	1548	2738	77	
	PFHpA	20	20	-	
	PFOA	680	1180	74	
GW3	PFBA	450	1420	215	-16
	PFPeA	1760	3500	98	<10
	PFHxA	1574	3727	136	<10
	PFHpA	440	640	45	<10
	PFOA	1090	1970	80	-12
	PFNA	200	230	15	-
	6:2 FTS	2710	20	-99	-
	8:2 FTS	430	BDL	-100	-

Table A.7 Calculated EE/O Values of PFAS Treated as Single Solute Samples at 250 kGy of E-Beam Dose. Ranges Denote Maximum and Minimum EE/O Values Calculated. Initial Concentration: 100 µg/L.

Note: * Denotes EE/O Value for PFBA and PFBS Calculated at 1000 kGy. ** Denotes The Range Of EE/O Values for PFOA and PFOS Calculated at E-Beam Doses of 250-1000 kGy.

PFAS treated	Calculated EE/O values (kwh/m^3/order)
PFBA	139[*]
PFBS	503[*]
PFPEA	70-174
PFHXA	63-100
PFHXS	84
PFHPA	135
PFOA	58-140[**]
6:2 FTS	49
PFOS	108-155**
PFNA	45-265

EFFECT OF CHAIN LENGTH, ELECTROLYTE COMPOSITION AND AEROSOLIZATION ON THE REMOVAL OF PER- AND POLYFLUOROALKYL SUBSTANCES DURING ELECTROCHEMICAL TREATMENT OF WATER

This contains supporting information submitted along with the manuscript.

Table B.1 Variation of Anodic Voltage in Solutions Containing Different Electrolytes With Varying Applied Voltage.

Note: Solution Conductivity Maintained at 1000 ms/cm

Applied voltage	Anodic voltage vs Ag/AgCl in		
	Na_2SO_4	NaCl	$NaNO_3$
5	3.6	3.5	3.5
7.5	5.6	5.5	5.5
10	7.6	7.5	7.5
12	9.2	9.1	9.1
15	11.6	11.5	11.5
20	15.7	15.5	15.5
28	22.3	22.1	22.1

Table B.2 Average Surrogate Recoveries for PFAS Using Wax Cartridges

PFAS analyzed	Average SPE surrogate recovery (%)
PFBS	104
PFOA	95
PFOS	89
6:FTS	88
PFNA	90
Average	93
stdev	6

Power supply   Multimeter   Cathode and anode in electrolyte solution
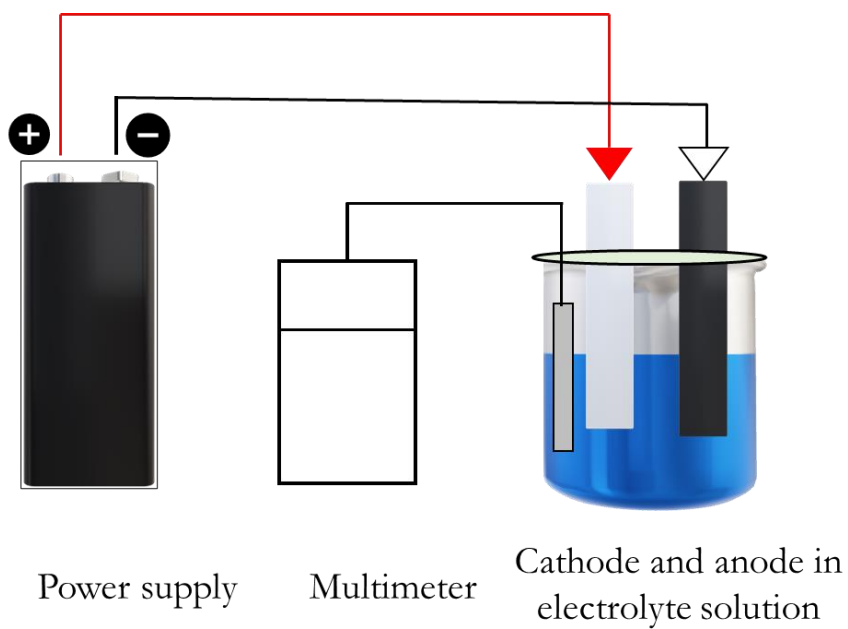
Figure B.1 Schematic of the eAOP system

APPENDIX C

AIR-BUBBLING ASSISTED SOIL WASHING APPROACHES FOR PFAS CONTAMINATED SOILS

Table C.1 Average Surrogate Recoveries for PFAS Using Wax Cartridges and Average Standard Addition Recovery in soil Spiked Prior to Soil Washing

PFAS analyzed	Average SPE surrogate recovery* (%)	Average SPE surrogate recovery** (%)	Average standard addition recovery (%)
PFBA	88	-	
PFBS	75	-	
PFOA	85	-	
PFOS	76	52	25
PFDA	90		

* Recovery calculated in soil

** Recovery calculated in non-settleable organic carbon phase

REFERENCES

1.   Ross, R. What Are PFAS? https://www.livescience.com/65364-pfas.html (accessed November 2023)

2.   Rahman, M. F.; Peldszus, S.; Anderson, W. B., Behaviour and fate of perfluoroalkyl and polyfluoroalkyl substances (PFASs) in drinking water treatment: a review. *Water Res* **2014,** *50*, 318-40.

3.   Nzeribe, B. N.; Crimi, M.; Mededovic Thagard, S.; Holsen, T. M., Physico-Chemical Processes for the Treatment of Per- And Polyfluoroalkyl Substances (PFAS): A review. *Crit. Rev. Environ. Sci. Technol.* **2019,** *49* (10), 866-915.

4.   Casal, P.; Gonzalez-Gaya, B.; Zhang, Y.; Reardon, A. J.; Martin, J. W.; Jimenez, B.; Dachs, J., Accumulation of Perfluoroalkylated Substances in Oceanic Plankton. *Environ. Sci. Technol.* **2017,** *51* (5), 2766-2775.

5.   Pike, K. A.; Edmiston, P. L.; Morrison, J. J.; Faust, J. A., Correlation Analysis of Perfluoroalkyl Substances in Regional U.S. Precipitation Events. *Water Res* **2021,** *190*, 116685.

6.   Londhe, K.; Lee, C. S.; McDonough, C. A.; Venkatesan, A. K., The Need for Testing Isomer Profiles of Perfluoroalkyl Substances to Evaluate Treatment Processes. *Environ.Sci. Technol.* **2022,** *56* (22), 15207-15219.

7.   Buck, R. C.; Franklin, J.; Berger, U.; Conder, J. M.; Cousins, I. T.; de Voogt, P.; Jensen, A. A.; Kannan, K.; Mabury, S. A.; van Leeuwen, S. P., Perfluoroalkyl and polyfluoroalkyl substances in the environment: terminology, classification, and origins. *Integr. Environ. Assess. Manag.* **2011,** *7* (4), 513-41.

8.   Herkert, N. J.; Kassotis, C. D.; Zhang, S.; Han, Y.; Pulikkal, V. F.; Sun, M.; Ferguson, P. L.; Stapleton, H. M., Characterization of Per- and Polyfluorinated Alkyl Substances Present in Commercial Anti-fog Products and Their In Vitro Adipogenic Activity. *Environ. Sci. Technol* **2022**.

9.   Brown, J. B.; Conder, J. M.; Arblaster, J. A.; Higgins, C. P., Assessing Human Health Risks from Per- and Polyfluoroalkyl Substance (PFAS)-Impacted Vegetable Consumption: A Tiered Modeling Approach. *Environ. Sci. Technol.* **2020,** *54* (23), 15202-15214.

10.   McDonough, C. A.; Choyke, S.; Barton, K. E.; Mass, S.; Starling, A. P.; Adgate, J. L.; Higgins, C. P., Unsaturated PFOS and Other PFASs in Human Serum and Drinking Water from an AFFF-Impacted Community. *Environ.Sci. Technol.* **2021**.

11.   McDonough, C. A.; Li, W.; Bischel, H. N.; De Silva, A. O.; DeWitt, J. C., Widening the Lens on PFASs: Direct Human Exposure to Perfluoroalkyl Acid Precursors (pre-PFAAs). *Environ.Sci. Technol.* **2022**.

12.   ATSDR What are the health effects of PFAS? https://www.atsdr.cdc.gov/pfas/health-effects/index.html (accessed November 2023).

13.   Sinclair, G. M.; Long, S. M.; Jones, O. A. H., What are the effects of PFAS exposure at environmentally relevant concentrations? *Chemosphere* **2020,** *258*, 127340.

14.   Gagliano, E.; Sgroi, M.; Falciglia, P. P.; Vagliasindi, F. G. A.; Roccaro, P., Removal of poly- and perfluoroalkyl substances (PFAS) from water by adsorption: Role of PFAS chain length, effect of organic matter and challenges in adsorbent regeneration. *Water Res* **2020,** *171*, 115381.

15.   Appleman, T. D.; Higgins, C. P.; Quinones, O.; Vanderford, B. J.; Kolstad, C.; Zeigler-Holady, J. C.; Dickenson, E. R., Treatment of poly- and perfluoroalkyl substances in U.S. full-scale water treatment systems. *Water Res* **2014,** *51*, 246-55.

16.   Londhe, K.; Lee, C.-S.; Zhang, Y.; Grdanovska, S.; Kroc, T.; Cooper, C. A.; Venkatesan, A. K., Energy Evaluation of Electron Beam Treatment of Perfluoroalkyl Substances in Water: A Critical Review. *ACS ES&T Engineering* **2021,** *1* (5), 827-841.

17.   Li, D.; Londhe, K.; Chi, K.; Lee, C. S.; Venkatesan, A. K.; Hsiao, B. S., Functionalized bio-adsorbents for removal of perfluoroalkyl substances: A perspective. *AWS* **2021,** *3* (6).

18.   Cleland, M. R., Fernald, R. A., & Maloof, S. R., Electron beam process design for the treatment of wastes and economic feasibility of the process. *Radiat. Phys. Chem* **1977,** *24* (1), 179-190.

19.   Kurucz, C. N., Waite, T. D., Cooper, W. J., & Nickelsen, M. J., High Energy Electron Beam Irradiation of Water, Wastewater and Sludge. *J Nucl Sci Technol* **1991,** *22*, 1-43.

20.   Cooper, W. J., Nickelsen, M. G., Meacham, D. E., Cadavid, E., Waite, T. D., & Kurucz, C. N, High energy electron beam irradiation: An innovative process for the treatment of aqueous based organic hazardous wastes. *J. Environ. Sci. Health A* **1990,** *27*, 219-244.

21.   Nickelsen, M. G., Cooper, W. J., Lin, K., Kurucz, C. N., & Waite, T. D, High energy electron beam generation of oxidants for the treatment of benzene and toluene in the presence of radical scavengers. *Water Res* **1994,** *28* (5), 1227-1237.

22.   Woods, R. J., & Pikaev, A. K, *Applied Radiation Chemistry: Radiation Processing*. John Wiley & Sons: Canada, 1994.

23.   Hanna, S. M. In *Role of linear accelerators in water treatment*, Eleventh International Water Technology Conference, Sharm El-Sheikh, Egypt, Sharm El-Sheikh, Egypt, 2007.

24.   Getoff, N., Radiation-induced degradation of water pollutants--state of the art. *Radiat. Phys. Chem* **1996,** *47*, 581-593.

25.   Kurucz, C. N., Waite, T. D., & Cooper, W. J., The Miami Electron Beam Research Facility: a large scale wastewater treatment application. *Radiat. Phys. Chem* **1995,** *45*, 299-308.

26.   Kume, T. M., Y In *Proccedings of the Takasaki symposium on radiation processing of natural polymers*, JAERI, Takasaki, Japan, Japan Atomic Energy Research Institute: Takasaki, Japan, 2001.

27.   Cooper, W. J., Curry, R. D., & O'Shea, K. E., Environmental applications of ionizing radiation. John Wiley and sons: Unites States of America, 1998; p 21.

28.   Getoff, N., Factors influencing the efficiency of radiation-induced degradation of water pollutants. *Radiat. Phys. Chem* **2002,** (65), 437-446.

29.   Song, Z.; Tang, H.; Wang, N.; Zhu, L., Reductive defluorination of perfluorooctanoic acid by hydrated electrons in a sulfite-mediated UV photochemical system. *J. Hazard. Mater.* **2013,** *262*, 332-8.

30.   Bentel, M. J.; Yu, Y.; Xu, L.; Li, Z.; Wong, B. M.; Men, Y.; Liu, J., Defluorination of Per- and Polyfluoroalkyl Substances (PFASs) with Hydrated Electrons: Structural Dependence and Implications to PFAS Remediation and Management. *Environ. Sci. Technol.* **2019,** *53* (7), 3718-3728.

31.   Trojanowicz, M.; Bartosiewicz, I.; Bojanowska-Czajka, A.; Kulisa, K.; Szreder, T.; Bobrowski, K.; Nichipor, H.; Garcia-Reyes, J. F.; Nałęcz-Jawecki, G.; Męczyńska-Wielgosz, S.; Kisała, J., Application of ionizing radiation in decomposition of perfluorooctanoate (PFOA) in waters. *J. Chem. Eng* **2019,** *357*, 698-714.

32.   Zhang, Z.; Chen, J. J.; Lyu, X. J.; Yin, H.; Sheng, G. P., Complete mineralization of perfluorooctanoic acid (PFOA) by gamma-irradiation in aqueous solution. *Sci Rep.* **2014,** *4*, 7418.

33.   Szajdzinska-Pietek, E., & Gebicki, J. L., Pulse radiolytic investigation of perfluorinated surfactants in aqueous solutions. *Res. Chem. Intermed.* **2000,** *26*, 897-912.

34.   Trojanowicz, M.; Bartosiewicz, I.; Bojanowska-Czajka, A.; Szreder, T.; Bobrowski, K.; Nałęcz-Jawecki, G.; Męczyńska-Wielgosz, S.; Nichipor, H., Application of ionizing radiation in decomposition of perfluorooctane sulfonate (PFOS) in aqueous solutions. *Chem. Eng. J.* **2020,** *379*.

35.   Kim, T.-H.; Lee, S.-H.; Kim, H. Y.; Doudrick, K.; Yu, S.; Kim, S. D., Decomposition of perfluorooctane sulfonate (PFOS) using a hybrid process with electron beam and chemical oxidants. *Chem. Eng. J.* **2019,** *361*, 1363-1370.

36.   Trojanowicz, M.; Bojanowska-Czajka, A.; Bartosiewicz, I.; Kulisa, K., Advanced Oxidation/Reduction Processes treatment for aqueous perfluorooctanoate (PFOA) and perfluorooctanesulfonate (PFOS) – A review of recent advances. *Chem. Eng. J.* **2018,** *336*, 170-199.

37.   Ma, S.-H.; Wu, M.-H.; Tang, L.; Sun, R.; Zang, C.; Xiang, J.-J.; Yang, X.-X.; Li, X.; Xu, G., EB degradation of perfluorooctanoic acid and perfluorooctane sulfonate in aqueous solution. *Nucl. Sci. Tech.* **2017,** *28* (9), 137.

38.   Kim, T. H.; Yu, S.; Choi, Y.; Jeong, T. Y.; Kim, S. D., Profiling the decomposition products of perfluorooctane sulfonate (PFOS) irradiated using an electron beam. *Sci Total Environ* **2018,** *631-632*, 1295-1303.

39.   Micic, O. I., Nenadovic, M.T., & Markovic, V.M *Radiation chemical destruction of phenol in oxygenated aqueous solutions*; International Atomic Energy Agency (IAEA): IAEA.: 1975.

40.   Pikaev, A. K., Shubin, V.M.,, Radiation treatment of liquid wastes. *Radiat. Phys. Chem* **1984,** *24*, 77-83.

41.   Nickelsen, M. G., Cooper, W. J., Secker, D. A., Rosocha, L. A., Kurucz, C. N., & Waite, T. D., Kinetic modeling and simulation of PCE and TCE removal in aqueous solutions by electron-beam irradiation. *Radiat. Phys. Chem.* **2002,** *65*, 579-587.

42.   Podgorsak, E. B., *Radiation Oncology Physics: A Handbook for Teachers and Students*. IAEA: Vienna, Austria, 2005.

43.   Wang, S.; Yang, Q.; Chen, F.; Sun, J.; Luo, K.; Yao, F.; Wang, X.; Wang, D.; Li, X.; Zeng, G., Photocatalytic degradation of perfluorooctanoic acid and perfluorooctane sulfonate in water: A critical review. *Chem. Eng. J.* **2017,** *328*, 927-942.

44.   Kim, T. H.; Kim, S. D.; Kim, H. Y.; Lim, S. J.; Lee, M.; Yu, S., Degradation and toxicity assessment of sulfamethoxazole and chlortetracycline using electron beam, ozone and UV. *J. Hazard. Mater.* **2012,** *227-228*, 237-42.

45.   Emami-Meibodi, M.; Parsaeian, M. R.; Amraei, R.; Banaei, M.; Anvari, F.; Tahami, S. M. R.; Vakhshoor, B.; Mehdizadeh, A.; Fallah Nejad, N.; Shirmardi, S. P.; Mostafavi, S. J.; Mousavi, S. M. J., An experimental investigation of wastewater treatment using electron beam irradiation. *Radiat. Phys. Chem.* **2016,** *125*, 82-87.

46.   Lee, C. S.; Venkatesan, A. K.; Walker, H. W.; Gobler, C. J., Impact of groundwater quality and associated byproduct formation during UV/hydrogen peroxide treatment of 1,4-dioxane. *Water Res* **2020,** *173*, 115534.

47.   Trucci, R. H., Harwood, William S., Herring, F. G., and Madura Jeffrey D, *General Chemistry: Principles and Modern Applications. 9th ed.* Pearson Education, Inc: Upper Saddle River, 2007.

48.   Kwon, M.; Yoon, Y.; Cho, E.; Jung, Y.; Lee, B. C.; Paeng, K. J.; Kang, J. W., Removal of iopromide and degradation characteristics in electron beam irradiation process. *J. Hazard. Mater.* **2012,** *227-228*, 126-34.

49.   Cooper, W. J., Cadavid, E., Nickelsen, M. G., Lin, K., Kurucz, C. N., & Waite, T. D Removing THMs From Drinking Water Using High-Energy Electron-Beam Irradiation. *J Am Water Works Assoc* **1993,** *85*.

50.   He, S.; Wang, J.; Ye, L.; Zhang, Y.; Yu, J., Removal of diclofenac from surface water by electron beam irradiation combined with a biological aerated filter. *Radiat. Phys. Chem.* **2014,** *105*, 104-108.

51.   Qing X, H. J., Yu XW, Zhang SK, Yang YY, Ren MZ, Wen YL, Concentrations, distribution characteristics and electron beam radiolysis degradation of PCDD/Fs in waste water from a paper mill. *Europe PMC* **2014,** *35* (7), 2645-2649.

52.   Wang, L.; Batchelor, B.; Pillai, S. D.; Botlaguduru, V. S. V., Electron beam treatment for potable water reuse: Removal of bromate and perfluorooctanoic acid. *Chem. Eng. J.* **2016,** *302*, 58-68.

53.   Trojanowicz, M., Removal of persistent organic pollutants (POPs) from waters and wastewaters by the use of ionizing radiation. *Sci Total Environ* **2020,** *718*, 134425.

54.   Gu, Y.; Dong, W.; Luo, C.; Liu, T., Efficient Reductive Decomposition of Perfluorooctanesulfonate in a High Photon Flux UV/Sulfite System. *Environ. Sci. Technol* **2016,** *50* (19), 10554-10561.

55.   Schulz, K.; Silva, M. R.; Klaper, R., Distribution and effects of branched versus linear isomers of PFOA, PFOS, and PFHxS: A review of recent literature. *Sci. Total Environ* **2020**.

56.   Gobelius, L.; Hedlund, J.; Durig, W.; Troger, R.; Lilja, K.; Wiberg, K.; Ahrens, L., Per- and Polyfluoroalkyl Substances in Swedish Groundwater and Surface Water: Implications for Environmental Quality Standards and Drinking Water Guidelines. *Environ. Sci. Technol.* **2018,** *52* (7), 4340-4349.

57.   Ahrens, L., Vogel, L., & Wiberg, K *Analysis of per- and polyfluoroalkyl substances (PFASs) and phenolic compounds in Swedish rivers over four different seasons*; Swedish University of Agricultural sciences: Uppsala, Sweden, 2018.

58.   Huang, D.; Yin, L.; Lu, X.; Lin, S.; Niu, Z.; Niu, J., Directional electron transfer mechanisms with graphene quantum dots as the electron donor for photodecomposition of perfluorooctane sulfonate. *Chem. Eng. J.* **2017,** *323*, 406-414.

59.   Buxton, G. V. In *Basic Radiation Chemistry of Liquid Water*, Dordrecht, Springer Netherlands: Dordrecht, 1982; pp 241-266.

60.   Buxton, G. V.; Greenstock, C. L.; Helman, W. P.; Ross, A. B., Critical Review of rate constants for reactions of hydrated electrons, hydrogen atoms and hydroxyl radicals ($\cdot$OH/$\cdot$O− in Aqueous Solution. *J. Phys. Chem. Ref. Data* **1988,** *17* (2), 513-886.

61.   Banks, D.; Jun, B.-M.; Heo, J.; Her, N.; Park, C. M.; Yoon, Y., Selected advanced water treatment technologies for perfluoroalkyl and polyfluoroalkyl substances: A review. *Sep. Purif. Technol.* **2020,** *231*, 115929.

62.   Lewis, A. J.; Joyce, T.; Hadaya, M.; Ebrahimi, F.; Dragiev, I.; Giardetti, N.; Yang, J.; Fridman, G.; Rabinovich, A.; Fridman, A. A.; McKenzie, E. R.; Sales, C. M., Rapid degradation of PFAS in aqueous solutions by reverse vortex flow gliding arc plasma. *Environ. Sci. Water Res. Technol.* **2020,** *6* (4), 1044-1057.

63.   Lu, D.; Sha, S.; Luo, J.; Huang, Z.; Zhang Jackie, X., Treatment train approaches for the remediation of per- and polyfluoroalkyl substances (PFAS): A critical review. *J. Hazard. Mater.* **2020,** *386*, 121963.

64.   Yasuoka, K.; Sasaki, K.; Hayashi, R., An energy-efficient process for decomposing perfluorooctanoic and perfluorooctane sulfonic acids using dc plasmas generated within gas bubbles. *Plasma Sources Sci T* **2011,** *20* (3).

65.   Grdanovska,S , C. C. *Electron Beam Driven Industrial Chemistries*; Fermi National Accelerator Laboratory: Illinois Accelerator Research Center, 2019; https://web.fnal.gov/organization/iarc/Shared%20Documents/Electron-Beam-Driven-Industrial-Chemistries.pdf.

66.   In *Accelerators for America's Future*, Accelerators for America's Future, United States, Department of Energy's Office of High Energy Physics: United States, 2010, https://www.osti.gov/servlets/purl/1358082.

67.   Carter, K. E., & Farrell, J. , Oxidative Destruction of Perfluorooctane Sulfonate Using Boron-Doped Diamond Film Electrodes. *Environ. Sci. Technol.* **2008,** *42*, 6111–6115.

68.   Wang, Y.; Pierce, R. D.; Shi, H.; Li, C.; Huang, Q., Electrochemical degradation of perfluoroalkyl acids by titanium suboxide anodes. *Environ. Sci. Water Res. Technol.* **2020,** *6* (1), 144-152.

69.   Guzilov, I., Maslennikov, O., Egorov, R., Syratchev, I., Kobets, V., & Sumbaev, A In *Comparison of 6 MW S-band pulsed BAC MBK with the existing SBKs*, Eighteenth International Vacuum Electronics Conference (IVEC), 2017.

70.   Wang, H., Rimmer, R. A., Nelson, R., Neubauer, M., Dudas, A., Coriton, B. R., & Moeller, C. P In *Magnetron R&D for high efficiency cw rf sources of particle accelerators*, 10th Int. Particle Accelerator Conf, Melbourne, Australia, Melbourne, Australia, 2019.

71.   Read, M.; Ives, R. L.; Bui, T.; Collins, G.; Marsden, D.; Chase, B.; Reid, J.; Walker, C.; Conant, J., A 100-kW 1300-MHz Magnetron With Amplitude and Phase Control for Accelerators. *IEEE Trans Plasma Sci* **2019,** *47* (9), 4268-4273.

72.   Cooper, C. *Conceptual Design of an Electron Accelerator for Bio-Solid Waste Treatment*; United States, 2017.

73.   Ciovati, G., Anderson, J., Coriton, B., Guo, J., Hannon, F., Holland, L., LeSher, M., Marhauser, F., Rathke, J., Rimmer, R. and Schultheiss, T, Design of a cw, low energy, high power superconducting linac for environmental applications. *Phys. Rev. Accel. Beams* **2018,** *21*.

74.   Dhuley, R. *Cryocooler conduction-cooled SRF cavities for particle accelerators*; FERMILAB-SLIDES-20-018-DI-LDRD-TD; Fermi National Accelerator Lab: United States, 2020; https://www.osti.gov/biblio/1633742-cryocooler-conduction-cooled-srf-cavities-compact-particle-accelerators.

75.   Ciovati, G., Anderson, J., Coriton, B., Guo, J., Hannon, F., Holland, L., LeSher, M., Marhauser, F., Rathke, J., Rimmer, R. and Schultheiss, T, First demonstration of a cryocooler conduction cooled superconducting radiofrequency cavity operating at practical cw accelerating gradients. *Supercond. Sci. Technol.* **2020,** *33* (6).

76.   Kim, T.-H.; Lee, S.-H.; Kim, H. Y.; Doudrick, K.; Yu, S.; Kim, S. D., Decomposition of perfluorooctane sulfonate (PFOS) using a hybrid process with electron beam and chemical oxidants. *J. Chem. Eng* **2019,** *361*, 1363-1370.

77.   Kim, T. H.; Yu, S.; Choi, Y.; Jeong, T. Y.; Kim, S. D., Profiling the decomposition products of perfluorooctane sulfonate (PFOS) irradiated using an electron beam. *Sci.Total. Environ.* **2018,** *631-632*, 1295-1303.

78.   Ma, S.-H.; Wu, M.-H.; Tang, L.; Sun, R.; Zang, C.; Xiang, J.-J.; Yang, X.-X.; Li, X.; Xu, G., EB degradation of perfluorooctanoic acid and perfluorooctane sulfonate in aqueous solution. *NST* **2017,** *28* (9), 137.

79.   Wang, L.; Batchelor, B.; Pillai, S. D.; Botlaguduru, V. S. V., Electron beam treatment for potable water reuse: Removal of bromate and perfluorooctanoic acid. *J. Chem. Eng* **2016,** *302*, 58-68.

80.   Trojanowicz, M.; Bartosiewicz, I.; Bojanowska-Czajka, A.; Szreder, T.; Bobrowski, K.; Nałęcz-Jawecki, G.; Męczyńska-Wielgosz, S.; Nichipor, H., Application of ionizing radiation in decomposition of perfluorooctane sulfonate (PFOS) in aqueous solutions. *J. Chem. Eng* **2020,** *379*.

81.   Lassalle, J.; Gao, R.; Rodi, R.; Kowald, C.; Feng, M.; Sharma, V. K.; Hoelen, T.; Bireta, P.; Houtz, E. F.; Staack, D.; Pillai, S. D., Degradation of PFOS and PFOA in soil and groundwater samples by high dose Electron Beam Technology. *Radiat. Phys. Chem* **2021,** *189*.

82.   Jiao, C.; Men, X.; Li, Z.; Zhang, M.; Gao, Y.; Liu, J.; Li, Y.; Zhao, H., Degradation of representative perfluorinated and hydrocarbon surfactants by electron beam irradiation. *JRNC* **2022,** *331* (4).

83.   Feng, M.; Gao, R.; Staack, D.; Pillai, S. D.; Sharma, V. K., Degradation of perfluoroheptanoic acid in water by electron beam irradiation. *Environ. Chem. Lett.* **2021,** *19* (3), 2689-2694.

84.   Kowald, C.; Brorman, E.; Shankar, S.; Klemashevich, C.; Staack, D.; Pillai, S. D., PFOA and PFOS breakdown in experimental sand, laboratory-grade water, investigation-derived groundwater and wastewater effluent samples at 50 kGy electron beam dose. *Radiat. Phys. Chem.* **2021,** *180*.

85.   Gao, Y.; Liang, Y.; Gao, K.; Wang, Y.; Wang, C.; Fu, J.; Wang, Y.; Jiang, G.; Jiang, Y., Levels, spatial distribution and isomer profiles of perfluoroalkyl acids in soil, groundwater and tap water around a manufactory in China. *Chemosphere* **2019,** *227*, 305-314.

86.   Schulz, K.; Silva, M. R.; Klaper, R., Distribution and effects of branched versus linear isomers of PFOA, PFOS, and PFHxS: A review of recent literature. *Sci Total Environ* **2020,** *733*, 139186.

87.   Baabish, A.; Sobhanei, S.; Fiedler, H., Priority perfluoroalkyl substances in surface waters - A snapshot survey from 22 developing countries. *Chemosphere* **2021,** *273*, 129612.

88.   Cousins, I. T.; DeWitt, J. C.; Gluge, J.; Goldenman, G.; Herzke, D.; Lohmann, R.; Miller, M.; Ng, C. A.; Scheringer, M.; Vierke, L.; Wang, Z., Strategies for grouping per- and polyfluoroalkyl substances (PFAS) to protect human and environmental health. *Environ. Sci. Process. Impacts.* **2020,** *22* (7), 1444-1460.

89.   Getoff, N., Factors influencing the efficiency of radiation-induced degradation of water pollutants. *Radiat. Phys. Chem.* **2002,** (65), 437-446.

90.   Tian, S.; Xu, T.; Fang, L.; Zhu, Y.; Li, F.; Zhao, D.; Soong, T.-Y.; Shi, H., A 'Concentrate-&-Destroy' technology for enhanced removal and destruction of per- and polyfluoroalkyl substances in municipal landfill leachate. *Sci. Total Environ.* **2021**.

91.   Patch, D.; O'Connor, N.; Koch, I.; Cresswell, T.; Hughes, C.; Davies, J. B.; Scott, J.; O'Carroll, D.; Weber, K., Elucidating degradation mechanisms for a range of per- and polyfluoroalkyl substances (PFAS) via controlled irradiation studies. *Sci. Total. Environ.* **2022**, 154941.

92.   Trojanowicz, M.; Bojanowska-Czajka, A.; Bartosiewicz, I.; Kulisa, K., Advanced Oxidation/Reduction Processes treatment for aqueous perfluorooctanoate (PFOA) and perfluorooctanesulfonate (PFOS) – A review of recent advances. *J. Chem. Eng* **2018,** *336*, 170-199.

93.   Bentel, M. J.; Liu, Z.; Yu, Y.; Gao, J.; Men, Y.; Liu, J., Enhanced Degradation of Perfluorocarboxylic Acids (PFCAs) by UV/Sulfite Treatment: Reaction Mechanisms and System Efficiencies at pH 12. *Environ. Sci. Technol. Lett* **2020,** *7* (5), 351-357.

94.   Cheng, Z.; Chen, Q.; Liu, Z.; Liu, J.; Liu, Y.; Liu, S.; Gao, X.; Tan, Y.; Shen, Z., Interpretation of Reductive PFAS Defluorination with Quantum Chemical Parameters. *Environ. Sci. Technol. Lett.* **2021,** *8* (8).

95.   Yamamoto, T.; Noma, Y.; Sakai, S.; Shibata, Y., Photodegradation of perfluorooctane sulfonate by UV irradiation in water and alkaline 2-propanol. *Environ. Sci. Technol.* **2007,** *41* (16), 5660-5.

96.   Houtz, E. F.; Sedlak, D. L., Oxidative conversion as a means of detecting precursors to perfluoroalkyl acids in urban runoff. *Environ. Sci. Technol* **2012,** *46* (17), 9342-9.

97.   Martin, D.; Munoz, G.; Mejia-Avendano, S.; Duy, S. V.; Yao, Y.; Volchek, K.; Brown, C. E.; Liu, J.; Sauve, S., Zwitterionic, cationic, and anionic perfluoroalkyl and polyfluoroalkyl substances integrated into total oxidizable precursor assay of contaminated groundwater. *Talanta* **2019,** *195*, 533-542.

98.   Tenorio, R.; Liu, J.; Xiao, X.; Maizel, A.; Higgins, C. P.; Schaefer, C. E.; Strathmann, T. J., Destruction of Per- and Polyfluoroalkyl Substances (PFASs) in Aqueous Film-Forming Foam (AFFF) with UV-Sulfite Photoreductive Treatment. *Environ Sci Technol* **2020,** *54* (11), 6957-6967.

99.   Abusallout, I.; Wang, J.; Hanigan, D., Emerging investigator series: rapid defluorination of 22 per- and polyfluoroalkyl substances in water using sulfite irradiated by medium-pressure UV. *Environ. Sci. Water Res. Technol.* **2021,** *7* (9), 1552-1562.

100.   Chaplin, B. P., Critical review of electrochemical advanced oxidation processes for water treatment applications. *Environ. Sci. Process. Impacts.* **2014,** *16* (6), 1182-203.

101.   Lee, C.-S.; Londhe, K.; Grdanovska, S.; Cooper, C. A.; Venkatesan, A. K., Emerging investigator series: low doses of electron beam irradiation effectively degrade 1,4-dioxane in water within a few seconds. *Environ. Sci. Water Res. Technol.* **2023,** *9* (9), 2226-2237.

102.   Sun, Y.; Zhang, B.; Zheng, T.; Wang, P., Regeneration of activated carbon saturated with chloramphenicol by microwave and ultraviolet irradiation. *J. Chem. Eng.* **2017,** *320*, 264-270.

103.   Dehdashti, A. K., A; Rezaei, ; Assilian, H; Soleimanian, A, Using Microwave Radiation to Recover GAC exposed to toulene vapor. *Iran. J. Environ. Health. Sci. Eng.* **2011,** *8*, 85-94.

104.   Emami-Meibodi, M.; Parsaeian, M. R.; Amraei, R.; Banaei, M.; Anvari, F.; Tahami, S. M. R.; Vakhshoor, B.; Mehdizadeh, A.; Fallah Nejad, N.; Shirmardi, S. P.; Mostafavi, S. J.; Mousavi, S. M. J., An experimental investigation of wastewater treatment using electron beam irradiation. *Radiat. Phys. Chem* **2016**, *125*, 82-87.

105.   Beltran, F. J., *Ozone Reaction Kinetics for Water and Wastewater Systems*. Lewis Publishers: Boca Raton, Florida., 2004.

106.   von Gunten, U., Ozonation of drinking water: Part I. Oxidation kinetics and product formation. *Water Res* **2003,** *37* (7), 1443-1467.

107.   Venkatesan, A. K.; Lee, C. S.; Gobler, C. J., Hydroxyl-radical based advanced oxidation processes can increase perfluoroalkyl substances beyond drinking water standards: Results from a pilot study. *Sci. Total Environ.* **2022,** *847*, 157577.

108.   Radjenovic, J.; Sedlak, D. L., Challenges and Opportunities for Electrochemical Processes as Next-Generation Technologies for the Treatment of Contaminated Water. *Environ.Sci. Technol.* **2015,** *49* (19), 11292-302.

109.   Fang, C.; Sobhani, Z.; Niu, J.; Naidu, R., Removal of PFAS from aqueous solution using PbO2 from lead-acid battery. *Chemosphere* **2019,** *219*, 36-44.

110.   Niu, J.; Lin, H.; Xu, J.; Wu, H.; Li, Y., Electrochemical mineralization of perfluorocarboxylic acids (PFCAs) by ce-doped modified porous nanocrystalline PbO2 film electrode. *Environ.Sci. Technol.* **2012,** *46* (18), 10191-8.

111.   Sharma, S.; Shetti, N. P.; Basu, S.; Nadagouda, M. N.; Aminabhavi, T. M., Remediation of per- and polyfluoroalkyls (PFAs) via electrochemical methods. *J. Chem. Eng.* **2021**.

112.   Radjenovic, J.; Duinslaeger, N.; Avval, S. S.; Chaplin, B. P., Facing the Challenge of Poly- and Perfluoroalkyl Substances in Water: Is Electrochemical Oxidation the Answer? *Environ.Sci. Technol.* **2020**.

113.   Barisci, S.; Suri, R., Electrooxidation of short and long chain perfluorocarboxylic acids using boron doped diamond electrodes. *Chemosphere* **2020,** *243*, 125349.

114.   Barisci, S.; Suri, R., Electrooxidation of Short- and Long-chain Perfluoroalkyl Substances (PFASs) under different Process Conditions. *J. Environ. Chem. Eng* **2021**.

115.   Fenti, A.; Jin, Y.; Rhoades, A. J. H.; Dooley, G. P.; Iovino, P.; Salvestrini, S.; Musmarra, D.; Mahendra, S.; Peaslee, G. F.; Blotevogel, J., Performance testing of mesh anodes for in situ electrochemical oxidation of PFAS. *Adv. Chem. Eng* **2022,** *9*.

116.   Duinslaeger, N.; Radjenovic, J., Electrochemical degradation of per- and polyfluoroalkyl substances (PFAS) using low-cost graphene sponge electrodes. *Water Res* **2022,** *213*.

117.   Radjenovic, J.; Bagastyo, A.; Rozendal, R. A.; Mu, Y.; Keller, J.; Rabaey, K., Electrochemical oxidation of trace organic contaminants in reverse osmosis concentrate using RuO2/IrO2-coated titanium anodes. *Water Res* **2011,** *45* (4), 1579-86.

118. Le, T. X. H.; Haflich, H.; Shah, A. D.; Chaplin, B. P., Energy-Efficient Electrochemical Oxidation of Perfluoroalkyl Substances Using a Ti4O7 Reactive Electrochemical Membrane Anode. *Environ. Technol. Lett.* **2019,** *6* (8), 504-510.

119. Le, T. X. H.; Haflich, H.; Shah, A. D.; Chaplin, B. P., Energy-Efficient Electrochemical Oxidation of Perfluoroalkyl Substances Using a Ti4O7 Reactive Electrochemical Membrane Anode. *Environ. Sci. Technol. Lett.* **2019,** *6* (8), 504-510.

120. Urtiaga, A.; Fernandez-Gonzalez, C.; Gomez-Lavin, S.; Ortiz, I., Kinetics of the electrochemical mineralization of perfluorooctanoic acid on ultrananocrystalline boron doped conductive diamond electrodes. *Chemosphere* **2015,** *129*, 20-6.

121. Pierpaoli, M.; Szopinska, M.; Wilk, B. K.; Sobaszek, M.; Luczkiewicz, A.; Bogdanowicz, R.; Fudala-Ksiazek, S., Electrochemical oxidation of PFOA and PFOS in landfill leachates at low and highly boron-doped diamond electrodes. *J. Hazard. Mater.* **2021,** *403*, 123606.

122. Rao, U.; Su, Y.; Khor, C. M.; Jung, B.; Ma, S.; Cwiertny, D. M.; Wong, B. M.; Jassby, D., Structural Dependence of Reductive Defluorination of Linear PFAS Compounds in a UV/Electrochemical System. *Environ.Sci. Technol.* **2020**.

123. Nienhauser, A. B.; Ersan, M. S.; Lin, Z.; Perreault, F.; Westerhoff, P.; Garcia-Segura, S., Boron-doped diamond electrodes degrade short- and long-chain per- and polyfluorinated alkyl substances in real industrial wastewaters. *J. Environ. Chem. Eng* **2022,** *10* (2).

124. Armstrong, D. A.; Huie, R. E.; Koppenol, W. H.; Lymar, S. V.; Merényi, G.; Neta, P.; Ruscic, B.; Stanbury, D. M.; Steenken, S.; Wardman, P., Standard electrode potentials involving radicals in aqueous solution: inorganic radicals (IUPAC Technical Report). *IUPAC* **2015,** *87* (11-12), 1139-1150.

125. Chen, Z.; Wang, X.; Feng, H.; Chen, S.; Niu, J.; Di, G.; Kujawski, D.; Crittenden, J. C., Electrochemical Advanced Oxidation of Perfluorooctanoic Acid: Mechanisms and Process Optimization with Kinetic Modeling. *Environ Sci Technol* **2022**.

126. Schaefer, C. E.; Andaya, C.; Burant, A.; Condee, C. W.; Urtiaga, A.; Strathmann, T. J.; Higgins, C. P., Electrochemical treatment of perfluorooctanoic acid and perfluorooctane sulfonate: Insights into mechanisms and application to groundwater treatment. *J. Chem. Eng.* **2017,** *317*, 424-432.

127. Duinslaeger, N.; Doni, A.; Radjenovic, J., Impact of supporting electrolyte on electrochemical performance of borophene-functionalized graphene sponge anode and degradation of per- and polyfluoroalkyl substances (PFAS). *Water Res* **2023,** *242*, 120232.

128. Zhuo, Q.; Deng, S.; Yang, B.; Huang, J.; Wang, B.; Zhang, T.; Yu, G., Degradation of perfluorinated compounds on a boron-doped diamond electrode. *Electrochim. Acta.* **2012,** *77*, 17-22.

129. Lin, H.; Xiao, R.; Xie, R.; Yang, L.; Tang, C.; Wang, R.; Chen, J.; Lv, S.; Huang, Q., Defect Engineering on a Ti4O7 Electrode by Ce(3+) Doping for the Efficient Electrooxidation of Perfluorooctanesulfonate. *Environ.Sci. Technol.* **2021,** *55* (4), 2597-2607.

130.	Shi, H.; Chiang, S.-Y.; Wang, Y.; Wang, Y.; Liang, S.; Zhou, J.; Fontanez, R.; Gao, S.; Huang, Q., An electrocoagulation and electrooxidation treatment train to remove and degrade per- and polyfluoroalkyl substances in aqueous solution. *Sci Total Environ* **2021**.

131.	Wang, L.; Lu, J.; Li, L.; Wang, Y.; Huang, Q., Effects of chloride on electrochemical degradation of perfluorooctanesulfonate by Magneli phase Ti4O7 and boron doped diamond anodes. *Water Res* **2020**, *170*, 115254.

132.	Cao, Y.; Lee, C.; Davis, E. T. J.; Si, W.; Wang, F.; Trimpin, S.; Luo, L., 1000-Fold Preconcentration of Per- and Polyfluorinated Alkyl Substances within 10 Minutes via Electrochemical Aerosol Formation. *Anal Chem* **2019,** *91* (22), 14352-14358.

133.	Wan, Z.; Cao, L.; Huang, W.; Zheng, D.; Li, G.; Zhang, F., Enhanced Electrochemical Destruction of Perfluorooctanoic Acid (PFOA) Aided by Overlooked Cathodically Produced Bubbles. *Environ. Sci. Technol. Lett* **2022**.

134.	CompTox Chemicals Dashboard. https://comptox.epa.gov/dashboard/ (accessed November 2022)

135.	Wang, Y.; Li, L.; Huang, Q., Electrooxidation of per- and polyfluoroalkyl substances in chloride-containing water on surface-fluorinated Ti4O7 anodes: Mitigation and elimination of chlorate and perchlorate formation. *Chemosphere* **2022**.

136.	Hayashi, R.; Obo, H.; Takeuchi, N.; Yasuoka, K., Decomposition of Perfluorinated Compounds in Water by DC Plasma within Oxygen Bubbles. *EEJ* **2015**, *190* (3), 9-16.

137.	Niu, J.; Lin, H.; Gong, C.; Sun, X., Theoretical and experimental insights into the electrochemical mineralization mechanism of perfluorooctanoic acid. *Environ.Sci. Technol.* **2013,** *47* (24), 14341-9.

138.	Veciana, M.; Bräunig, J.; Farhat, A.; Pype, M.-L.; Freguia, S.; Carvalho, G.; Keller, J.; Ledezma, P., Electrochemical oxidation processes for PFAS removal from contaminated water and wastewater: fundamentals, gaps and opportunities towards practical implementation. *J. Hazard. Mater.* **2022,** *434*.

139.	Liu, Z.; Bentel, M. J.; Yu, Y.; Ren, C.; Gao, J.; Pulikkal, V. F.; Sun, M.; Men, Y.; Liu, J., Near-Quantitative Defluorination of Perfluorinated and Fluorotelomer Carboxylates and Sulfonates with Integrated Oxidation and Reduction. *Environ.Sci. Technol.* **2021**.

140.	Ochiai, T.; Iizuka, Y.; Nakata, K.; Murakami, T.; Tryk, D. A.; Fujishima, A.; Koide, Y.; Morito, Y., Efficient electrochemical decomposition of perfluorocarboxylic acids by the use of a boron-doped diamond electrode. *DRM* **2011,** *20* (2), 64-67.

141.	Benskin, J. P., Yeung, L.W.Y., Yamashita, N., Taniyasu, S., Lam, P.K.S., Martin, J.W.,, Perfluorinated Acid Isomer Profiling in Water and Quantitative Assessment of Manufacturing Source. *Environ. Sci. Technol* **2010,** *44*, 9049–9054.

142.	Benotti, M. J.; Fernandez, L. A.; Peaslee, G. F.; Douglas, G. S.; Uhler, A. D.; Emsbo-Mattingly, S., A forensic approach for distinguishing PFAS materials. *Environ. Forensics* **2020,** *21* (3-4), 319-333.

143.   Reagen, W. K. L., K. R.; Jacoby, C. B.; Purcell, R. G.; Kestner, T. A.; Payfer, R. M.; Miller, J. W. In *Environmental characterization of 3M electrochemical fluorination derived perfluorooctanoate and perfluorooctanesulfonate*, 28th North American meeting, Milwaukee, WI, November; Society of Environmental Toxicology and Chemistry: Milwaukee, WI.

144.   Benskin, J. P.; De Silva, A. O.; Martin, J. W., Isomer profiling of perfluorinated substances as a tool for source tracking: a review of early findings and future applications. *Rev. Environ. Contam. Toxicol.* **2010,** *208*, 111-60.

145.   De Silva, A. O., Derek CG Muir, and Scott A. Mabury., Distribution of perfluorocarboxylate isomers in select samples from the North American environment. *Environ. Toxicol. Chem.* **2009,** *28*, 1801-1814.

146.   Wang, Z.; MacLeod, M.; Cousins, I. T.; Scheringer, M.; Hungerbühler, K., Using COSMOtherm to predict physicochemical properties of poly- and perfluorinated alkyl substances (PFASs). *Environ. Chem. Lett.* **2011,** *8* (4).

147.   Rayne, S.; Forest, K., Comparative semiempirical, ab initio, and density functional theory study on the thermodynamic properties of linear and branched perfluoroalkyl sulfonic acids/sulfonyl fluorides, perfluoroalkyl carboxylic acid/acyl fluorides, and perhydroalkyl sulfonic acids, alkanes, and alcohols. *J. Mol. Struct.* **2010,** *941* (1-3), 107-118.

148.   Chen, X.; Zhu, L.; Pan, X.; Fang, S.; Zhang, Y.; Yang, L., Isomeric specific partitioning behaviors of perfluoroalkyl substances in water dissolved phase, suspended particulate matters and sediments in Liao River Basin and Taihu Lake, China. *Water Res* **2015,** *80*, 235-44.

149.   Chen, M.; Wang, Q.; Shan, G.; Zhu, L.; Yang, L.; Liu, M., Occurrence, partitioning and bioaccumulation of emerging and legacy per- and polyfluoroalkyl substances in Taihu Lake, China. *Sci. Total. Environ.* **2018,** *634*, 251-259.

150.   Yu, N.; Shi, W.; Zhang, B.; Su, G.; Feng, J.; Zhang, X.; Wei, S.; Yu, H., Occurrence of perfluoroalkyl acids including perfluorooctane sulfonate isomers in Huai River Basin and Taihu Lake in Jiangsu Province, China. *Environ. Sci. Technol.* **2013,** *47* (2), 710-7.

151.   Belkouteb, N.; Franke, V.; McCleaf, P.; Kohler, S.; Ahrens, L., Removal of per- and polyfluoroalkyl substances (PFASs) in a full-scale drinking water treatment plant: Long-term performance of granular activated carbon (GAC) and influence of flow-rate. *Water Res* **2020,** *182*, 115913.

152.   Eschauzier, C.; Beerendonk, E.; Scholte-Veenendaal, P.; De Voogt, P., Impact of treatment processes on the removal of perfluoroalkyl acids from the drinking water production chain. *Environ. Sci. Technol.* **2012,** *46* (3), 1708-15.

153.   McCleaf, P.; Englund, S.; Ostlund, A.; Lindegren, K.; Wiberg, K.; Ahrens, L., Removal efficiency of multiple poly- and perfluoroalkyl substances (PFASs) in drinking water using granular activated carbon (GAC) and anion exchange (AE) column tests. *Water Res* **2017,** *120*, 77-87.

154.   Park, M.; Daniels, K. D.; Wu, S.; Ziska, A. D.; Snyder, S. A., Magnetic ion-exchange (MIEX) resin for perfluorinated alkylsubstance (PFAS) removal in groundwater: Roles of atomic charges for adsorption. *Water Res* **2020,** *181*, 115897.

155.   Park, M.; Wu, S.; Lopez, I. J.; Chang, J. Y.; Karanfil, T.; Snyder, S. A., Adsorption of perfluoroalkyl substances (PFAS) in groundwater by granular activated carbons: Roles of hydrophobicity of PFAS and carbon characteristics. *Water Res* **2020,** *170*, 115364.

156.   Rodowa, A. E.; Knappe, D. R. U.; Chiang, S.-Y. D.; Pohlmann, D.; Varley, C.; Bodour, A.; Field, J. A., Pilot scale removal of per- and polyfluoroalkyl substances and precursors from AFFF-impacted groundwater by granular activated carbon. *Environ.Sci. Technol.* **2020,** *6* (4), 1083-1094.

157.   Valeria Ochoa-Herrera, R. S.-A., Arpad Somogyi, Neil E. Jacobsen, Vicki H. Wysocki, Jim A. Field, Reductive Defluorination of PFOS. *Environ. Sci. Technol. Lett* **2008,** *42*, 3260-3264.

158.   Charbonnet, J. A.; Rodowa, A. E.; Joseph, N. T.; Guelfo, J. L.; Field, J. A.; Jones, G. D.; Higgins, C. P.; Helbling, D. E.; Houtz, E. F., Environmental Source Tracking of Per- and Polyfluoroalkyl Substances within a Forensic Context: Current and Future Techniques. *Environ. Sci. Technol.* **2021,** *55* (11), 7237-7245.

159.   Liu, J.; Zhong, G.; Li, W.; Mejia Avendaño, S., Isomer-specific biotransformation of perfluoroalkyl sulfonamide compounds in aerobic soil. *Sci. Total. Environ.* **2019,** *651*, 766-774.

160.   Chen, M.; Qiang, L.; Pan, X.; Fang, S.; Han, Y.; Zhu, L., In Vivo and in Vitro Isomer-Specific Biotransformation of Perfluorooctane Sulfonamide in Common Carp (Cyprinus carpio). *Environ. Sci. Technol.* **2015,** *49* (23), 13817-24.

161.   Benskin, J. P., Application of Perfluorinated Acid Isomer Profiles for Manufacturing and Exposure Source Determination. Alberta, U. o., Ed. Edmonton, Alberta, 2011.

162.   Ali, A. M.; Higgins, C. P.; Alarif, W. M.; Al-Lihaibi, S. S.; Ghandourah, M.; Kallenborn, R., Per- and polyfluoroalkyl substances (PFASs) in contaminated coastal marine waters of the Saudi Arabian Red Sea: a baseline study. *Environ. Sci. Pollut. Res. Int.* **2021,** *28* (3), 2791-2803.

163.   Ali, A. M.; Langberg, H. A.; Hale, S. E.; Kallenborn, R.; Hartz, W. F.; Mortensen, A. K.; Ciesielski, T. M.; McDonough, C. A.; Jenssen, B. M.; Breedveld, G. D., The fate of poly- and perfluoroalkyl substances in a marine food web influenced by land-based sources in the Norwegian Arctic. *Environ. Sci. Process. Impacts.* **2021,** *23* (4), 588-604.

164.   Benskin, J. P.; Ahrens, L.; Muir, D. C.; Scott, B. F.; Spencer, C.; Rosenberg, B.; Tomy, G.; Kylin, H.; Lohmann, R.; Martin, J. W., Manufacturing origin of perfluorooctanoate (PFOA) in Atlantic and Canadian Arctic seawater. *Environ. Sci. Technol.* **2012,** *46* (2), 677-85.

165.   Fang, S.; Chen, X.; Zhao, S.; Zhang, Y.; Jiang, W.; Yang, L.; Zhu, L., Trophic magnification and isomer fractionation of perfluoroalkyl substances in the food web of Taihu Lake, China. *Environ. Sci. Technol.* **2014,** *48* (4), 2173-82.

166.   Feng, X.; Ye, M.; Li, Y.; Zhou, J.; Sun, B.; Zhu, Y.; Zhu, L., Potential sources and sediment-pore water partitioning behaviors of emerging per/polyfluoroalkyl substances in the South Yellow Sea. *J. Hazard. Mater.* **2020,** *389*, 122124.

167.   Furdui, V. I., Paul A. Helm, Patrick W. Crozier, Corina Lucaciu, Eric J. Reiner, Chris H. Marvin, D. Michael Whittle, Scott A. Mabury, and Gregg T. Tomy, Temporal Trends of Perfluoroalkyl Compounds with Isomer Analysis in Lake Trout from Lake Ontario (1979-2004). *Environ. Sci. Technol* **2008,** *42*, 4739–4744.

168.   Houde, M., Gertje Czub, Jeff M. Small, Sean Backus, Xiaowa Wang, Mehran Alaee, and Derek CG Muir., Fractionation and bioaccumulation of perfluorooctane sulfonate (PFOS) isomers in a Lake Ontario food web. *Environ. Sci. Technol. Lett* **2008,** *42*, 9397-9403.

169.   Hu, H.; Zhang, Y.; Zhao, N.; Xie, J.; Zhou, Y.; Zhao, M.; Jin, H., Legacy and emerging poly- and perfluorochemicals in seawater and sediment from East China Sea. *Sci.Total. Environ.* **2021,** *797*, 149052.

170.   Johansson, J. H.; Salter, M. E.; Acosta Navarro, J. C.; Leck, C.; Nilsson, E. D.; Cousins, I. T., Global transport of perfluoroalkyl acids via sea spray aerosol. *Environ. Sci. Process. Impacts.* **2019,** *21* (4), 635-649.

171.   Kärrman, A.; Elgh-Dalgren, K.; Lafossas, C.; Møskeland, T., Environmental levels and distribution of structural isomers of perfluoroalkyl acids after aqueous fire-fighting foam (AFFF) contamination. *Environ. Chem* **2011,** *8* (4).

172.   Kumar, K. S., Yasuyuki Zushi, Shigeki Masunaga, Matthew Gilligan, Carol Pride, and Kenneth S. Sajwan., Perfluorinated organic contaminants in sediment and aquatic wildlife, including sharks, from Georgia, USA. *Mar. Pollut. Bull.* **2009,** *58*, 621-629.

173.   Langberg, H. A.; Arp, H. P. H.; Breedveld, G. D.; Slinde, G. A.; Hoiseter, A.; Gronning, H. M.; Jartun, M.; Rundberget, T.; Jenssen, B. M.; Hale, S. E., Paper product production identified as the main source of per- and polyfluoroalkyl substances (PFAS) in a Norwegian lake: Source and historic emission tracking. *Environ. Pollut.* **2020,** *273*, 116259.

174.   Ma, X.; Shan, G.; Chen, M.; Zhao, J.; Zhu, L., Riverine inputs and source tracing of perfluoroalkyl substances (PFASs) in Taihu Lake, China. *Sci. Total. Environ.* **2018,** *612*, 18-25.

175.   Munoz, G.; Labadie, P.; Botta, F.; Lestremau, F.; Lopez, B.; Geneste, E.; Pardon, P.; Devier, M. H.; Budzinski, H., Occurrence survey and spatial distribution of perfluoroalkyl and polyfluoroalkyl surfactants in groundwater, surface water, and sediments from tropical environments. *Sci. Total. Environ.* **2017,** *607-608*, 243-252.

176.   Picard, J.-C.; Munoz, G.; Vo Duy, S.; Sauvé, S., Longitudinal and vertical variations of waterborne emerging contaminants in the St. Lawrence Estuary and Gulf during winter conditions. *Sci. Total. Environ.* **2021,** *777*.

177.   Powley, C. R.; George, S. W.; Russell, M. H.; Hoke, R. A.; Buck, R. C., Polyfluorinated chemicals in a spatially and temporally integrated food web in the Western Arctic. *Chemosphere* **2008,** *70* (4), 664-72.

178.   Roscales, J. L.; Suarez de Puga, B. R.; Vicente, A.; Munoz-Arnanz, J.; Sanchez, A. I.; Ros, M.; Jimenez, B., Levels and trends of perfluoroalkyl acids (PFAAs) in water (2013-2020) and fish from selected riverine basins in Spain. *Chemosphere* **2022,** *286* (Pt 3), 131940.

179.   Shan, G.; Qian, X.; Chen, X.; Feng, X.; Cai, M.; Yang, L.; Chen, M.; Zhu, L.; Zhang, S., Legacy and emerging per- and poly-fluoroalkyl substances in surface seawater from northwestern Pacific to Southern Ocean: Evidences of current and historical release. *J Hazard Mater* **2021,** *411*, 125049.

180.   Shi, Y.; Vestergren, R.; Nost, T. H.; Zhou, Z.; Cai, Y., Probing the Differential Tissue Distribution and Bioaccumulation Behavior of Per- and Polyfluoroalkyl Substances of Varying Chain-Lengths, Isomeric Structures and Functional Groups in Crucian Carp. *Environ.Sci. Technol.* **2018,** *52* (8), 4592-4600.

181.   Zhou, J.; Li, S.; Liang, X.; Feng, X.; Wang, T.; Li, Z.; Zhu, L., First report on the sources, vertical distribution and human health risks of legacy and novel per- and polyfluoroalkyl substances in groundwater from the Loess Plateau, China. *J. Hazard. Mater.* **2021,** *404* (Pt A), 124134.

182.   Jiang, W.; Zhang, Y.; Zhu, L.; Deng, J., Serum levels of perfluoroalkyl acids (PFAAs) with isomer analysis and their associations with medical parameters in Chinese pregnant women. *Environ. Int.* **2014,** *64*, 40-7.

183.   Torres, F. J.; Ochoa-Herrera, V.; Blowers, P.; Sierra-Alvarez, R., Ab initio study of the structural, electronic, and thermodynamic properties of linear perfluorooctane sulfonate (PFOS) and its branched isomers. *Chemosphere* **2009,** *76* (8), 1143-9.

184.   Xu, Y.; Fletcher, T.; Pineda, D.; Lindh, C. H.; Nilsson, C.; Glynn, A.; Vogs, C.; Norstrom, K.; Lilja, K.; Jakobsson, K.; Li, Y., Serum Half-Lives for Short- and Long-Chain Perfluoroalkyl Acids after Ceasing Exposure from Drinking Water Contaminated by Firefighting Foam. *Environ. Health. Perspect.* **2020,** *128* (7), 77004.

185.   McDonough, C. A.; Choyke, S.; Ferguson, P. L.; DeWitt, J. C.; Higgins, C. P., Bioaccumulation of Novel Per- and Polyfluoroalkyl Substances in Mice Dosed with an Aqueous Film-Forming Foam. *Environ.Sci. Technol.* **2020,** *54*, 5700-5709.

186.   De Silva, A. O., Benskin, J. P., Martin, L. J., Arsenault, G., McCrindle, R., Riddell, N., ... & Mabury, S. A., Disposition of perfluorinated acid isomers in sprague-dawley rats; Part 2: Subchronic dose. *Environ. Toxicol. Chem.* **2009,** *28*, 555-567.

187.   Beesoon, S.; Martin, J. W., Isomer-Specific Binding Affinity of Perfluorooctanesulfonate (PFOS) and Perfluorooctanoate (PFOA) to Serum Proteins. *Environ. Sci. Technol.* **2015,** *49* (9), 5722-31.

188.   Yu, N.; Wang, X.; Zhang, B.; Yang, J.; Li, M.; Li, J.; Shi, W.; Wei, S.; Yu, H., Distribution of perfluorooctane sulfonate isomers and predicted risk of thyroid hormonal perturbation in drinking water. *Water Res.* **2015,** *76*, 171-80.

189.   Han, X.; Nabb, D. L.; Russell, M. H.; Kennedy, G. L.; Rickard, R. W., Renal elimination of perfluorocarboxylates (PFCAs). *Chem. Res. Toxicol.* **2012,** *25* (1), 35-46.

190.   Schultes, L.; Vestergren, R.; Volkova, K.; Westberg, E.; Jacobson, T.; Benskin, J. P., Per- and polyfluoroalkyl substances and fluorine mass balance in cosmetic products from the Swedish market: implications for environmental emissions and human exposure. *Environ Sci Process Impacts* **2018,** *20* (12), 1680-1690.

191.   Rodgers, K. M.; Swartz, C. H.; Occhialini, J.; Bassignani, P.; McCurdy, M.; Schaider, L. A., How Well Do Product Labels Indicate the Presence of PFAS in Consumer Items Used by Children and Adolescents? *Environ.Sci. Technol.* **2022,** *56* (10), 6294-6304.

192.   Liu, J.; Van Hoomissen, D. J.; Liu, T.; Maizel, A.; Huo, X.; Fernández, S. R.; Ren, C.; Xiao, X.; Fang, Y.; Schaefer, C. E.; Higgins, C. P.; Vyas, S.; Strathmann, T. J., Reductive Defluorination of Branched Per- and Polyfluoroalkyl Substances with Cobalt Complex Catalysts. *Environ. Technol. Lett.* **2018,** *5* (5), 289-294.

193.   Uwayezu, J. N.; Yeung, L. W. Y.; Backstrom, M., Sorption of PFOS isomers on goethite as a function of pH, dissolved organic matter (humic and fulvic acid) and sulfate. *Chemosphere* **2019,** *233*, 896-904.

194.   Uwayezu, J. N.; Carabante, I.; Lejon, T.; van Hees, P.; Karlsson, P.; Hollman, P.; Kumpiene, J., Electrochemical degradation of per- and poly-fluoroalkyl substances using boron-doped diamond electrodes. *J. Environ. Manage.* **2021,** *290*, 112573.

195.   Vyas, S. M.; Kania-Korwel, I.; Lehmler, H. J., Differences in the isomer composition of perfluoroctanesulfonyl (PFOS) derivatives. *J. Environ. Sci. Health. A. Tox. Hazard. Subst. Environ. Eng.* **2007,** *42* (3), 249-55.

196.   Benskin, J. P.; Bataineh, M.; Martin, J. W., Simultaneous Characterization of Perfluoroalkyl Carboxylate, Sulfonate, and Sulfonamide Isomers by Liquid Chromatography−Tandem Mass Spectrometry. *Anal. Chem.* **2007,** *79* (17), 6455-6464.

197.   Ahrens, L.; Gashaw, H.; Sjoholm, M.; Gebrehiwot, S. G.; Getahun, A.; Derbe, E.; Bishop, K.; Akerblom, S., Poly- and perfluoroalkylated substances (PFASs) in water, sediment and fish muscle tissue from Lake Tana, Ethiopia and implications for human exposure. *Chemosphere* **2016,** *165*, 352-357.

198.   Barzen-Hanson, K. A.; Roberts, S. C.; Choyke, S.; Oetjen, K.; McAlees, A.; Riddell, N.; McCrindle, R.; Ferguson, P. L.; Higgins, C. P.; Field, J. A., Discovery of 40 Classes of Per- and Polyfluoroalkyl Substances in Historical Aqueous Film-Forming Foams (AFFFs) and AFFF-Impacted Groundwater. *Environ. Sci. Technol.* **2017,** *51* (4), 2047-2057.

199.   Langlois, I.; Oehme, M., Structural identification of isomers present in technical perfluorooctane sulfonate by tandem mass spectrometry. *Rapid. Commun. Mass. Spectrom.* **2006,** *20* (5), 844-50.

200.   Martin JW, K. K., Berger U, de Voogt P, Field J, Franklin J, Giesy JP, Harner T, Muir DC, Scott B, Kaiser M, Jarnberg U, Jones KC, Mabury SA, Schroeder H, Simcik M, Sottani C, van Bavel B, Karrman A, Lindstrom G, van Leeuwen SP, Analytical challenges hamper perfluoroalkyl research. *Environ.Sci. Technol.* **2004,** *38*, 248A–255A.

201.   Riddell N, A. G., Benskin JP, Chittim B, Martin JW, McAlees A, McCrindle R, Branched Perfluorooctane Sulfonate Isomer Quantification and Characterization in Blood Serum Samples by HPLC/ESI-MS(/MS). *Environ.Sci. Technol.* **2007,** *43*, 7902-7908.

202.   Bagenstose, K. New Jersey approves drinking water standards for toxic PFAS chemicals. Will legal battles follow? https://www.usatoday.com/story/news/2020/04/07/new-jersey-approves-drinking-water-standards-toxic-pfas-chemicals/2963032001/ (accessed November 2020).

203.   BCLP State-by-State Regulation of PFAS Substances in Drinking Water. https://www.bclplaw.com/en-US/insights/state-by-state-regulation-of-pfas-substances-in-drinking-water.html (accessed June 2021)

204.   AWWA Per- and Polyfluoroalkyl Substances (PFAS) Summary of State Regulation to Protect Drinking Water. https://www.awwa.org/Portals/0/AWWA/Government/SummaryofStateRegulationtoProtectDrinkingWater.pdf (accessed June 2021)

205.   BBKLaw California Issues the Nation's Strictest Notice Levels for PFAS in Drinking Water. https://www.bbklaw.com/news-events/insights/2019/legal-alerts/09/california-issues-the-nations-strictest-notice-le (accessed November 2020).

206.   Crone, B. C.; Speth, T. F.; Wahman, D. G.; Smith, S. J.; Abulikemu, G.; Kleiner, E. J.; Pressman, J. G., Occurrence of Per- and Polyfluoroalkyl Substances (PFAS) in Source Water and Their Treatment in Drinking Water. *Crit. Rev. Environ. Sci. Technol.* **2019,** *49* (24), 2359-2396.

207.   Xiao, F.; Simcik, M. F.; Gulliver, J. S., Mechanisms for removal of perfluorooctane sulfonate (PFOS) and perfluorooctanoate (PFOA) from drinking water by conventional and enhanced coagulation. *Water Res.* **2013,** *47* (1), 49-56.

208.   USEPA EPA Announces New Drinking Water Health Advisories for PFAS Chemicals, $1 Billion in Bipartisan Infrastructure Law Funding to Strengthen Health Protections. https://www..epa.gov/newsreleases/epa-announces-new-drinking-water-health-advisories-pfas-chemicals-1-billion-bipartisan (accessed June 2022).

209.   Strynar, M. J.; Lindstrom, A. B.; Nakayama, S. F.; Egeghy, P. P.; Helfant, L. J., Pilot scale application of a method for the analysis of perfluorinated compounds in surface soils. *Chemosphere* **2012,** *86* (3), 252-7.

210.   Brusseau, M. L.; Anderson, R. H.; Guo, B., PFAS concentrations in soils: Background levels versus contaminated sites. *Sci. Total. Environ.* **2020,** *740*, 140017.

211.   Fernández, M. D.; Sánchez-Arguello, P. S.; García-Gómez, C., Soil pollution remediation. In *Reference Module in Biomedical Sciences*, 2022.

212.   Pang, H.; Dorian, B.; Gao, L.; Xie, Z.; Cran, M.; Muthukumaran, S.; Sidiroglou, F.; Gray, S.; Zhang, J., Remediation of poly-and perfluoroalkyl substances (PFAS) contaminated soil using gas fractionation enhanced technology. *Sci Total Environ* **2022**, 154310.

213.   Hoisaeter, A.; Arp, H. P. H.; Slinde, G.; Knutsen, H.; Hale, S. E.; Breedveld, G. D.; Hansen, M. C., Excavated vs novel in situ soil washing as a remediation strategy for sandy soils impacted with per- and polyfluoroalkyl substances from aqueous film forming foams. *Sci Total Environ* **2021,** *794*, 148763.

214. Grimison, C.; Knight, E. R.; Nguyen, T. M. H.; Nagle, N.; Kabiri, S.; Braunig, J.; Navarro, D. A.; Kookana, R. S.; Higgins, C. P.; McLaughlin, M. J.; Mueller, J. F., The efficacy of soil washing for the remediation of per- and poly-fluoroalkyl substances (PFASs) in the field. *J. Hazard. Mater.* **2023,** *445*, 130441.

215. Deshpande, S., Shiau, B. J., Wade, D., Sabatini, D. A., & Harwell, J. H., Surfactant selection for enhancing ex situ soil washing. *Water Res* **1999,** *33*, 551-560.

216. Chu, W., Remediation of Contaminated Soils by Surfactant-Aided Soil Washing. *Pract. period. hazard., toxic, radioact. waste manag.* **2003,** *7* (1), 19-24.

217. Befkadu, A. A.; Chen, Q., Surfactant-Enhanced Soil Washing for Removal of Petroleum Hydrocarbons from Contaminated Soils: A Review. *Pedosphere* **2018,** *28* (3), 383-410.

218. Campos-Pereira, H.; Kleja, D. B.; Ahrens, L.; Enell, A.; Kikuchi, J.; Pettersson, M.; Gustafsson, J. P., Effect of pH, surface charge and soil properties on the solid-solution partitioning of perfluoroalkyl substances (PFASs) in a wide range of temperate soils. *Chemosphere* **2023,** *321*, 138133.

219. Quinnan, J.; Morrell, C.; Nagle, N.; Maynard, K. G., Ex situ soil washing to remove PFAS adsorbed to soils from source zones. *Remediation* **2022,** *32* (3), 151-166.

220. Brusseau, M. L., Influence of chain length on field-measured distributions of PFAS in soil and soil porewater. *JHM Letters* **2023,** *4*.

221. Hubert, M.; Arp, H. P. H.; Hansen, M. C.; Castro, G.; Meyn, T.; Asimakopoulos, A. G.; Hale, S. E., Influence of grain size, organic carbon and organic matter residue content on the sorption of per- and polyfluoroalkyl substances in aqueous film forming foam contaminated soils - Implications for remediation using soil washing. *Sci.Total. Environ.* **2023**, 162668.

222. Uwayezu, J. N.; Ren, Z.; Sonnenschein, S.; Leiviska, T.; Lejon, T.; van Hees, P.; Karlsson, P.; Kumpiene, J.; Carabante, I., Combination of separation and degradation methods after PFAS soil washing. *Sci. Total Environ.* **2023**, 168137.

223. Fabregat-Palau, J.; Vidal, M.; Rigol, A., Modelling the sorption behaviour of perfluoroalkyl carboxylates and perfluoroalkane sulfonates in soils. *Sci. Total. Environ.* **2021**.

224. Smith, S. J.; Lewis, J.; Wiberg, K.; Wall, E.; Ahrens, L., Foam fractionation for removal of per- and polyfluoroalkyl substances: Towards closing the mass balance. *Sci Total Environ* **2023,** *871*, 162050.

225. Wang, Y.; Ji, Y.; Tishchenko, V.; Huang, Q., Removing per- and polyfluoroalkyl substances (PFAS) in water by foam fractionation. *Chemosphere* **2022**.

226. Fang, Y.; Ellis, A.; Choi, Y. J.; Boyer, T. H.; Higgins, C. P.; Schaefer, C. E.; Strathmann, T. J., Removal of Per- and Polyfluoroalkyl Substances (PFASs) in Aqueous Film-Forming Foam (AFFF) Using Ion-Exchange and Nonionic Resins. *Environ Sci Technol* **2021**.

227. Wanzek, T.; Stults, J. F.; Johnson, M. G.; Field, J. A.; Kleber, M., Role of Mineral-Organic Interactions in PFAS Retention by AFFF-Impacted Soil. *Environ Sci Technol* **2023**.

228.   Agency, U. S. E. P. CompTox Chemicals Dashboard. https://comptox.epa.gov/dashboard/ (accessed November 2023)

229.   Zhang, Y.; Thomas, A.; Apul, O.; Venkatesan, A. K., Coexisting ions and long-chain per- and polyfluoroalkyl substances (PFAS) inhibit the adsorption of short-chain PFAS by granular activated carbon. *J. Hazard. Mater.* **2023**, *460*, 132378.

230.   Zhang, C.; Hopkins, Z. R.; McCord, J.; Strynar, M. J.; Knappe, D. R. U., Fate of Per- and Polyfluoroalkyl Ether Acids in the Total Oxidizable Precursor Assay and Implications for the Analysis of Impacted Water. *Environ. Technol. Lett.* **2019**.

231.   Al Amin, M.; Luo, Y.; Nolan, A.; Robinson, F.; Niu, J.; Warner, S.; Liu, Y.; Dharmarajan, R.; Mallavarapu, M.; Naidu, R.; Fang, C., Total oxidisable precursor assay towards selective detection of PFAS in AFFF. *J. Clean. Prod.* **2021**, *328*.

232.   Place, B. *Suspect List of Possible Per-and Polyfluoroalkyl Substances (PFAS)*; National Institute of Standards and Technology: 2021.

233.   Charbonnet, J. A.; McDonough, C. A.; Xiao, F.; Schwichtenberg, T.; Cao, D.; Kaserzon, S.; Thomas, K. V.; Dewapriya, P.; Place, B. J.; Schymanski, E. L.; Field, J. A.; Helbling, D. E.; Higgins, C. P., Communicating Confidence of Per- and Polyfluoroalkyl Substance Identification via High-Resolution Mass Spectrometry. *Environ. Sci. Technol. Lett.* **2022,** *9* (6), 473-481.

234.   Hao, S.; Choi, Y. J.; Wu, B.; Higgins, C. P.; Deeb, R.; Strathmann, T. J., Hydrothermal Alkaline Treatment for Destruction of Per- and Polyfluoroalkyl Substances in Aqueous Film-Forming Foam. *Environ. Sci. Technol* **2021,** *55* (5), 3283-3295.

235.   Cui, J.; Gao, P.; Deng, Y., Destruction of Per- and Polyfluoroalkyl Substances (PFAS) with Advanced Reduction Processes (ARPs): A Critical Review. *Environ. Sci. Technol.* **2020**.